The Pennsylvania State University

The Graduate School

College of Engineering

# DETECTION AND ESTIMATION IN ULTRAWIDEBAND MIMO NOISE RADAR

A Dissertation in

Electrical Engineering

by

Wei-Jen Chen



Submitted in Partial Fulfillment
of the Requirements
for the Degree of

Doctor of Philosophy

August 2010

The dissertation of Wei-Jen Chen was reviewed and approved* by the following:

Ram M. Narayanan
Professor of Electrical Engineering
Dissertation Advisor
Chair of Committee

John F. Doherty
Professor of Electrical Engineering

Julio Urbina
Assistant Professor of Electrical Engineering

Soundar R.T. Kumara
Professor of Industrial and Manufacturing Engineering

Ken Jenkins
Professor of Electrical Engineering
Head of the Department of Electrical Engineering

*Signatures are on file in the Graduate School

## ABSTRACT

In radar systems, the wider the bandwidth, the better is the range resolution. While a variety of transmit waveforms can be used, noise and noise-like waveforms are preferred from the standpoint of covertness and immunity to jamming and interference. Moreover, multi-input-multi-output (MIMO) spatial diversity radar significantly improves radar detection and estimation performances. Based to the above advantages, ultrawideband (UWB) MIMO noise radar systems are garnering more and more attention recently. In this dissertation, two issues concerning detection and estimation in UWB MIMO noise radar are investigated in detail.

First, we consider the problem of estimating target directions in UWB MIMO noise radar. In our system, transmitters are sufficiently separated and transmit UWB independent noise waveforms to satisfy the requirements of MIMO spatial diversity. Receivers are assumed to be spaced half-wavelength apart to eliminate directional ambiguity. We apply the tapped-delay line (TDL) based beamforming technique to concentrate on receiving signals from a certain direction, and to efficiently suppress the interferences from the others. According to the TDL outputs, the CLEAN-sense conditional generalized likelihood ratio test (CGLRT) is applied for detecting the targets given the average of the square of the absolute value of the residual signal resulting from the CLEAN algorithm. Then, we propose a new mechanism called the iterative CGLRT (ICGLRT) to determine their directions by implementing these two techniques iteratively. Simulation results show that ICGLRT is able to sequentially detect the targets and improve target direction estimation accuracy even when their reflections are seriously interfered with by others.

Then, with some simplifications to the system model, we analyze the mean square error (MSE) of target velocity and location estimation in UWB MIMO noise radar. The ambiguity function (AF) formulation is applied to implement the estimations. Since the maximum of the AF is attained when the time-delay and Doppler stretch of replica signals are exactly matched with

the ones corresponding to the reflections, this estimation is also a peak localization problem. When noise is added, the peak may be located in a different place causing error. In this dissertation, we develop probability density functions (pdfs) to approximate the distributions of coherent and non-coherent ambiguity functions (CAFs and NCAFs) and apply the pdfs to analyze MSE of their estimates. Based on the analyses, we explain and demonstrate that the NCAF is the better estimation approach in spatial diversity MIMO radar. Finally, the error floor resulting from NCAF approach is further discussed.

# TABLE OF CONTENTS

# LIST OF FIGURES

# LIST OF TABLES

# NOTATIONS

| | |
|---|---|
| $N$ , $M$ | Number of transmit and receive antennas, respectively |
| $S_n(t) = s_n(t)e^{-j2\pi f_c t}$ | UWB noise waveform transmitted by the $n$-th antenna |
| $B$ | Bandwidth of $s_n(t)$ |
| $\sigma_s^2$ | Variance of $s_n(t)$ |
| $f_c$ | Center frequency |
| $Q$ | Number of scatterers in a complex target |
| $\alpha_q$ | Reflectivity of the $q$-th scatterer |
| $\phi_n$ , $\theta$ | Target directions corresponding to the $n$-th transmit antenna and the receive antenna array in the direction estimation issue |
| $P$ | Number of targets |
| $g_{n,p}(\tau)$ | The $p$-th target impulse response corresponds to $n$-th transmit antenna |
| $S_p^r(t)$ | Summation of the reflections from the $p$-th target |
| $ja(t)$ | Jammer signal emitted from direction $\theta_{ja}$ with variance $\sigma_{ja}^2$ and bandwidth $BW_{ja}$ |
| $K$ | Number of taps in TDL |
| $T_m$ | The delay time of the first tap for the $m$-th receive antenna |
| $\tau_{tdl}$ | The delay time of the taps except the first one |

| | |
|---|---|
| $\theta_{pre}$ | The pre-steered direction of the receiver array |
| $r_{TDL}(t)$ | TDL outputs |
| $\Gamma(\theta_{pre})$ | Likelihood ratio corresponds to direction $\theta_{pre}$ |
| $\mathbf{v} = (v_x, v_y)$ | Target velocity vector |
| $\mathbf{x} = (x, y)$ | Target location vector |
| $\theta_n^t,\ \theta_m^r$ | Target directions correspond to the $n$-th transmit antenna and the $m$-th receive antenna in the location and velocity estimation issue |
| $o$ | Reference point |
| $r_m(t)$ | Signal received by the $m$-th receive antenna |
| $z_m(t)$ | Thermal noise in the $m$-th receive antenna |
| $S_{n,m}^r(t)$ | Reflected signals for the $n$-th transmit antenna and the $m$-th receiver antenna pair |
| $\alpha_{n,m} = \alpha_{R,n,m} + j\alpha_{I,n,m}$ | Amplitude factor of $S_{n,m}^r(t)$ |
| $\beta_{n,m}$ | Doppler stretch factor of $S_{n,m}^r(t)$ |
| $\tau_{n,m}$ | Delay time of $S_{n,m}^r(t)$ |
| $R_{n,m}$ | Propagation path distance from the $n$-th transmit antenna, though the reference point, and ending in the $m$-th receive antenna |
| $T_o$ | Observed duration |

| | |
|---|---|
| $t_s$ | Sample duration |
| $L$ | Number of total samples |
| $c$ | Speed of light |
| $\widetilde{\beta}_{n,m}$ | Doppler stretch factor corresponding to reference signal |
| $\tilde{\tau}_{n,m}$ | Delay time corresponding to reference signal |
| $\tilde{\mathbf{v}}$ | Velocity vector corresponding to reference signal |
| $\tilde{\mathbf{x}}$ | Location vector corresponding to reference signal |
| CAF | Coherent ambiguity function |
| NCAF | Non-coherent ambiguity function |
| $\boldsymbol{\beta}$ , $\tilde{\boldsymbol{\beta}}$ | Vectors piled up with all $\beta_{n,m}$ and $\tilde{\beta}_{n,m}$ values, respectively |
| $\boldsymbol{\tau}$ , $\tilde{\boldsymbol{\tau}}$ | Vectors piled up with all $\tau_{n,m}$ and $\tilde{\tau}_{n,m}$ values, respectively |
| $A^{1/2}\left(\tilde{\mathbf{v}}_{u,h},\tilde{\mathbf{x}}_{\mathrm{u,h}}\right)$ | Square root of CAF result when $\tilde{\mathbf{v}}=\left(\tilde{v}_{x,u},\tilde{v}_{y,h}\right)$ and $\tilde{\mathbf{x}}=\left(\tilde{x}_{\mathrm{u}},\tilde{y}_{\mathrm{h}}\right)$ correspond to the reference signal |
| $A_{nc}^{1/2}\left(\tilde{\mathbf{v}}_{u,h},\tilde{\mathbf{x}}_{\mathrm{u,h}}\right)$ | Square root of NCAF result when $\tilde{\mathbf{v}}=\left(\tilde{v}_{x,u},\tilde{v}_{y,h}\right)$ and $\tilde{\mathbf{x}}=\left(\tilde{x}_{\mathrm{u}},\tilde{y}_{\mathrm{h}}\right)$ corresponding to the reference signal |
| $\hat{\mathbf{v}}$ , $\hat{\mathbf{v}}_{nc}$ | Estimates of velocity vector resulting from CAF and NCAF approaches, respectively |
| $\Delta\tilde{v}_x$ | Step size for $\tilde{v}_x$ |
| **A** , **ncA** | Vectors piled up with all $A^{1/2}\left(\tilde{\mathbf{v}}_{u,h},\tilde{\mathbf{x}}_{\mathrm{u,h}}\right)$ and $A_{nc}^{1/2}\left(\tilde{\mathbf{v}}_{u,h},\tilde{\mathbf{x}}_{\mathrm{u,h}}\right)$ values, respectively |

$w_{n,m}(t)$ Signals received by the $m$-th receive antenna except the reflection of the $n$-th transmit signal, given $r_m(t) - S^r_{n,m}(t)$

$\chi^{[u,h,\mathrm{u},\mathrm{h}]}_{R,n,m,\ell,\tilde{\mathbf{v}},\tilde{\mathbf{x}}} + j\chi^{[u,h,\mathrm{u},\mathrm{h}]}_{I,n,m,\ell,\tilde{\mathbf{v}},\tilde{\mathbf{x}}}$ $\ell$-th sample of the product of the received signal of the $m$-th receiver antenna, and the $n$-th reference signal while $\tilde{\mathbf{v}} = (\tilde{v}_{x,u}, \tilde{v}_{y,h})$ and $\tilde{\mathbf{x}} = (\tilde{x}_{\mathrm{u}}, \tilde{y}_{\mathrm{h}})$, given by $r_m[\ell t_s] S^*_n\left[\widetilde{\beta}_{n,m}(\ell t_s - \tilde{\tau}_{n,m})\right]$

$\mu^{[u,h,\mathrm{u},\mathrm{h}]}_{R,n,m,\ell,\tilde{\mathbf{v}},\tilde{\mathbf{x}}}$, $\left(\sigma^{[u,h,\mathrm{u},\mathrm{h}]}_{R,n,m,\ell,\tilde{\mathbf{v}},\tilde{\mathbf{x}}}\right)^2$ Mean and the variance of $\chi^{[u,h,\mathrm{u},\mathrm{h}]}_{R,n,m,\ell,\tilde{\mathbf{v}},\tilde{\mathbf{x}}}$

$\overline{\chi}^{[u,h,\mathrm{u},\mathrm{h}]}_{C,n,m,\tilde{\mathbf{v}},\tilde{\mathbf{x}}} = \overline{\chi}^{[u,h,\mathrm{u},\mathrm{h}]}_{R,n,m,\tilde{\mathbf{v}},\tilde{\mathbf{x}}} + j\overline{\chi}^{[u,h,\mathrm{u},\mathrm{h}]}_{I,n,m,\tilde{\mathbf{v}},\tilde{\mathbf{x}}}$ Correlator outputs in the $m$-th receiver antenna with the $n$-th reference signal

$\overline{\mu}^{[u,h,\mathrm{u},\mathrm{h}]}_{R,n,m,\tilde{\mathbf{v}},\tilde{\mathbf{x}}}$, $\left(\overline{\sigma}^{[u,h,\mathrm{u},\mathrm{h}]}_{R,n,m,\tilde{\mathbf{v}},\tilde{\mathbf{x}}}\right)^2$ Mean and the variance of $\overline{\chi}^{[u,h,\mathrm{u},\mathrm{h}]}_{R,n,m,\tilde{\mathbf{v}},\tilde{\mathbf{x}}}$

$D^{[u,h,\mathrm{u},\mathrm{h}]}_{\ell,n,m,\tilde{\mathbf{v}},\tilde{\mathbf{x}}}$ Time difference between the $\ell$-th sample of the reflection for the $n$-th transmit signal and the $\ell$-th sample of the $n$-th reference signal in the $m$-th receiver antenna, given by $\beta_{n,m}(\ell t_s - \tau_{n,m}) - \tilde{\beta}_{n,m}(\ell t_s - \tilde{\tau}_{n,m})$

$D^{[u,h,\mathrm{u},\mathrm{h}]}_{\ell,\tilde{n},m,\tilde{\mathbf{v}},\tilde{\mathbf{x}}}$ Time difference between the $\ell$-th sample of the reflection for the $\tilde{n}$-th transmit antenna and the $\ell$-th sample of the $n$-th reference signal in the $m$-th receiver antenna, given by $\beta_{\tilde{n},m}(\ell t_s - \tau_{\tilde{n},m}) - \tilde{\beta}_{n,m}(\ell t_s - \tilde{\tau}_{n,m})$

$\rho^{[u,h,\mathrm{u},\mathrm{h}]}_{n,m,\tilde{\mathbf{v}},\tilde{\mathbf{x}}}$ Correlation coefficient between $\overline{\chi}^{[u,h,\mathrm{u},\mathrm{h}]}_{R,n,m,\tilde{\mathbf{v}},\tilde{\mathbf{x}}}$ and $\overline{\chi}^{[u,h,\mathrm{u},\mathrm{h}]}_{I,n,m,\tilde{\mathbf{v}},\tilde{\mathbf{x}}}$

| | |
|---|---|
| $\overline{\chi}_{R,\tilde{\mathbf{v}},\tilde{\mathbf{x}}}^{[u,h,\mathrm{u},\mathrm{h}]} = \sum_{m=1}^{M}\sum_{n=1}^{N}\overline{\chi}_{R,n,m,\tilde{\mathbf{v}},\tilde{\mathbf{x}}}^{[u,h,\mathrm{u},\mathrm{h}]}$ | Real part of the summation of all correlator outputs |
| $\overline{\chi}_{I,\tilde{\mathbf{v}},\tilde{\mathbf{x}}}^{[u,h,\mathrm{u},\mathrm{h}]} = \sum_{m=1}^{M}\sum_{n=1}^{N}\overline{\chi}_{I,n,m,\tilde{\mathbf{v}},\tilde{\mathbf{x}}}^{[u,h,\mathrm{u},\mathrm{h}]}$ | Imaginary part of the summation of all correlator outputs |
| $\overline{\mu}_{R,\tilde{\mathbf{v}},\tilde{\mathbf{x}}}^{[u,h,\mathrm{u},\mathrm{h}]}$, $\left(\overline{\sigma}_{R,\tilde{\mathbf{v}},\tilde{\mathbf{x}}}^{[u,h,\mathrm{u},\mathrm{h}]}\right)^2$ | Mean and the variance of $\overline{\chi}_{R,\tilde{\mathbf{v}},\tilde{\mathbf{x}}}^{[u,h,\mathrm{u},\mathrm{h}]}$ |
| $\rho_{\tilde{\mathbf{v}},\tilde{\mathbf{x}}}^{[u,h,\mathrm{u},\mathrm{h}]}$ | Correlation coefficient between $\overline{\chi}_{R,\tilde{\mathbf{v}},\tilde{\mathbf{x}}}^{[u,h,\mathrm{u},\mathrm{h}]}$ and $\overline{\chi}_{I,\tilde{\mathbf{v}},\tilde{\mathbf{x}}}^{[u,h,\mathrm{u},\mathrm{h}]}$ |
| $\widehat{\mu}_{n,m,\tilde{\mathbf{v}},\tilde{\mathbf{x}}}^{[u,h,\mathrm{u},\mathrm{h}]}$, $\left(\widehat{\sigma}_{n,m,\tilde{\mathbf{v}},\tilde{\mathbf{x}}}^{[u,h,\mathrm{u},\mathrm{h}]}\right)^2$ | Mean and the variance approximations of $\left\lvert\overline{\chi}_{C,n,m,\tilde{\mathbf{v}},\tilde{\mathbf{x}}}^{[u,h,\mathrm{u},\mathrm{h}]}\right\rvert$ |
| $\widehat{\mu}_{\tilde{\mathbf{v}},\tilde{\mathbf{x}}}^{[u,h,\mathrm{u},\mathrm{h}]}$, $\left(\widehat{\sigma}_{\tilde{\mathbf{v}},\tilde{\mathbf{x}}}^{[u,h,\mathrm{u},\mathrm{h}]}\right)^2$ | Mean and the variance approximations of $A_{nc}^{1/2}\left(\tilde{\mathbf{v}}_{u,h},\tilde{\mathbf{x}}_{\mathrm{u},\mathrm{h}}\right)$ |
| $F(\bullet)$ | Cumulative distribution function of a standard normal distribution |
| $\hat{\varepsilon}_{\mathbf{v}}$, $\hat{\varepsilon}_{nc,\mathbf{v}}$ | Mean square errors of velocity estimation resulting from CAF and NCAF, respectively |
| $\phi_A^{[u,h,\mathrm{u},\mathrm{h}]}(\bullet)$ | Probability density function of $A^{1/2}\left(\tilde{\mathbf{v}}_{u,h},\tilde{\mathbf{x}}_{\mathrm{u},\mathrm{h}}\right)$ |
| $\Phi_{\mathbf{A}\mid\zeta}^{[u,h,\mathrm{u},\mathrm{h}]}(\bullet)$ | Conditional cumulative distribution function of $\mathbf{A}$ given $A^{1/2}\left(\tilde{\mathbf{v}}_{u,h},\tilde{\mathbf{x}}_{\mathrm{u},\mathrm{h}}\right)=\zeta$ |

# ACKNOWLEDGMENTS

I would like to thank my advisor Dr. Ram Narayanan for his help, support and encouragement, my committee members Dr. John F. Doherty, Dr. Julio Urbina, and Dr. Soundar R.T. Kumara for their insightful advice, and all my laboratory colleagues for their sincere support. Last but not the least, we appreciate valuable comments and suggestions received from Dr. Jon Sjogren of the U.S. Air Force Office of Scientific Research (AFOSR). This grant was supported by AFOSR Contract # FA9550-06-1-0029.

# Chapter 1

# Introduction

## 1.1. UWB noise radar and MIMO radar introductions

While narrow band noise radars have been proposed and refined over the past fifty years [1-7], the concept of ultrawideband (UWB) random noise radar has seen significant development more recently [8-13]. In contrast to conventional radar, the UWB noise radar transmits a noise or noise-like waveform having a fractional bandwidth of greater than 25%. The return from the target is cross-correlated with a time-delayed replica of the transmit waveform to determine the range to the target with a range resolution inversely proportional to the bandwidth. Noise radars satisfy important requirements for military systems, such as low probability of interception (LPI) and low probability of detection (LPD), owing to the featureless characteristics of its waveform [14]. Moreover, the aperiodicity of the waveform also causes the suppressed ambiguity in range/velocity [15]. Another advantage of UWB noise radars is their ability to efficiently share the frequency spectrum. A number of UWB noise radars can operate over the same frequency band with minimal cross-interference since each noise waveform is uncorrelated with the others. For example, recently, multichannel noise radar architectures have been proposed and theoretically studied [16].

Multi-input and multi-output (MIMO) radar systems have captured the attention of many researchers in recent years. An innovative concept in designing MIMO radar systems is to stabilize the reflected power instead of enhancing it as in phase array radar systems. In order to limit the reflected power variations resulting from target radar cross section (RCS) scintillations, these systems apply independent probing signals, and sufficiently separated radars to ensure

adequate averaging to reduce amplitude variations. Such a radar system is called spatial diversity MIMO radar system to reflect its unique features. Spatial diversity MIMO radar systems have been further investigated in various applications and many advantages have been discovered. First, it has been shown that MIMO radar detection performance is dramatically improved which has contributed to the efforts in stabilizing the reflected power [17]. Second, since spatial diversity provides independent realizations of the radar reflectivity of the target, the Cramer-Rao bound (CRB) for the direction of arrival (DOA) estimation is effectively reduced [18]. Third, ambiguity function formulation proved that coherent processing over widely dispersed sensors elements may lead to range resolutions higher than supported by the waveform's bandwidth [19]. Finally, the different spatial spread characteristics of a small target and clutter in a spatial diversity MIMO radar can enhance the target detection probability [20].

Since an independent waveform set is necessary for MIMO operation, waveform design is very critical. Early work focused on creating orthogonal waveforms, for which the sidelobe level in the autocorrelation and cross correlation functions are approximately zero. Examples include polyphase orthogonal sequences based on the Hadamard matrix [21] as well as an integration of Genetic Algorithm and the traditional iterative code selection method [22]. Then, the idea that the waveform set should maximize the total radar return or match the illumination to the scene was recognized and developed [23]. Another interesting criterion for designing waveforms, namely, maximizing the conditional mutual information between the random target impulse response and the reflected waveforms, was then developed [24].

Considering the independent signals requirement combined with its benefits, the UWB noise waveform is indeed a great candidate. Several works initialized the investigation of this application. The comparisons between element and beam space beamforming approaches and their corresponding matched filter designs and coarrays concepts for MIMO noise radar are discussed in [25] and [26] respectively. Then, nonparametric copula based detection algorithms

for UWB MIMO noise radars are suggested in [27]. In fact, the development of MIMO UWB noise radar is still in the beginning stage. Therefore, it is worthy to study further. Several topics will be discussed as follows.

## 1.2. Interesting topics for UWB MIMO noise radar

First of all, since most discussions about stabilizing the reflected power are focused on narrow band signals [17, 18], the criteria for limiting reflection power fluctuations in UWB noise waveform should be studied before applying it to spatial diversity MIMO radar system.

### 1.2.1 Target direction estimation

In contrast to investigations on MIMO radar advantages and waveform design, the practical issue of MIMO radar operation in multi-target and powerful jammer environment has not received adequate attention it deserves. In one of limited studies in this topic, an iterative generalized likelihood ratio test algorithm (iGLRT) for locating targets [28] is proposed. The iGLRT does not only iteratively examine target existence over the entire surveillance area, but also exploits the information about observed targets to help detect new targets. As a result, localization accuracy is improving sequentially, and almost reaches the Cramer-Rao bound (CRB) when the iterative procedure is completed. However, since the discussion is restricted to narrow band signals, its extension to MIMO UWB noise radar is advantageous.

Prior work on noise radar system design and implementation employ a power divider or a directional coupler to pass the replica of the transmitted signal to the receiver [5, 6, 8, 9, 15]. Moreover, a delay line and a mixer are used to implement the correlator operation. The correlation between the reflected signal and the transmit replica depends on the time difference

between the delay for the replica and the round trip propagation time from the transmitter to the receiver through the target. This feature causes a lobe in the correlator output as a function of the delay. By observing the peak of the lobe, not only is the target distance and target impulse response measured, but also the lobe implies the existence of the target [1, 11, 12]. However, it is not a precise approach for detecting the target especially when the lobe is not noticeable due to high thermal noise levels. Therefore, it is critical to develop a more robust detection mechanism.

In addition, target direction is another important parameter for locating the target. Since multiple antennas are used in the receiver, target direction is solvable. The signal subspace approach is one of the most popular methods in direction finding [29]. First, the covariance matrix of signals in different antennas is calculated. Then, the eigenvectors corresponding to smaller eigenvalues of the covariance matrix are the vectors for the noise subspace. If the noise subspace is determined, the signal direction can be solved, since the signal vector resulting from its direction is orthogonal to the noise subspace. Even though the subspace approach is a well developed approach in direction finding, it has several primary disadvantages when applied to radar. First, in order to gather the information for deciding the noise subspace, the number of targets has to be smaller than the number of receiver antennas. Second, it may need a lot of samples to estimate the covariance matrix. Third, this approach is unable to distinguish target reflections from jammers. Therefore, in our considered environment where multiple targets and strong jammers exist, an alternate direction finding approach needs to be developed.

In this dissertation, the widely discussed broadband beamforming technique, namely the tapped delay line (TDL) system [30-33], is applied to concentrate on receiving the desired signal from a certain angle and to suppress the interferences from other angles. We first review the TDL beamforming approach and the CLEAN algorithm. Then, we introduce the CLEAN-sense generalized likelihood ratio test (CGLRT), which is a likelihood ratio test given residual signals resulting from the CLEAN algorithm to determine the target existence of the certain angle. Next,

we integrate the CGLRT and TDL system and propose an iterative CGLRT (ICGLRT) mechanism to estimate the target directions in multi-target and powerful jammer environment. Finally, we demonstrate the ICGLRT procedure and verify that our proposed algorithm can iteratively improve the performance via numerical examples.

### 1.2.2 Target location and velocity estimation

In recent years, the estimation of target parameters using noise radar is also gathering considerable attention. As we mentioned, in order to determine the range to the target, the return from the target is cross-correlated with a time-delayed replica of the transmit waveform. However, the accuracy of the range estimation has not been further analyzed in detail.

Moreover, the target velocity estimation is another widely investigated issue. Doppler estimation in a coherent UWB random noise radar system was proposed and demonstrated in [34]. In this system, in-phase and quadrature (I/Q) detector is applied to estimate the Doppler frequency. However, since, in practice, all frequencies are not always present within a finite observation interval, it is essential that the frequency components be averaged over longer intervals. Furthermore, since the Doppler stretch factor in random amplitudes is ignored, the performance of this approach is degraded when the target moves at high speed.

In addition, evaluation of the estimation performance is emerging as a topic of great interest. The Doppler visibility, i.e., the ability to extract Doppler information under clutter spectra and noisy microwave components influences was studied in [35]. However, this discussion focused on evaluating the I/Q detector approach in estimating the velocity of a slow moving target. A more general performance evaluation, the Cramer-Rao bound approximation of Doppler error in correlation processing was developed in [36]. However, this study was restricted

to narrowband noise radar, and most approximations used are not satisfied for UWB noise waveforms.

Moreover, ambiguity function is another valuable reference in understanding the characteristics of the UWB noise waveforms [37-38]. Ambiguity function provides the statistical features when the parameters in the transmit replica are not exactly matched with the parameters in the reflected signal, but it is not an indicator as precise as the mean square error (MSE) to characterize the estimation performance.

Based upon the previous discussion, it is imperative to investigate the location and velocity estimation approach which can be implemented within a limited observation interval and to analyze its MSEs for a high-speed target using a UWB MIMO noise radar system.

Inspired by the proposed method in [39], in this dissertation, location and velocity corresponding to delay time and Doppler stretch are jointly estimated using the coherent ambiguity function (CAF) and non-coherent ambiguity function (NCAF) approaches. We first develop the probability density functions (pdfs) for approximating the distributions of their results, and use the pdfs to analyze the MSE in estimating target parameters. Then, according to the pdfs, we explain the relation between reflectivity sets and estimation performances resulted from different approaches. Last, we demonstrate the pdfs are proper for modeling the distributions of CAF and of NCAF results and verify that NCAF approach can achieve better estimation performance in spatial diversity MIMO radar system via simulation.

This dissertation contains four subsequent chapters. Chapter 2 provides the system overview of MIMO radar and the criteria for achieving spatial diversity in UWB MIMO radar system. The applied detection algorithm, proposed iterative processing mechanism, and related simulation results are introduced in Chapter 3. In Chapter 4, the estimation performances for velocity and location are analyzed. Moreover, the comparisons between analyses and simulations are also attached. Finally, the conclusions and future works are shown in Chapter 5.

## Chapter 2

# System overview

### 2.1. Signal model

For target direction estimation issue, we consider the scenario presented in Figure 2.1, which was studied in [18], and assume that the transmitter, receiver arrays, and targets are all static. In a manner similar to [18], we also apply this model to investigate the criteria for reflected power stabilization. Then, we apply the wideband beamforming TDL technique since multiple targets and a strong jammer are included in the environment. For target location and velocity estimation issue, the scenario is a little different from Figure 2.1. Since we focus on analyzing the estimation performance and only one point target is considered, TDL could be discarded to simplify the system. More details about the scenario for moving target will be introduced in Chapter 4.

Consider a UWB MIMO noise radar system with two uniform linear arrays of $N$ omni-directional antennas at the transmitter and $M$ antennas at the receiver. Noise signal transmitted by the $n$-th antenna is denoted as $S_n(t) = s_n(t)e^{-j2\pi f_c t}$, where the amplitude $s_n(t)$ is a wide-sense stationary (WSS) random process and normally distributed with zero mean and variance $\sigma_s^2$, whose autocorrelation $E\left[s_n(t)s_n(t+\tau)\right] = \mathrm{sinc}(B\tau)$, where $B$ is the bandwidth of the transmitted signal and $f_c$ is the carrier frequency. In order to gain the advantages of spatial diversity, the signals transmitted by different transmitters are orthogonal to each other, which means that $E\left[s_{n1}(t)s_{n2}(t)\right] = 0$, $\forall n1 \neq n2$. Since the non-periodic noise waveform is applied, the transmitter structure can be further simplified by illuminating signals continuously.

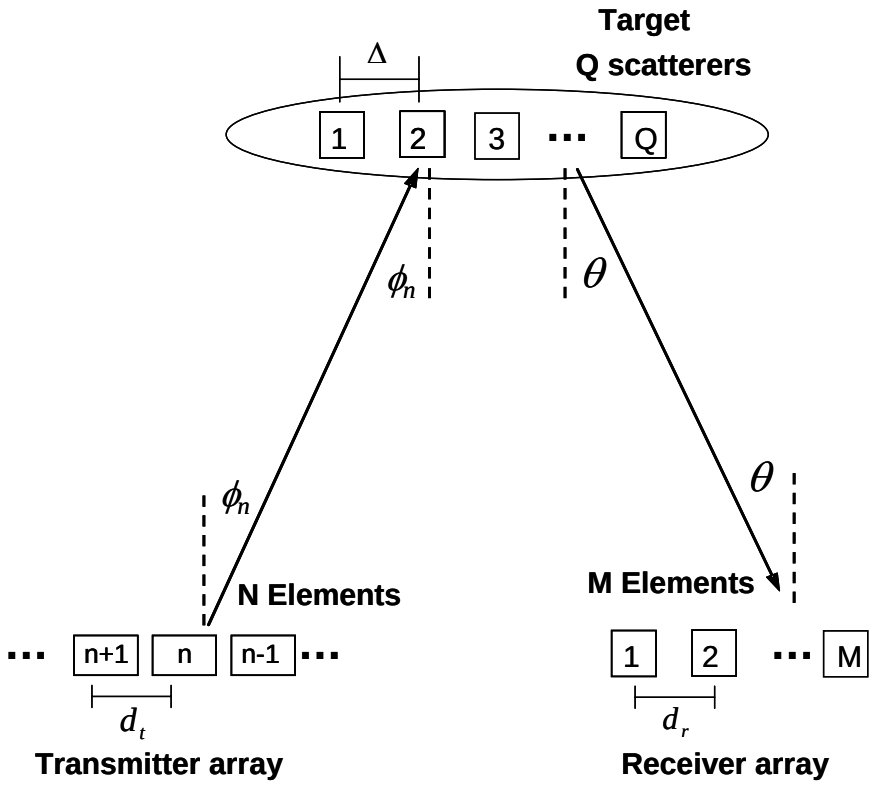


Figure 2.1: Bistatic radar scenario.

In Figure 2.1, the receiver, transmitter and target array are orderly numbered as shown. Moreover, we consider a far field complex target which consists of $Q$ independent and isotropic scatterers, and is illuminated by UWB random noise signals. Moreover, the $Q$ scatterers are organized in the form of a uniform linear array which is parallel to the transmitter and receiver arrays, and the reflectivity of $q$-th scatterer is denoted as $\alpha_q$. The signal radiated by the $n$-th transmit antenna impinges on each of $Q$ scatterers at different angles, $\phi_{n,q}$, $n = 1,...,N$, $q = 1,...,Q$. However, since the length of the target array is much smaller than the distance between the $n$-th transmit antenna and the target, the arrival angles at the target can be assumed to be the same and independent of the scatterer, i.e. $\phi_{n,q} = \phi_n$. Moreover, since the distance

between receiver and the target array is much larger than their lengths, the angles $\theta_{m,q}$, $m = 1,...,M$, and, $q = 1,...,Q$ denoting the angles indicating the signals reflected by the $q$-th target scatterer toward the $m$-th receiver antenna are all equal to $\theta$. Therefore, the reflected signals which are radiated by $n$-th transmit antenna are represented in vector form as $\boldsymbol{\alpha}\mathbf{S_n}$ where

$\boldsymbol{\alpha} = \left[\alpha_1,...,\alpha_Q\right]$,

$\mathbf{S_n} = \left[S_n\left(t-\tau_n-(Q-1)\tau_\theta\right), S_n\left(t-\tau_n-\tau_{\phi_n}-(Q-2)\tau_\theta\right),..., S_n\left(t-\tau_n-(Q-1)\tau_{\phi_n}\right)\right]^T$,

$\tau_\theta = \left(\Delta\sin\theta/c\right)$, and

$\tau_{\phi_n} = \left(\Delta\sin\phi_n/c\right)$.

In the above expressions, $\Delta$ is the distance between two successive scatterers, and $\tau_n$ is the propagation time from the $n$-th transmit antenna to the first receive antenna through the first scatterer in the concerned target.

The reflected signal of the $n$-th antenna illumination can be represented as

$$S_n^r(t) = \boldsymbol{\alpha}\mathbf{S_n} = g_n(t) \otimes S_n\left(t-\tau_n\right) = \int_\tau g_n(\tau) S_n\left(t-\tau_n-\tau\right) d\tau \qquad 2.1$$

where $g_n(t) = \sum_{q=1}^{Q} \alpha_q \delta\left(t-\tau_q\right)$; $\tau_q = (q-1)\tau_{\phi_n} + (Q-q)\tau_\theta$, and $\otimes$ stands for the convolution operation.

Therefore, considering $N$ transmit antennas in the system, the composite $p$-th target reflection received by the first receiver antenna can be expressed as

$$S_p^r(t) = \frac{1}{\sqrt{N}} \sum_{n=1}^{N} \int_\tau g_{n,p}(\tau) S_n\left(t-\tau_{n,p}-\tau\right) d\tau, \qquad 2.2$$

where $g_{n,p}(t)$ is the target impulse response of the $p$-th target corresponding to $n$-th transmitted signal, $\alpha_{q,p}$ is the reflectivity of the $q$–th scatterer of the $p$–th target, $\phi_{n,p}$, and $\theta_p$

are the $p$ -th target directions to the $n$ -th transmit antenna, and to receive antenna array, respectively. $\tau_{n,p}$ is the propagation time corresponding to the $p$ -th target. The factor $1/\sqrt{N}$ is used for normalizing the total transmission power to be equal to $\sigma_s^2$.

Next, we extend the signal expression to a multitarget environment, consisting of $P$ targets. The reflections from these received by the first receiver antenna can be represented as the summation of equation 2.2 over all targets, i.e., $\sum_{p=1}^{P} S_p^r(t)$.

In order to lead our consideration to be more practical, we assume that one jammer in direction $\theta_{ja}$ is also present in the environment. The jamming signal is usually band-limited white noise or multi-tone [31]. Since in a UWB radar system, partial band noise affects the system performance more seriously than does multi-tone, we assume that the jamming signal is partial band noise which is normally distributed with zero mean and variance, $\sigma_{ja}^2$.

Last, the receiver antenna is a uniformly linear array and signals in different antennas are polluted by independent thermal noise. Therefore, the received signal of the $m$ -th receiver antenna is

$$r_m(t) = \sum_{p=1}^{P} S_p^r(t - \tau_{m,p}) + ja(t - \tau_{m,ja}) + z_m(t), \qquad 2.3$$

Also, $\tau_{m,p} = \left\{\left((m-1)d_r \sin\theta_p\right)/c\right\}$ and $\tau_{m,ja} = \left\{\left((m-1)d_r \sin\theta_{ja}\right)/c\right\}$ represent the arrival time delays for $m$ -th receive antenna corresponding to the $p$ -th target and the jammer, respectively, where $d_r = c/2f_c$ to ensure unambiguous direction finding. Also, $z_m(t)$ is the thermal noise at the $m$ -th receive antenna, which is complex Gaussian distributed with zero mean and variance $\sigma_{z_m}^2$. Moreover, $E\left[z_{m1}(t) z_{m2}(t)\right] = 0$, $\forall m1 \neq m2$.

## 2.2. Reflection power variation

We first investigate the characteristics of UWB noise waveforms in reducing the reflected power variation. In this section, we are consistent with the assumptions in [17] and [18] that the reflectivity of each scatterer of the target is modeled as an independent complex Gaussian random variable with zero-mean and variance $1/Q$.

We start from studying the reflection of the $n$-th antenna illumination. The reflected signals can be represented as $S_n^r(t) = \boldsymbol{\alpha}\mathbf{S_n}$. Then, the reflected power for a snapshot at time $t$ is denoted as $\xi_n$ which is equal to

$$\xi_n = \left|S_n^r(t)\right|^2 = \boldsymbol{\alpha}\mathbf{S_n}\mathbf{S_n}^H\boldsymbol{\alpha}^H = \tilde{\boldsymbol{\alpha}}_\mathbf{n}\mathbf{s_n}\mathbf{s_n}^T\tilde{\boldsymbol{\alpha}}_\mathbf{n}^H \tag{2.4}$$

The $\tilde{\boldsymbol{\alpha}}_\mathbf{n}$ and $\mathbf{s_n}$ in equation 2.4 are given by

$$\tilde{\boldsymbol{\alpha}}_\mathbf{n} = \left[\alpha_1 e^{-j2\pi f_c\left(t-\tau_n-(Q-1)\tau_\theta\right)},\ldots,\alpha_q e^{-j2\pi f_c\left(t-\tau_n-(Q-q)\tau_\theta-(q-1)\tau_{\phi_n}\right)},\ldots,\alpha_Q e^{-j2\pi f_c\left(t-\tau_n-(Q-1)\tau_{\phi_n}\right)}\right]$$

and

$$\mathbf{s_n} = \left[s_n\left(t-\tau_n-(Q-1)\tau_\theta\right), s_n\left(t-\tau_n-\tau_{\phi_n}-(Q-2)\tau_\theta\right),\ldots,s_n\left(t-\tau_n-(Q-1)\tau_{\phi_n}\right)\right]^T$$

It is obvious that the second moment of $\xi_n$ depends on the correlation between the elements of $\mathbf{s_n}$. When the bandwidth of the transmitted waveform, $B$ is much smaller than $c/D$ where $D$ is the target extent in the range dimension, the elements in $\mathbf{s_n}$ are identical to each other, and $E\left[\xi_n^2\right]$ will achieve its maximum. In other words, its minimum can be achieved when $B$ is sufficient large and results in the elements of $\mathbf{s_n}$ being orthogonal to each other. Therefore, a larger bandwidth is helpful in further reducing the reflected power variation.

The reflections of the $n$-th and $n+1$-th antenna illuminations can be represented as $\frac{1}{\sqrt{2}}\left(S_n^r(t)+S_{n+1}^r(t)\right)=\frac{1}{\sqrt{2}}\left(\boldsymbol{\alpha}\mathbf{S_n}+\boldsymbol{\alpha}\mathbf{S_{n+1}}\right)$, where the factor $\sqrt{2}$ is used for normalizing the total transmission power. Its reflected power for a snapshot at time $t$ is denoted as $\xi_{n,n+1}$ which is equal to

$$\xi_{n,n+1}=\frac{1}{2}\left|S_n^r(t)+S_{n+1}^r(t)\right|^2=\frac{1}{2}\left(\boldsymbol{\alpha}\mathbf{S_n}+\boldsymbol{\alpha}\mathbf{S_{n+1}}\right)\left(\mathbf{S_n}^H\boldsymbol{\alpha}^H+\mathbf{S_{n+1}}^H\boldsymbol{\alpha}^H\right) \tag{2.5}$$

Since $s_n(t)$ and $s_{n+1}(t)$ are independent of each other, $E\left[\xi_{n,n+1}\right]$ is equal to $\sigma_s^2$ which is identical to $E\left[\xi_n\right]$. The second moment of $\xi_{n,n+1}$ is

$$E\left[\xi_{n,n+1}^2\right]=\frac{1}{4}\left\{E\left[\xi_n^2\right]+E\left[\xi_{n+1}^2\right]+6E\left[\xi_n\xi_{n+1}\right]\right\} \tag{2.6}$$

If $E\left[\xi_n^2\right]$ and $E\left[\xi_{n+1}^2\right]$ are similar, we can conclude $E\left[\xi_{n,n+1}^2\right]<E\left[\xi_n^2\right]$ because of the independence between $\mathbf{s_n}$ and $\mathbf{s_{n+1}}$. Then, we concentrate on $E\left[\xi_n\xi_{n+1}\right]$. After some calculation, it can be shown to be

$$E\left[\tilde{\boldsymbol{\alpha}}_\mathbf{n}\mathbf{s_n}\mathbf{s_n}^T\tilde{\boldsymbol{\alpha}}_\mathbf{n}^H\tilde{\boldsymbol{\alpha}}_\mathbf{n+1}\mathbf{s_{n+1}}\mathbf{s_{n+1}}^T\tilde{\boldsymbol{\alpha}}_\mathbf{n+1}^H\right]=E\left[\tilde{\boldsymbol{\alpha}}_\mathbf{n}\mathbf{R}_{\mathbf{s_n}}\tilde{\boldsymbol{\alpha}}_\mathbf{n}^H\tilde{\boldsymbol{\alpha}}_\mathbf{n+1}\mathbf{R}_{\mathbf{s_{n+1}}}\tilde{\boldsymbol{\alpha}}_\mathbf{n+1}^H\right], \tag{2.7}$$

and

$$\begin{aligned}&E\left[\tilde{\boldsymbol{\alpha}}_\mathbf{n}\mathbf{R}_{\mathbf{s_n}}\tilde{\boldsymbol{\alpha}}_\mathbf{n}^H\tilde{\boldsymbol{\alpha}}_\mathbf{n+1}\mathbf{R}_{\mathbf{s_{n+1}}}\tilde{\boldsymbol{\alpha}}_\mathbf{n+1}^H\right]\\&=Q^{-1}\sigma_s^4+\sigma_s^4\\&+Q^{-2}\sum_{q_1=1}^{Q}\sum_{\substack{q_2=1\\q_1\neq q_2}}^{Q}\mathbf{R}_{\mathbf{s_n}}(q_1,q_2)\mathbf{R}_{\mathbf{s_{n+1}}}(q_2,q_1)\exp\left(j2\pi f_c(q_1-1)\left(\tau_{\phi_n}-\tau_{\phi_{n+1}}\right)\right)\exp\left(j2\pi f_c(q_2-1)\left(\tau_{\phi_{n+1}}-\tau_{\phi_n}\right)\right)\end{aligned} \tag{2.8}$$

The first two terms are the results from our assumption that the reflectivity of each scatterer is independent and identically complex normally distributed with zero-mean and $1/2Q$ variance for the real and imaginary parts. $\mathbf{R}_{\mathbf{s_n}}(q_1,q_2)$, the element in the $q_1$-th row and the $q_2$-

th column in $\mathbf{R}_{\mathbf{s_n}}$ , which is the covariance matrix of $\mathbf{s_n}$ , is equal to $\mathrm{sinc}\left(B\left(q_2-q_1\right)\left(\tau_{\phi_n}-\tau_\theta\right)\right)\sigma_s^2$. Therefore, the last term is significant when $\left|\tau_{\phi_n}-\tau_\theta\right| \ll \frac{1}{B}$ and $\left|\tau_{\phi_{n+1}}-\tau_\theta\right| \ll \frac{1}{B}$.

We assume that $R_n \approx R_{n+1} \approx R$ where $R_n$ is the distance between the $n$-th transmit antenna and the target array, and the transmitter array is parallel to the target array. From the definition of $\tau_{\phi_n}$, we can show that

$$\tau_{\phi_{n+1}}-\tau_{\phi_n}=\left(\Delta/c\right)\cdot\left(\sin\phi_{n+1}-\sin\phi_n\right).$$

Therefore, under the far field conditions stated above, $\sin\phi_{n+1}-\sin\phi_n \approx \frac{d_t}{R}$. For a certain $q_1$, we obtain

$$\sum_{\substack{q_2=1 \\ q_1\neq q_2}}^{Q} \mathbf{R}_{\mathbf{s_n}}\left(q_1,q_2\right)\mathbf{R}_{\mathbf{s_{n+1}}}\left(q_2,q_1\right)\exp\left(j2\pi f_c\left(q_2-1\right)\left(\tau_{\phi_{n+1}}-\tau_{\phi_n}\right)\right)\approx 0, \tag{2.9}$$

if

$$\frac{f_c d_t \Delta}{Rc} > \frac{1}{Q},\ d_t > \frac{Rc}{Qf_c\Delta} = \frac{R\lambda}{D} \tag{2.10}$$

for large value of $Q$, where $D = Q\cdot\Delta$. This criterion is exactly the same as the one for narrow band signals. Therefore, the UWB noise waveforms radar system can also limit the reflected power fluctuations using widely separated transmitter antennas.

All in all, since the UWB noise waveform is helpful to further reduce the power variation and its achievable criterion for spatial diversity, we can conclude that it is very suitable for exploitation in spatial diversity MIMO radar.

## 2.3. Tapped-delay line based beamformer

Since a powerful jammer is assumed to exist in the environment, the received signals are dominated by the jammer power. In order to concentrate on target reflections and to suppress the jamming signals, a suitable beamforming technique must be applied. However, the techniques for narrow and wide band signals are very different.

If a narrow band signal is transmitted, the target reflection obtained by different receiver antenna will have equal amplitudes at different phases. Therefore, the principle of beamformer design is to compensate the phase differences and guarantee observed signals in different receiver antennas are coherently summed up. This constructive summation efficiently increases not only the power of the target reflection, but also the probability of detecting the target. However, if a randomly wideband signal such as UWB noise is transmitted, the received signals at different receiver antennas at the same time instant are very possibly quite different from each other. As a result, constructive summation is not achievable using only one weight, and we need a more complex beamforming structure.

We apply the widely studied tapped-delay line (TDL) based beamformer to our MIMO UWB noise radar system, whose structure is presented in Figure 2.2 [31]. Received signals at each antenna are fed into a tapped-delay line which consists of $K$ taps and each of them is attached to an adjustable weight. Moreover, except for the first tap, the time delays for the remaining $K-1$ taps in all TDLs are identical and denoted as $\tau_{tdl}$. Then, we sum up the weighted outputs of all TDLs.

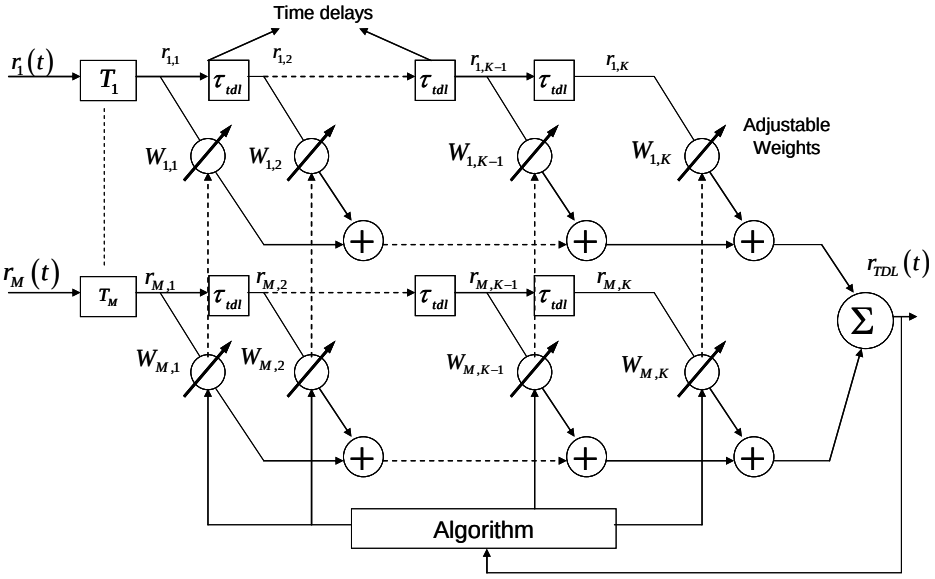


Figure 2.2: TDL beamformer structure.

The delay time of the first tap for the $m$-th receive antenna is denoted as $T_m$. The values of $T_m$, $m \in [1,...,M]$ are jointly designed for receive antennas to coherently collect the reflection from a pre-steered direction, $\theta_{pre}$. Therefore, $T_m = \left\{\left(\left[M-1-(m-1)\right]d_r \sin\theta_{pre}\right)/c\right\}$, and the outputs of the $k$-th tap in the $m$-th receive antenna is $r_{m,k}(t) = r_m\left(t - T_m - (k-1)\tau_{tdl}\right)$, which is denoted as $r_{m,k}$ in Figure 2.2. Also, $\tau_{tdl} = \left(2 f_{\max}\right)^{-1}$, where $f_{\max}$ is the maximum frequency of the transmit signal.

If $\theta_{pre}$, the pre-steered direction is along the $p_1$-th target direction, i.e. $\theta_{pre} = \theta_{p_1}$ and recalling the expression for its reflection received by the $m$-th antenna in equation 2.3, the reflected signal after the first tap can be represented as $S_{p_1}^r\left(t - \tau_{m,p_1} - T_m\right) = S_{p_1}^r\left(t - \tau_{M,p_1}\right)$ since $T_m = \tau_{M,p_1} - \tau_{m,p_1}$. Therefore, it is obvious that the signals reflected from this target will appear with identical delay time in all the receive antennas after the first tap.

Therefore, for this focused reflection, the TDLs attached to different antennas act like a single TDL and its weight parameter is the summation of the weights in the corresponding column. Moreover, the weights are designed to minimize the power of TDL output. Therefore, this is a linearly constrained minimum variance (LCMV) optimization problem, and can be formulated as

$$\min_{W} \mathbf{W}^H \mathbf{R}_\mathbf{r} \mathbf{W} \qquad \text{subject to } \mathbf{C}^T \mathbf{W} = \mathbf{F}. \tag{2.11}$$

where $\mathbf{C}$ and $\mathbf{W}$ can be expressed as

$$\mathbf{C} = \begin{bmatrix} \mathbf{c} & & \mathbf{0} \\ & \ddots & \\ \mathbf{0} & & \mathbf{c} \end{bmatrix} \in R^{MK \times K},\ \mathbf{c} = [1,1,...,1]^T \in R^{M \times 1}$$

$$\mathbf{W} = \left[ W_{1,1}, W_{2,1}, \ldots, W_{M,1}, W_{1,2}, \ldots, W_{M,K} \right]^T \in C^{MK \times 1}.$$

Furthermore, $\mathbf{F} = [F_1,...,F_K]^T \in C^{K \times 1}$ is the frequency response for the focused reflections, and $\mathbf{R}_\mathbf{r} = E\left[\mathbf{r}^H \mathbf{r}\right]$ is the autocorrelation matrix of the observed array data, where $\mathbf{r} = \left[ r_{1,1}(t), r_{2,1}(t), ..., r_{M,1}(t), r_{1,2}(t), ..., r_{M,K}(t) \right] \in C^{1 \times MK}$.

The optimum solution to the LCMV problem can be obtained by the method of Lagrange multipliers as follows,

$$\mathbf{W}_{opt} = \mathbf{R}_\mathbf{r}^{-1} \mathbf{C} \left( \mathbf{C}^T \mathbf{R}_\mathbf{r}^{-1} \mathbf{C} \right)^{-1} \mathbf{F}. \tag{2.12}$$

Therefore, if the $p_1$-th target exists in the pre-steered direction, i.e., $\theta_{pre} = \theta_{p_1}$, and $\mathbf{F}$ is simply designated as $[1,0,...,0]^T$, the TDL output is

$$r_{TDL}(t) = S_{p_1}^r \left( t - \tau_{M,p_1} \right) + \mathbf{S}_{\mathbf{P-1}}^r \times \mathbf{W}_{opt} + \mathbf{ja} \times \mathbf{W}_{opt} + \mathbf{z} \times \mathbf{W}_{opt} \tag{2.13}$$

Moreover, the above vectors are denoted as

$$\mathbf{ja} = \left[ ja_{1,1}(t), ja_{2,1}(t), ..., ja_{M,1}(t), ja_{1,2}(t), ..., ja_{M,K}(t) \right],$$

$$ja_{m,k}(t) = ja\left(t - \tau_{ja,m} - \tau_{M-m+1,p_1} - (k-1)\tau_{tdl}\right),$$

$$\mathbf{z} = \left[ z_{1,1}(t), z_{2,1}(t), ..., z_{M,1}(t), z_{1,2}(t), ..., z_{M,K}(t) \right],$$

$$z_{m,k}(t) = z_m\left(t - \tau_{M-m+1,p_1} - (k-1)\tau_{tdl}\right),$$

$$\mathbf{S}^r_{\mathbf{P\text{-}1}} = \left[ \sum_{\substack{p=1 \\ p \neq p_1}}^{P} S_p^r\left(t - \tau_{1,p} - \tau_{M,p_1}\right), ..., \sum_{\substack{p=1 \\ p \neq p_1}}^{P} S_p^r\left(t - \tau_{m,p} - \tau_{M-m+1,p_1} - (k-1)\tau_{tdl}\right), ... \right.$$

$$\left. ..., \sum_{\substack{p=1 \\ p \neq p_1}}^{P} S_p^r\left(t - \tau_{M,p} - \tau_{1,p_1} - (K-1)\tau_{tdl}\right) \right] .$$

# Chapter 3

# Target direction estimation

With the help of the TDL beamformer, we can concentrate on receiving signals from a chosen direction $\theta_{pre}$ and efficiently suppress the interferences from other directions. Therefore, the target direction estimation can be achieved by detecting whether a target exists in this pre-steered direction according to the observed TDL outputs. The generalized likelihood ratio test (GLRT), one of the most popular hypothesis tests is modified and applied to solve the detection problem.

## 3.1. CLEAN-sense generalized likelihood ratio tests

Before the likelihood ratio test is further discussed, the CLEAN algorithm which we apply in the likelihood ratio calculation should be introduced first. The CLEAN algorithm is basically a deconvolution tool [41-43]. In simple words, the CLEAN algorithm solves the target impulse response which is convolved with transmit signals by processing the following steps. First, a profile is created by cross correlating the transmitted and received signals. The residual signal is set equal to the received signal and the average of the square of its absolute value is calculated. Second, the largest peak in the profile is located. Third, the complex reflectivity corresponding to the peak is measured. Its effects are fractionally canceled in the profile, and the fraction of reflectivity is added to the peak location of the clean profile. Fourth, the residual signal is updated by deducting the convolution result of transmitted signal and fraction of reflectivity with its location from the residual signal. The average of the square of the absolute value of the updated residual signal is calculated and the new average is compared with the previous one.

Fifth, steps two to four are repeated until the average of the square of the absolute value of the residual signal stops decreasing.

According to the procedure of the CLEAN algorithm, we can conclude not only that the accumulated clean profile is the estimated target impulse response, but also that it tries to minimize the average of the square of the absolute value of the residual signal by cleaning the transmitted signal from the received signal. Moreover, a simpler CLEAN algorithm, called coherent CLEAN, is able to function properly only when the highest peak of the correlator result is a response to a real scatterer. If this requirement is not satisfied, but still some minor peaks exist corresponding to responses from actual scatterers, a more practical algorithm called the sequence CLEAN was proposed in [41].

In order to implement the CLEAN algorithm in our system, the correlators need the replicas of all transmitted signals. This can be easily accomplished by using cables to connect the transmitter and the receiver to ensure that the transmitter is able to send the replica to receiver. Moreover, the sampling rate operating in correlator and for CLEAN algorithm has to be equal or larger than $2 f_{\max}$, where $f_{\max}$ is the maximum frequency of the transmit signal.

The hypothesis 1 in likelihood ratio test is the situation that a target, say $p_1$-th target, exists in pre-steered direction, which means $\theta_{pre} = \theta_{p_1}$. Under this hypothesis and according to previous discussion, the TDL output can be represented as 2.13.

As shown in equation 2.13, the noise and jamming parts of $r_{TDL}(t)$ are the weighted summation of $ja(t)$ and $z_m(t)$ with various delays. Therefore, correlated values of $ja(t)$, or $ja(t)$ and $z_m(t)$, could appear in different samples of $r_{TDL}(t)$ at certain moments, leading to their noise and jamming parts being correlated. In order to avoid this correlation and simplify the probability density function (pdf) for hypothesis tests, only independent samples would be

selected. In other words, we perform downsampling on $r_{TDL}(t)$ for the likelihood ratio calculation. Its sample duration, $t_s$, should be larger than

$$\text{Max}\left\{\frac{1}{BW_{ja}}, 2\frac{(M-1)d_r}{c}+(K-1)\tau_{tdl}\right\} \tag{3.1}$$

to ensure that the noise and jamming parts of two successive downsamples in $r_{TDL}(t)$ are independent of each other, where $BW_{ja}$ is the bandwidth of jammer. The second term results from assuming $\theta_{ja}=90^{\circ}$ and $\theta_{pre}=-90^{\circ}$ where the negative values indicate angles on the right side of the dashed vertical line in the receiver antenna array in Figure 2.1.

Since the jammer, thermal noise, and other targets reflections are normally distributed, under hypothesis 1, the $p_1$-th target exists in the pre-steered direction, the pdf of $r_{TDL}(t)$ $L$ independent downsamples, $\mathbf{X}\in C^{1\times L}$ is

$$f\left(\mathbf{X}\middle|H_1\right)=\frac{1}{\pi^L\sigma_{H_1}^{2L}}\exp\left(-\sigma_{H_1}^{-2}\left(\mathbf{X}-\mathbf{S}_{d,p_1}^r\right)\left(\mathbf{X}-\mathbf{S}_{d,p_1}^r\right)^H\right) \tag{3.2}$$

where $\mathbf{S}_{d,p_1}^r=\left[S_{p_1}^r\left(t_s-\tau_{M,p_1}\right),S_{p_1}^r\left(2t_s-\tau_{M,p_1}\right),...,S_{p_1}^r\left(Lt_s-\tau_{M,p_1}\right)\right]$ are the downsamples of the maintained reflections from the $p_1$-th target. According to the principle of GLRT, $\hat{\mathbf{S}}_{d,p_1}^r$ and $\hat{\sigma}_{H_1}^2$ should be solved to maximize the value of equation 3.2 [40]. For the case that the mean vector is unknown, $\sigma_{H_1}^2$ is estimated as

$$\hat{\sigma}_{H_1}^2=\frac{1}{L}\left(\mathbf{X}-\hat{\mathbf{S}}_{d,p_1}^r\right)\left(\mathbf{X}-\hat{\mathbf{S}}_{d,p_1}^r\right)^H. \tag{3.3}$$

Therefore, maximizing equation 3.2 is equivalent to minimizing equation 3.3. Since each element in $\mathbf{S}_{d,p_1}^r$ is different from others, it is very difficult to determine their values from the $\mathbf{X}$ or $r_{TDL}(t)$. However, the idea embedded in equation 3.3 is removing the transmitted signals from

$r_{TDL}(t)$ to minimize the absolute value square average of the residual signals that is consistent with one of the CLEAN algorithm purposes. Therefore, we can apply the CLEAN algorithm to generate and downsample the residual signal which is denoted as $\mathbf{X}_{res}$. Then, $\hat{\sigma}^2_{H_1}$ is obtained by computing $\frac{1}{L}\mathbf{X}_{res}\mathbf{X}^H_{res}$.

If no target exists in $\theta_{pre}$, the pdf for $\mathbf{X}$ under hypothesis 0 is

$$f\left(\mathbf{X}\middle|H_0\right)=\frac{1}{\pi^L\sigma^{2L}_{H_0}}\exp\left(-\sigma^{-2}_{H_0}\mathbf{X}\mathbf{X}^H\right), \tag{3.4}$$

The ML estimation for

$$\sigma^2_{H_0} \text{ is } \hat{\sigma}^2_{H_0}=\frac{1}{L}\mathbf{X}\mathbf{X}^H. \tag{3.5}$$

According to the discussion from equations 3.2 to 3.5, the CLEAN-sense generalized likelihood ratio (CGLR) is

$$\Gamma\left(\theta_{pre}\right)=\log\left(\frac{\max\limits_{\sigma^2_{H_1}} f\left(\mathbf{X}\middle|H_1\right)}{\max\limits_{\sigma^2_{H_0}} f\left(\mathbf{X}\middle|H_0\right)}\right)=L\times\log\left(\frac{\mathbf{X}\mathbf{X}^H}{\mathbf{X}_{res}\mathbf{X}^H_{res}}\right) \tag{3.6}$$

In equation 3.6, one can easily infer that if a target exists, it is possible that most of the maintained reflections which are the combination of transmitted signals are removed from $\mathbf{X}$. That will lead to $\mathbf{X}_{res}\mathbf{X}^H_{res}\ll\mathbf{X}\mathbf{X}^H$ and the ratio in the right hand side of equation 3.6 to be much larger than the value when it is target free in $\theta_{pre}$. Therefore, if the ratio is larger than a threshold, we can claim that a target exists in $\theta_{pre}$ and that its parameters correspond to the clean profile resulting from the CLEAN algorithm.

Moreover, if $P_o$ targets are observed, their estimated reflections should be considered in the TDL beamformer and CGLRT. First of all, their estimated reflections could be deduced from the received signals,

$$r_{m|P_o}(t) = r_m(t) - \sum_{p=1}^{P_o} \hat{S}_p^r\left(t - \tau_{m,p}\right) \tag{3.7}$$

where the second term $\sum_{p=1}^{P_o} \hat{S}_p^r\left(t - \tau_{m,p}\right)$ represents the estimated reflections of $P_o$ targets for the $m$-th receive antenna, which are reconstructed with the estimated information, $\left\{\hat{g}_{n,p}(t), \hat{\tau}_{n,p}\right\}_{p=1}^{P_o}$ resulting from the CLEAN algorithm, $\left\{\hat{\theta}_p\right\}_{p=1}^{P_o}$ observed directions, and the replicas of transmit signals. Furthermore, the optimal solution for the weight vector in TDL beamformer is also updated as $\mathbf{W}_{opt|P_o}$ corresponding to the new signals $r_{m|P_o}(t)$ feed into TDLs. Therefore, under hypothesis $P_o + 1$, another target, namely the $P_o + 1$-th exists in $\theta_{pre}$, and the TDL outputs are

$$r_{TDL|P_o}(t) = S_{P_o+1}^r\left(t - \tau_{M,P_o+1}\right) + \left(\hat{\mathbf{S}}_{\mathbf{P}}^r - \hat{\mathbf{S}}_{\mathbf{P_o}}^r\right) \times \mathbf{W}_{opt|P_o} + \mathbf{ja} \times \mathbf{W}_{opt|P_o} + \mathbf{z} \times \mathbf{W}_{opt|P_o}, \tag{3.8}$$

where

$$\hat{\mathbf{S}}_{\mathbf{P_o}}^r = \left[\sum_{p=1}^{P_o} \hat{S}_p^r\left(t - \tau_{1,p} - \tau_{M,p_1}\right), ..., \sum_{p=1}^{P_o} \hat{S}_p^r\left(t - \tau_{m,p} - \tau_{M-m+1,p_1} - (k-1)\tau_{tdl}\right), ... \right.$$
$$\left. ..., \sum_{p=1}^{P_o} \hat{S}_p^r\left(t - \tau_{M,p} - \tau_{1,p_1} - (K-1)\tau_{tdl}\right)\right]$$

and the pdf of $r_{TDL|P_o}(t)$ $L$ independent samples, $\mathbf{X}_{P_o} \in C^{1\times L}$ is

$$f\left(\mathbf{X}_{P_o} \middle| H_{P_o+1}\right) = \frac{1}{\pi^L \sigma_{H_{P_o+1}}^{2L}} \exp\left(-\sigma_{H_{P_o+1}}^{-2}\left(\mathbf{X}_{P_o} - \mathbf{S}_{d,P_o+1}^r\right)\left(\mathbf{X}_{P_o} - \mathbf{S}_{d,P_o+1}^r\right)^H\right). \tag{3.9}$$

Moreover, for hypothesis $P_o$, non-additional target exists in $\theta_{pre}$, the pdf of $L$ independent TDL output samples is

$$f\left(\mathbf{X}_{P_o}\middle|H_{P_o}\right)=\frac{1}{\pi^L\sigma_{H_{P_o}}^{2L}}\exp\left(-\sigma_{H_{P_o}}^{-2}\mathbf{X}_{P_o}\mathbf{X}_{P_o}^H\right) \tag{3.10}$$

In addition, $\hat{\sigma}_{H_{P_o+1}}^2$ and $\hat{\sigma}_{H_{P_o}}^2$ can be calculated by using previously discussed approaches. As a result, the CGLR given $\left\{\hat{g}_{n,p}(t),\hat{\tau}_{n,p},\hat{\theta}_p\right\}_{p=1}^{P_o}$ is

$$\Gamma\left(\theta_{pre}\middle|\left\{\hat{g}_{n,p}(t),\hat{\tau}_{n,p},\hat{\theta}_p\right\}_{p=1}^{P_o}\right)=L\times\log\left(\frac{\mathbf{X}_{P_o}\mathbf{X}_{P_o}^H}{\mathbf{X}_{res|P_o}\mathbf{X}_{res|P_o}^H}\right) \tag{3.11}$$

### 3.2. Iterative CLEAN-sense generalized likelihood ratio tests

Applying the previously developed CGLRT, we propose an algorithm to sequentially detect targets and refine the estimated parameters of the observed targets. The detailed procedures are listed in Table 3.1, and each step is briefly discussed following the table.

Table 3.1: ICGLRT procedure

| |
|---|
| Step I: Save the received signals in different antennas |
| Step II: Process to detect the first target<br>II.1. Calculate $\Gamma\left(\theta_{pre}\right)$ for all $\theta_{pre}$<br>II.2. Compare $\Gamma\left(\theta_{pre}\right)$ to a threshold $\Gamma_0$: if $\Gamma\left(\theta_{pre}\right) < \Gamma_0$ for all directions, then stop;<br>otherwise $\hat{\theta}_1 = \arg\max_{\theta_{pre}} \Gamma\left(\theta_{pre}\right)$. Go to Step III |
| Step III: Process to detect another target given $P_o = 1, 2, \ldots$<br>III.1. Calculate $\Gamma\left(\theta_{pre} \middle\| \left\{\hat{g}_{n,p}(t), \hat{\tau}_{n,p}, \hat{\theta}_p\right\}_{p=1}^{P_o}\right)$ for all $\theta_{pre}$<br>III.2. Compare $\Gamma\left(\theta_{pre} \middle\| \left\{\hat{g}_{n,p}(t), \hat{\tau}_{n,p}, \hat{\theta}_p\right\}_{p=1}^{P_o}\right)$ to a threshold $\Gamma_0$: if<br>$\Gamma\left(\theta_{pre} \middle\| \left\{\hat{g}_{n,p}(t), \hat{\tau}_{n,p}, \hat{\theta}_p\right\}_{p=1}^{P_o}\right) < \Gamma_0$ for all directions, $\hat{P} = P_o$ then, stop after finishing Step IV;<br>otherwise $\hat{\theta}_{P_0+1} = \arg\max_{\theta_{pre}} \Gamma\left(\theta_{pre} \middle\| \left\{\hat{g}_{n,p}(t), \hat{\tau}_{n,p}, \hat{\theta}_p\right\}_{p=1}^{P_o}\right)$, $P_o = P_o + 1$ and repeat Step III after a complete computation of Step IV. |
| Step IV: Targets parameters update<br>IV.1. Complete the following two calculations by orderly assume $p_s = P_o - 1$,<br>$p_s = P_o - 2, \ldots,\ p_s = 1,\ p_s = P_o$<br>IV.2. Calculate $\Gamma\left(\theta_{pre} \middle\| \left\{\hat{g}_{n,p}(t), \hat{\tau}_{n,p}, \hat{\theta}_p\right\}_{\substack{p=1 \\ p \neq p_s}}^{P_o}\right)$ for all $\theta_{pre}$<br>IV.3. Update $\hat{\theta}_{p_s}$ by $\arg\max_{\theta_{pre}} \Gamma\left(\theta_{pre} \middle\| \left\{\hat{g}_{n,p}(t), \hat{\tau}_{n,p}, \hat{\theta}_p\right\}_{\substack{p=1 \\ p \neq p_s}}^{P_o}\right)$ and replace $\hat{g}_{n,p_s}(t)$ and $\hat{\tau}_{n,p_s}$ with the corresponding new results from CLEAN algorithm. |

In the first step of Table 3.1, we save the signals received by different receiver antennas, and the following procedures are designed to iteratively process these signals. Next, we feed the

stored signals into individual TDLs to compute the $\mathbf{W}_{opt}$ for certain $\theta_{pre}$ and the corresponding $\Gamma\left(\theta_{pre}\right)$. In general, since the number of targets is not *a priori* information, the algorithm is intended to detect targets one by one. Therefore, only the maximum $\Gamma\left(\theta_{pre}\right)$ is selected in Step II.2.

In Step III, we follow the introduction in last section to calculate $\Gamma\left(\theta_{pre}\left|\left\{\hat{g}_{n,p}(t),\hat{\tau}_{n,p},\hat{\theta}_{p}\right\}_{p=1}^{P_o}\right.\right)$. If no additional target is detected, $P_o$ is equal to $\hat{P}$, which is the estimated number of targets. However, if another target is detected, $P_o$ is updated by adding one. Moreover, in order to constrain the error accumulation in iterations, we update targets parameters by implementing Step IV once before starting another process.

In Step IV, we orderly select the target from the penultimate through the first, ending in the last observed one to update its parameters, and denote the selected target as $p_s$. Then, we calculate its $\Gamma\left(\theta_{pre}\left|\left\{\hat{g}_{n,p}(t),\hat{\tau}_{n,p},\hat{\theta}_{p}\right\}_{\substack{p=1\\p\neq p_s}}^{P_o}\right.\right)$ for various $\theta_{pre}$. New target parameters corresponding to $p_s$ target are determine by comparing the values of $\Gamma\left(\theta_{pre}\left|\left\{\hat{g}_{n,p}(t),\hat{\tau}_{n,p},\hat{\theta}_{p}\right\}_{\substack{p=1\\p\neq p_s}}^{P_o}\right.\right)$. Since the interferences resulted from the reflections of other observed targets are reduced by deducing $\sum_{p=1,p\neq p_s}^{P_o}\hat{S}_p^r\left(t-\tau_{m,p}\right)$ from saved signals, the new $\hat{g}_{n,p_s}(t)$, and $\hat{\tau}_{n,p_s}$ resulting from the CLEAN algorithm are supposed to be more accurate. The refinements in target impulse response and arrival time estimates lead to more precise target direction estimate, $\hat{\theta}_{p_s}$.

### 3.3. Numerical examples and discussions

In this section, we first demonstrate the detection mechanism, which integrates ICGLRT and TDL when the targets are widely dispersed in different directions. Then, we demonstrate this mechanism in a more severe situation wherein targets are dispersed along closer directions. Finally, we discuss the mean square error (MSE) of target direction estimation and show that ICGLRT is able to improve the accuracy.

In the numerical example, we extend the scenario in Figure 2.1 to a multitarget environment as presented in Figure 3.1. The transmit and receive arrays contain 5 and 10 antennas, respectively, and they are uniformly distributed. Also, $s_n(t)$ is normally distributed with zero mean and $\sigma_s^2 = 0.2$ for $n = 1,...,5$, and its bandwidth and carrier frequency are 1 GHz, and 1.5 GHz respectively. As a result, $d_r$ and $\tau_{tdl}$ are determined. Moreover, the length of TDL is assumed to be 13. The noise jammer direction angle $\theta_{ja}$ is $45^\circ$ towards the receive array, its frequency band is also over 1 to 2 GHz, and its variance, $\sigma_{ja}^2 = 10^4$. Then, according to these parameters and equation 3.1, the downsampling duration for CGLRT should be larger than 9 ns, say 10 ns. The duration of the saved signals is 250 ns, and the number of efficient samples for likelihood ratio test is 25. We assume that three targets exist in the environment. For simplicity, we assume all targets are consist of 10 isotropic, independent, and equally separated scatterers, with $\Delta = 5$ m.

First of all, we assume that the three targets are located in very different directions relative to receiver array, i.e., $\theta_1 = 20^\circ$, $\theta_2 = 60^\circ$, and $\theta_3 = 40^\circ$. We assume the distances between the fifth transmitter antenna and the first receiver antenna, the first, second, and third targets are 5, 5, 2.75, and 4.5 km respectively. As a result, $d_t$ is chosen to be 50 m to satisfy

equation 2.10. Then, doing some geometric calculations, $\phi_{n,p}$, $\forall n \in \{1,..,5\}, p \in \{1,2,3\}$ can be solved. Since the duration of the saved signals is short, it is reasonable to assume the reflectivity of each scatter in this duration does not change significantly. We further assume that the reflectivity values of all scatters in one target are identical, which are $2/\sqrt{10}$, $1/\sqrt{10}$, and $1.3/\sqrt{10}$ for the first, second, and third target respectively. The variance of the thermal noise in each antenna is 1. All procedures are presented in Figure 3.2.

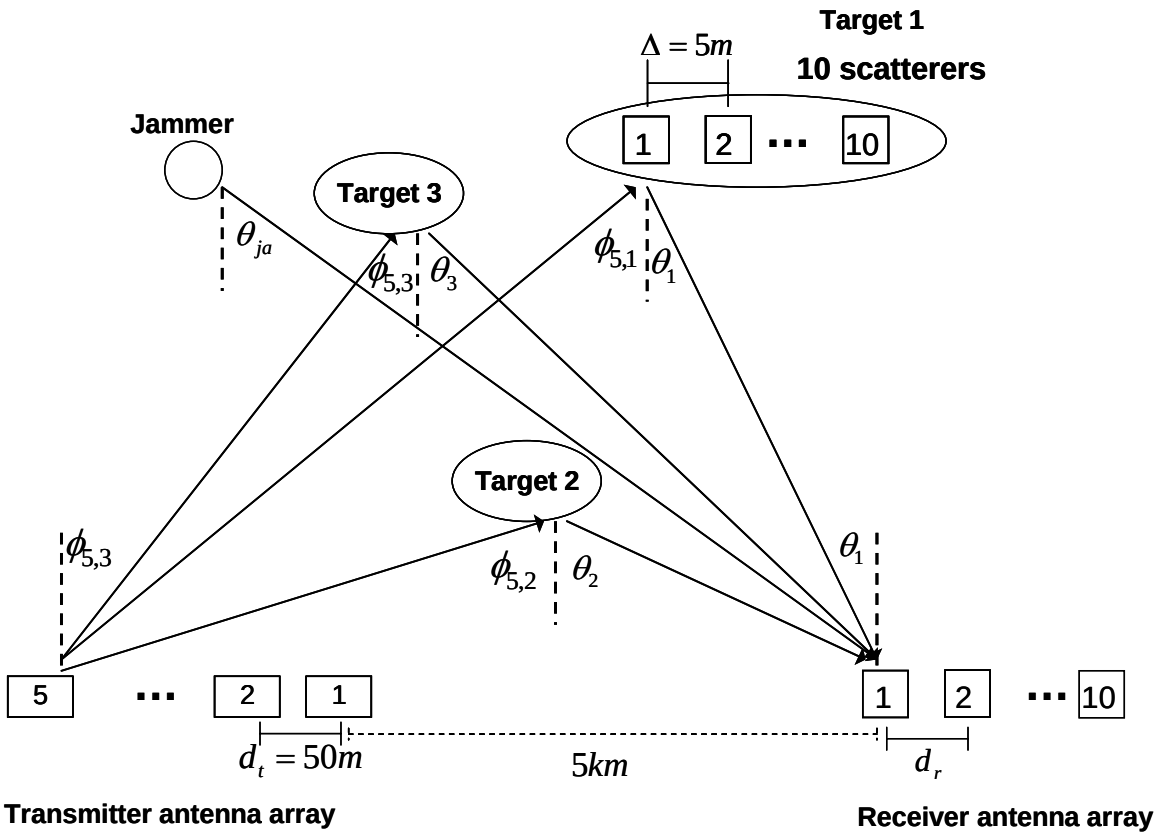


Figure 3.1: Scenario of bistatic radar with multiple targets.

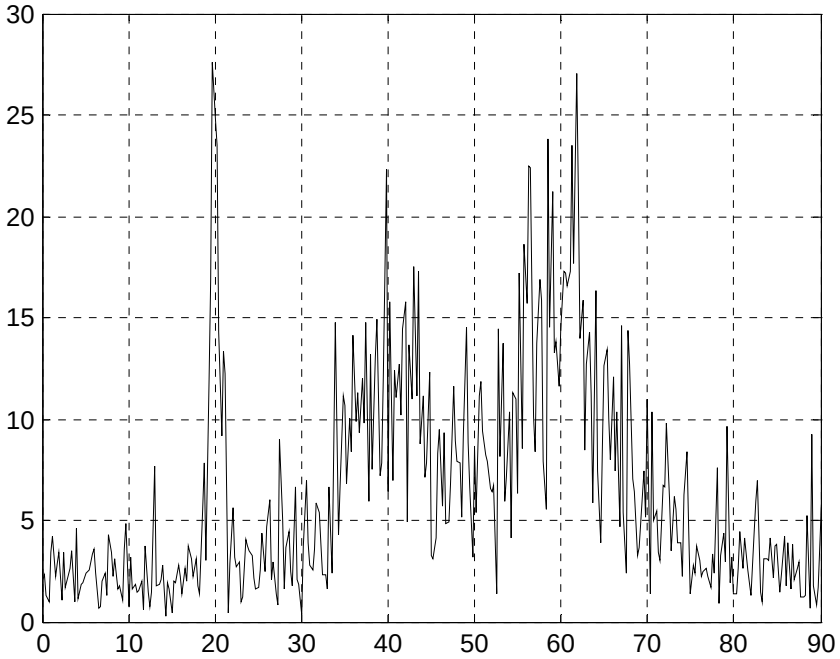


Fig. 3.2(a)

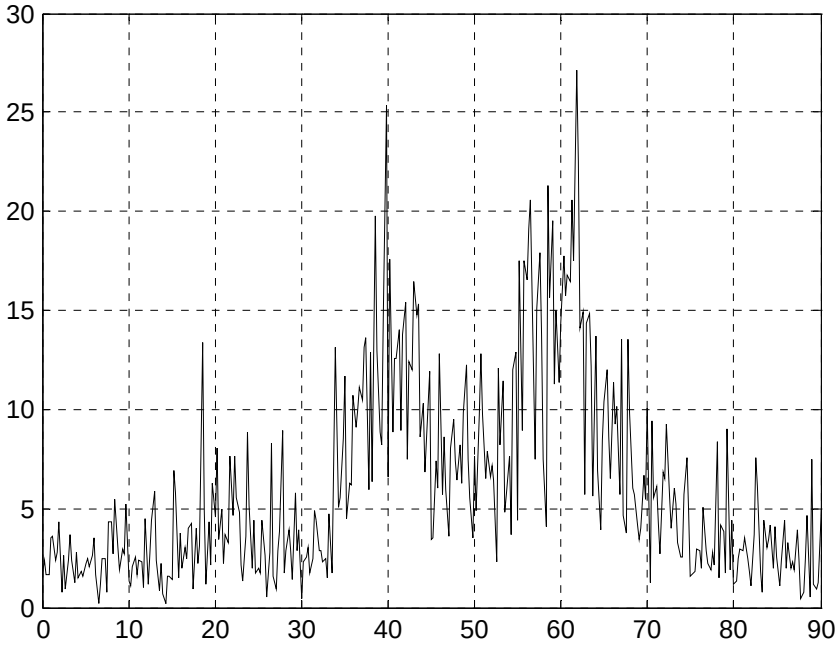


Fig. 3.2(b)

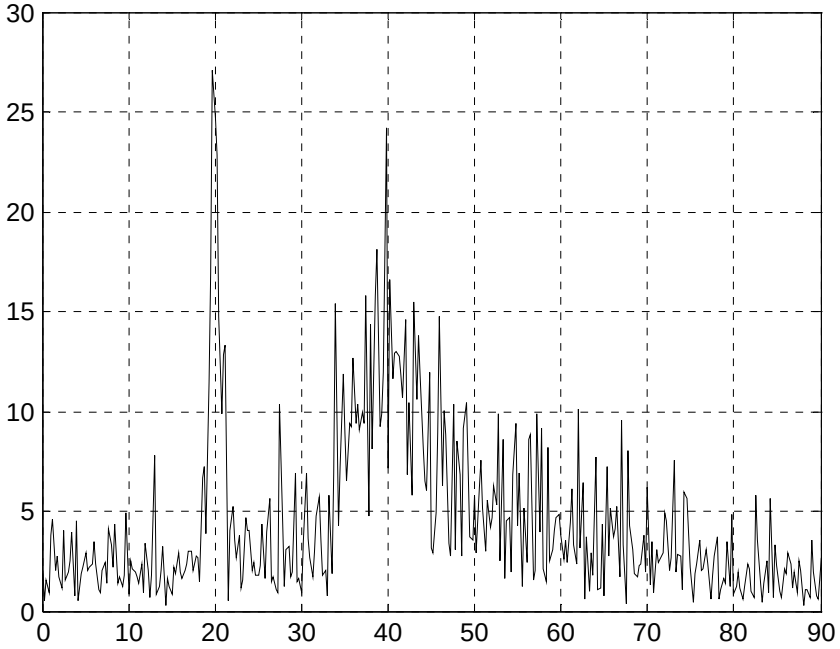


Fig. 3.2(c)

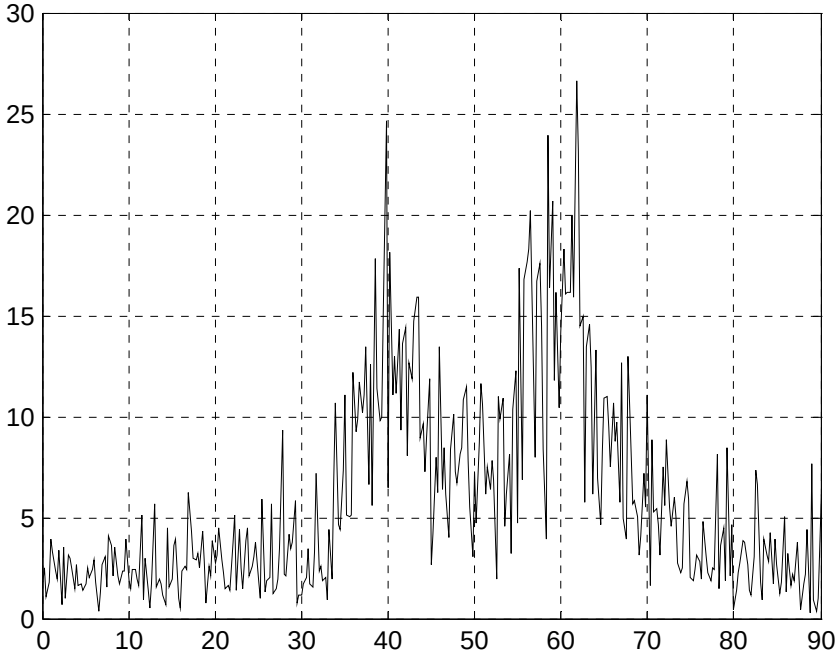


Fig. 3.2(d)

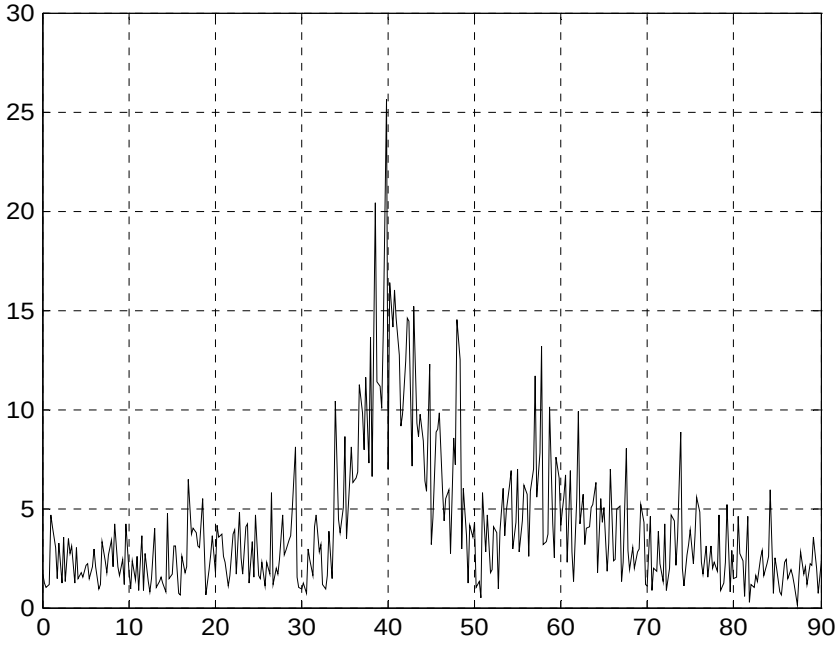


Fig. 3.2(e)

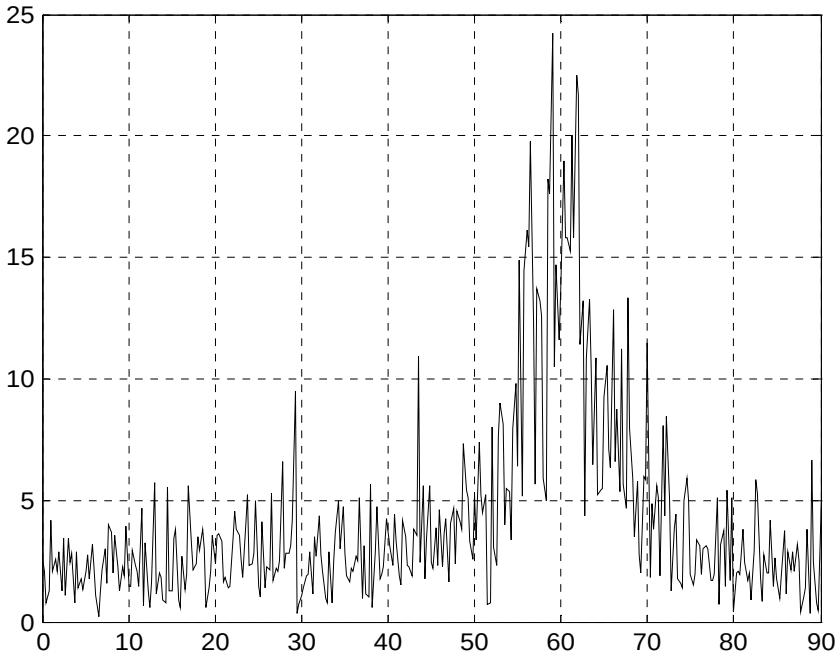


Fig. 3.2(f)

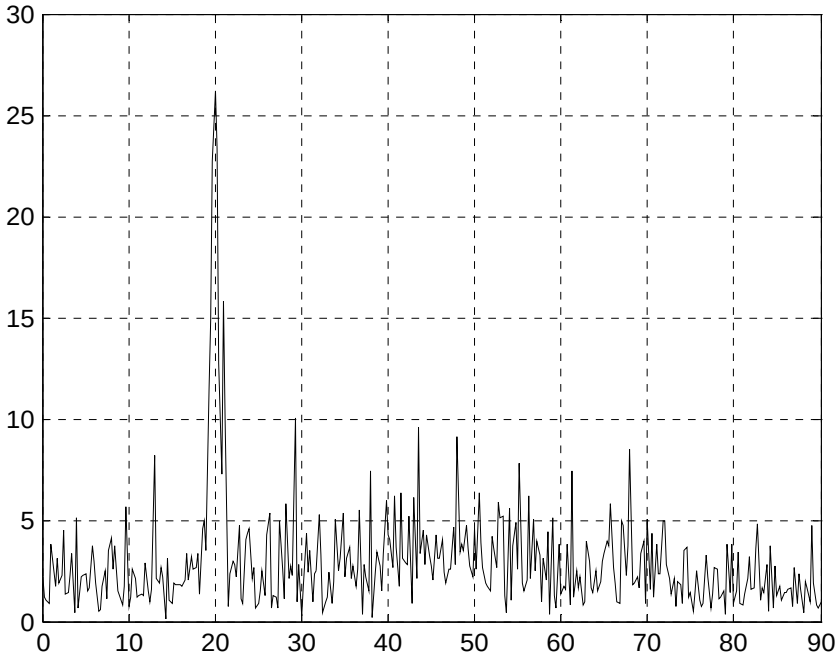


Fig. 3.2(g)

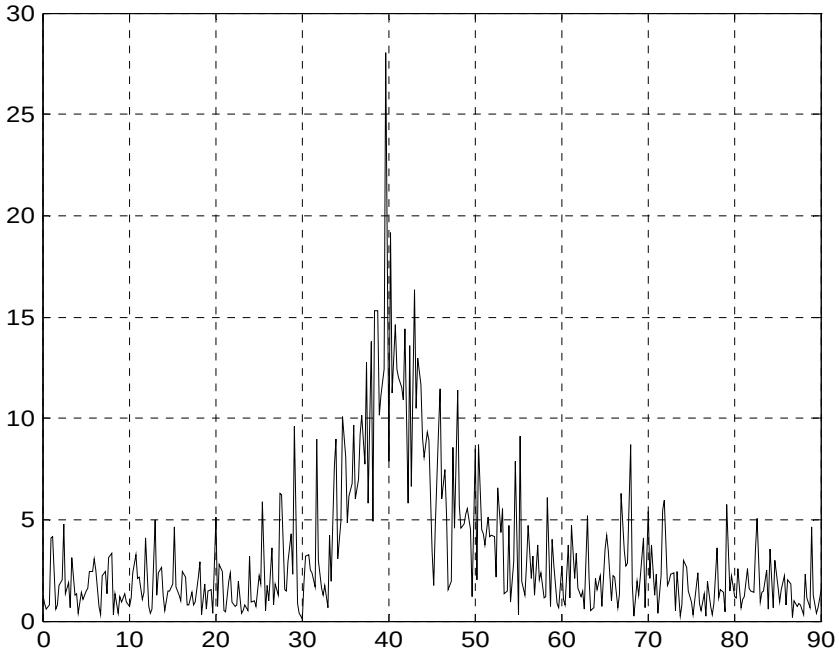


Fig. 3.2(h)

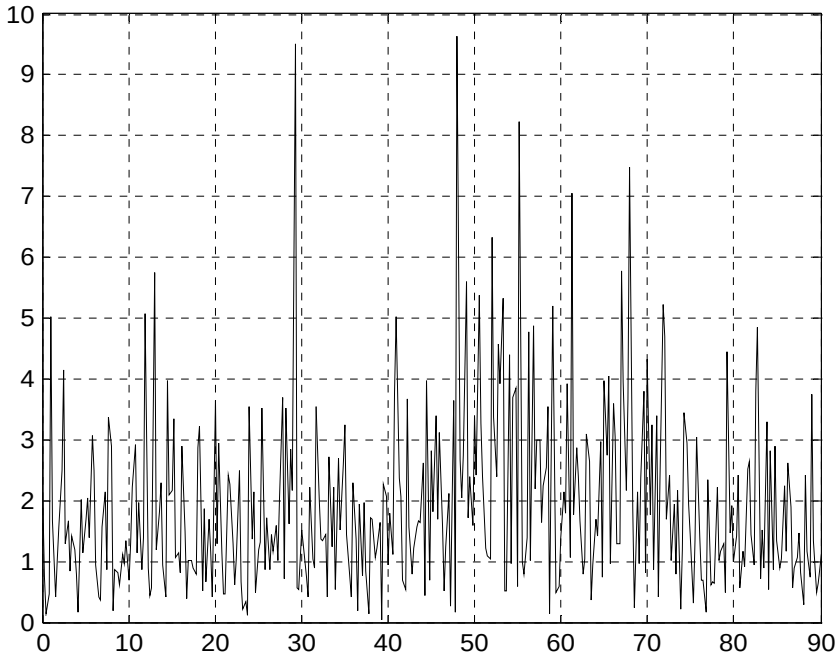


Fig. 3.2(i)

Figure 3.2: Various CGLRs for multi-target environment. (a) first process, (b) second process, (c) update the information of the first observed target after the second process, (d) update the information of the second observed target after the second process, (e) third process, (f) update the information of the second observed target after the third process, (g) update the information of the first observed target after the third process, (h) update the information of the third observed target after the third process, (i) the fourth process.

Since the transmitted signal is UWB random noise, the value of CGLR is also random. We can observe three primary lobes of different sizes around the targets directions in Figure 3.2(a) and no noticeable lobe in the direction of powerful jammer. Therefore, the jammer will not be misrecognized as a target. Moreover, it is obvious that the rough lobe width of the target located at $20^{\circ}$ is much smaller than the width of others. In order to explain this feature, we discuss the delay time difference of the first delay tap outputs in receiver antennas first. Taking

one scatterer illuminated by one transmit antenna as an example, the delay time difference between two successive receiver antenna first tap delay outputs is $\left(d_r(\sin\theta_{pre}-\sin\theta)/c\right)$, where $\theta_{pre}=\theta+\Delta\theta$. For a certain $\Delta\theta$, larger the $\theta$, smaller the difference between $\sin\theta_{pre}$ and $\sin\theta$. Since the signals in different first delay taps are similar, the reflections from $\theta$ is likely leaking out the filter even when $\theta_{pre}=\theta+\Delta\theta$. This leakage causes notable CGLR. Therefore, for a larger $\theta$, its lobe width is also larger.

Then, in Figure 3.2(b), since the reflections from $\theta_1=20^\circ$ are deduced with their estimates, no obvious peak is located around $20^\circ$. This deduction operation also leads to the absence of peaks in Figures 3.2(c)- 3.2(h). Then, since three targets reflections are significantly eliminated, and no more target exists, no obvious peak appears in Figure 3.2(i). Another update will be implemented to finish the iterative algorithm. However, since these results are similar to Figures 3.2(f)-(h), they are not presented.

In Figure 3.3, we show the mean square error (MSE) of target direction estimation at different signal to noise power ratios (SNRs). We define SNR as $E\left[\left|S_p^r(t)\right|^2\right]\Big/\sigma_{z_m}^2$ where $E\left[\left|S_p^r(t)\right|^2\right]$ is the average power of the $p$-th target refection. Reflecting the fact that smaller the $\theta$, smaller the lobe width, the estimation accuracy for $\theta_1=20^\circ$ is much better than others. Using the same argument, the estimation results of $\theta_3=40^\circ$ are supposed to be more accurate than the results for $\theta_2=60^\circ$. However, since $\theta_3=40^\circ$ is more seriously interfered by the jammer, which is emitted from an angle of $45^\circ$, the estimates for $\theta_2=60^\circ$ slightly outperforms the results for $\theta_3=40^\circ$. The target directions are widely dispersed lead the beamforming being able to efficiently suppress their reflection. Therefore, the focused target reflections are not

seriously influenced by other reflections and the iterative procedures. Since the results of the iterative procedures are similar along the lines in Figure 3.3, they are not shown.

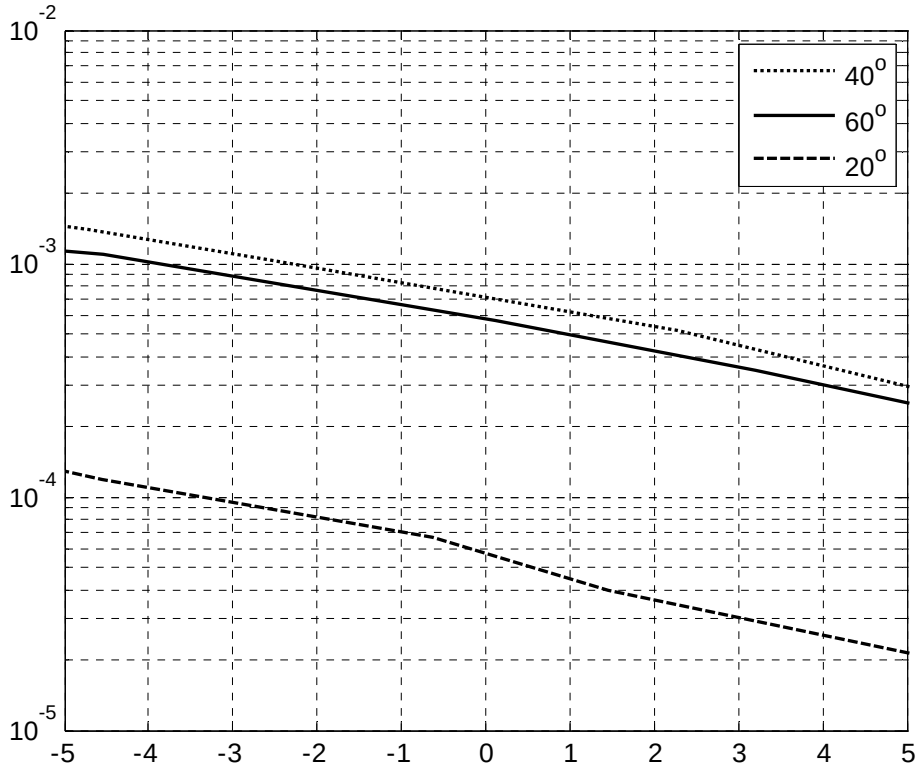


Figure 3.3: MSE of target direction estimation in different SNR.

Then, we assume $\theta_1 = 55^\circ$, $\theta_2 = 60^\circ$, and $\theta_3 = 50^\circ$, and the distances between the fifth transmitter antenna and the first, second, and third targets to be 3.1, 2.7, and 3.2 km, respectively. Then, $\phi_{n,p}$, $\forall n \in \{1,..,5\}, p \in \{1,2,3\}$ are determined. Other parameters are consistent with previous assumptions. The procedures are presented in Figure 3.4.

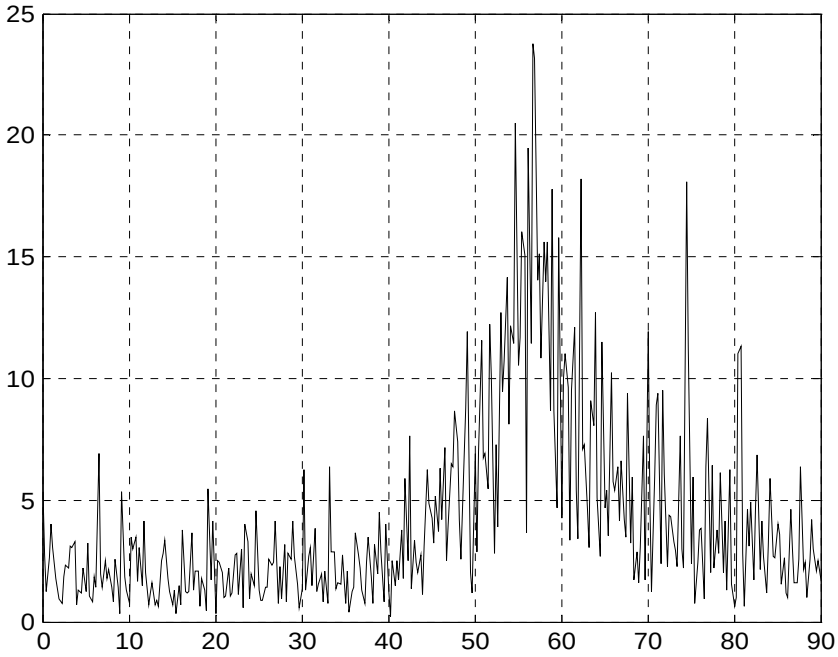


Fig. 3.4(a)

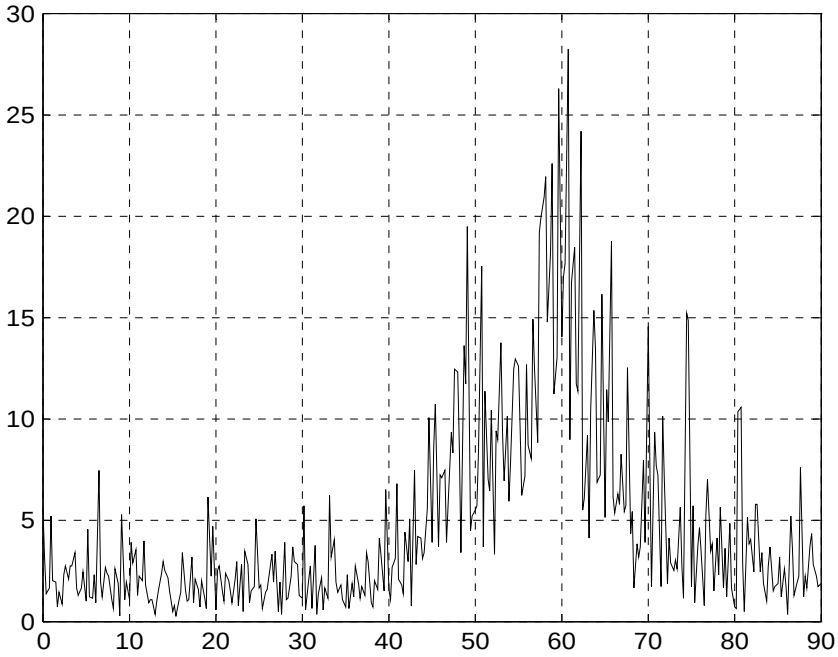


Fig. 3.4(b)

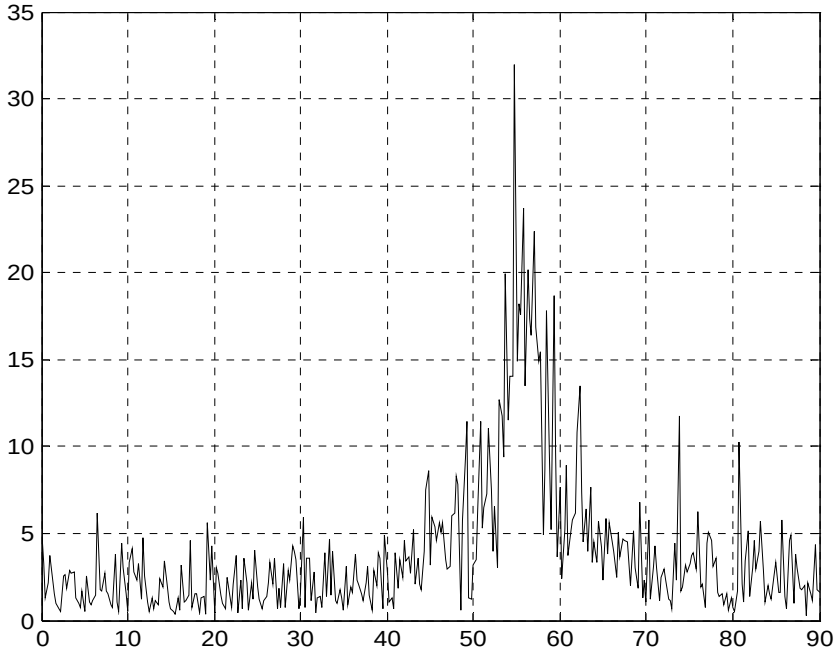


Fig. 3.4(c)

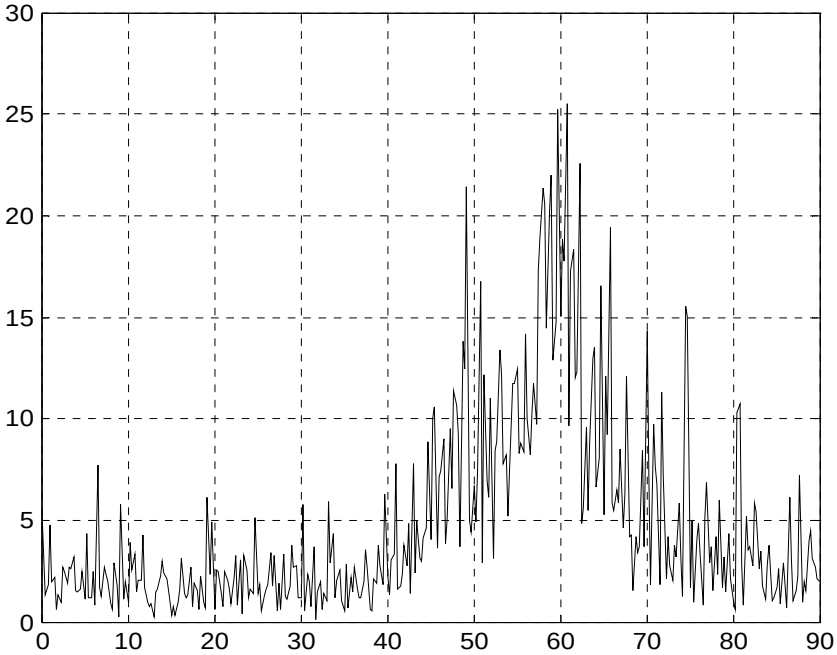


Fig. 3.4(d)

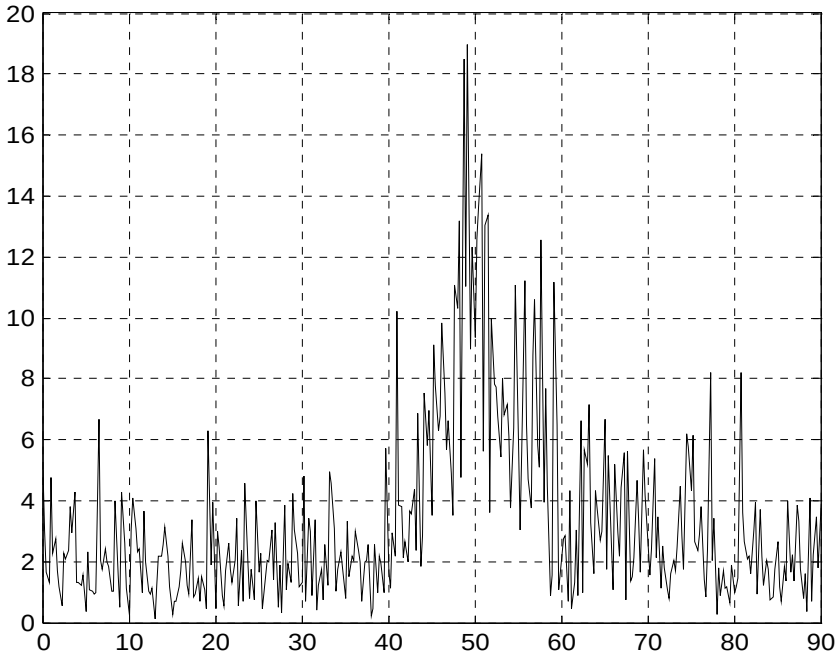


Fig. 3.4(e)

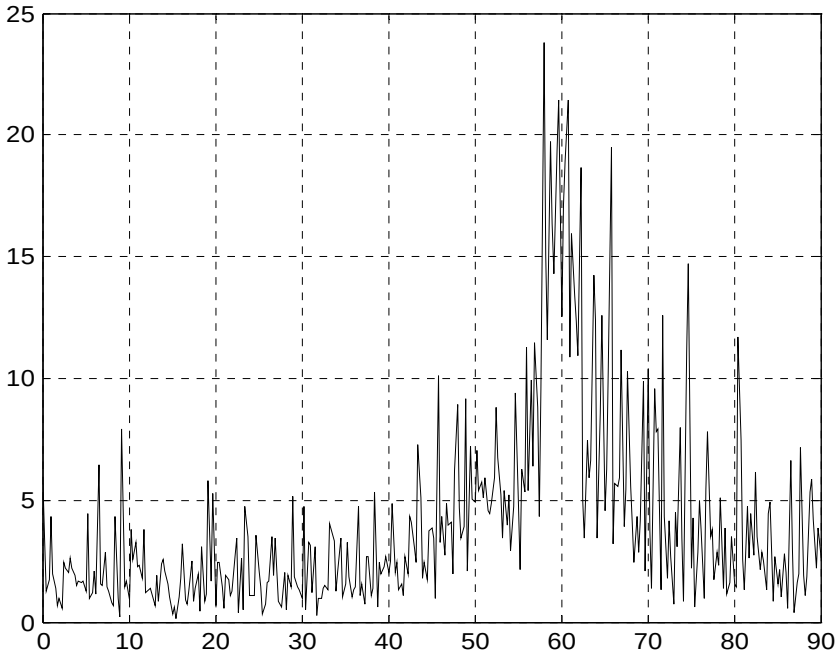


Fig. 3.4(f)

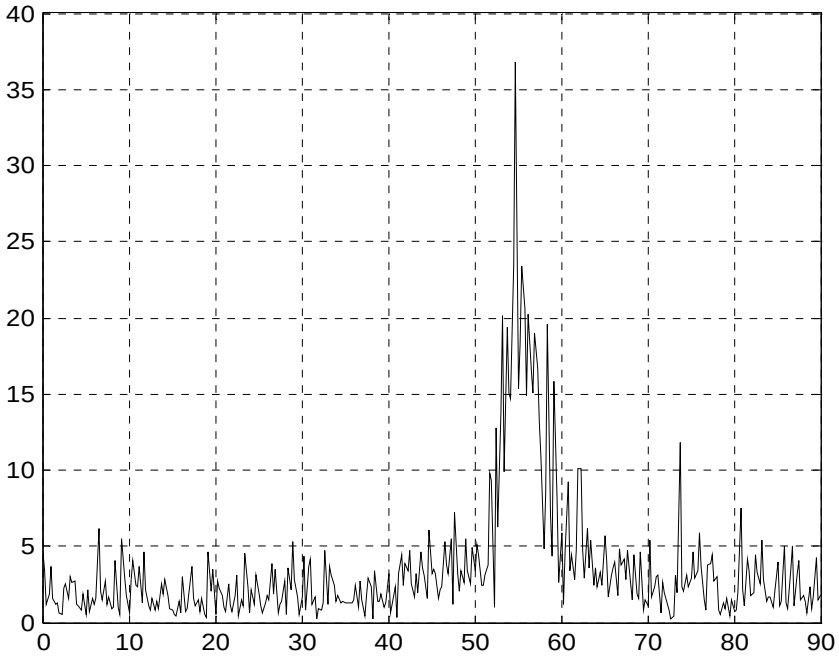


Fig. 3.4(g)

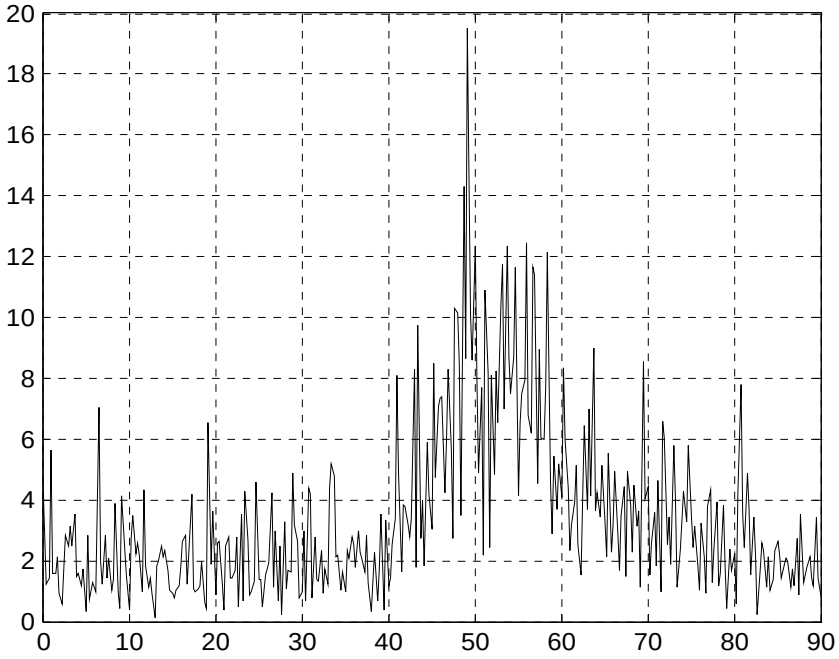


Fig. 3.4(h)

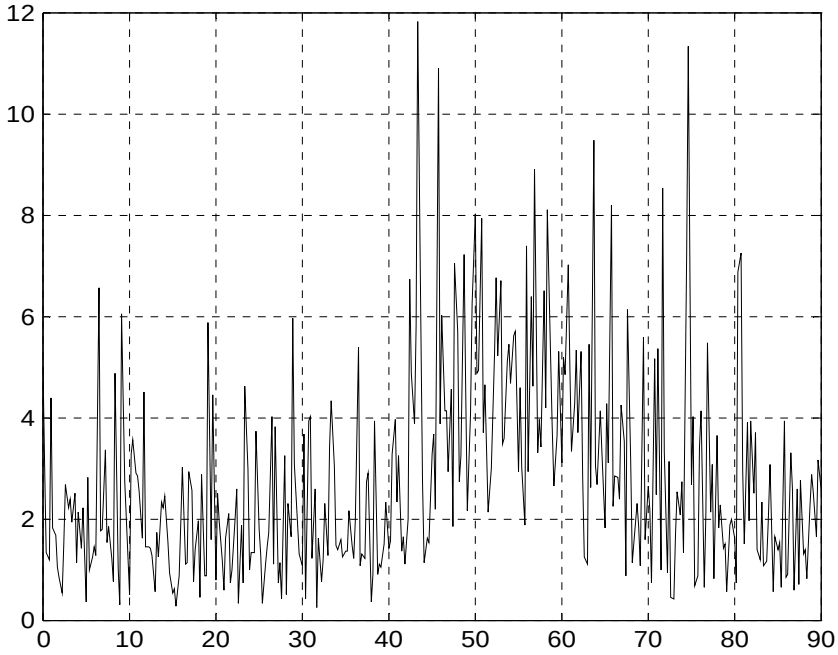


Fig. 3.4(i)

Figure 3.4: Various CGLRs for multi-target environment. (a) first process, (b) second process, (c) update the information of the first observed target after the second process, (d) update the information of the second observed target after the second process, (e) third process, (f) update the information of the second observed target after the third process, (g) update the information of the first observed target after the third process, (h) update the information of the third observed target after the third process, (i) fourth process.

Since the reflections of different targets interfere with each other, only one lobe is observed in Figure 3.4(a). Then, in Figure 3.4(b), the lobe of $\theta_2 = 60^\circ$ emerges, but the lobe for $\theta_3 = 50^\circ$ is not very obvious yet. After updating the parameters of targets $\theta_2 = 60^\circ$ and $\theta_1 = 55^\circ$ in Figure 3.4(c) and Figure 3.4(d) respectively, the lobe of target $\theta_3 = 50^\circ$ is obtained in Figure 3.4(e). Next, updating of target parameters is completed in Figures 3.4(f)-(h). In the fourth

iteration, since no additional target exists, no additional significant peak is observed in Figure 3.4(i).

In this example, $\theta_1 = 55^\circ$ is a target located half-way in angle between targets $\theta_2 = 60^\circ$ and $\theta_3 = 50^\circ$. Therefore, the improvements in target direction estimation accuracy during iterations are more obvious and are presented in Figure 3.5.

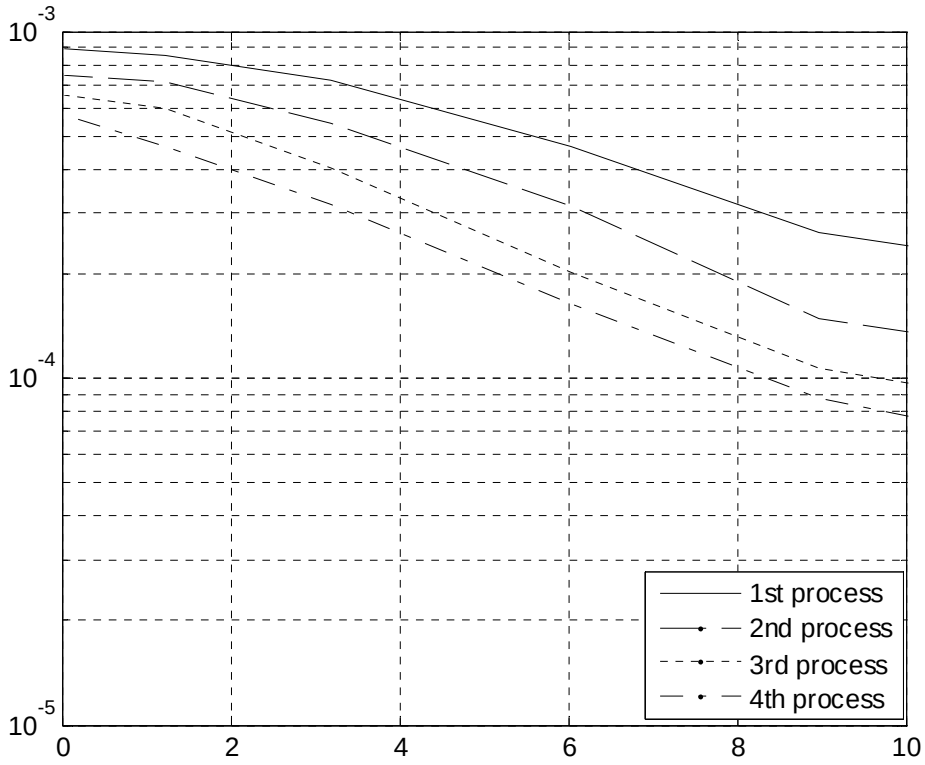


Figure 3.5: MSE of target direction estimation for $\theta_1 = 55^\circ$ in different SNR.

# Chapter 4

# Target velocity and location estimation

## 4.1. Problem formulation

Consider a UWB MIMO noise radar system equipped with $N$ and $M$ omni-directional antennas at the transmitter and receiver respectively that antennas do not need to linearly located and a moving target presented in Figure 4.1 whose velocity and location vectors are $\mathbf{v} = \left(v_x, v_y\right)$ and $\mathbf{x} = \left(x, y\right)$ respectively. Since the system is a little different from the previous one, we apply new notations to present the target directions relative to transmitter and receiver antennas. Furthermore, in Figure 4.1, although the angles $\theta_n^t$ and $\theta_m^r$ are defined with respect to the reference point $o$, they are also the angles to the target, since far field operation is assumed, which means that the distance between the target and reference point is much smaller than the distance between the target and transmit antennas or the distance between the target and receive antennas.

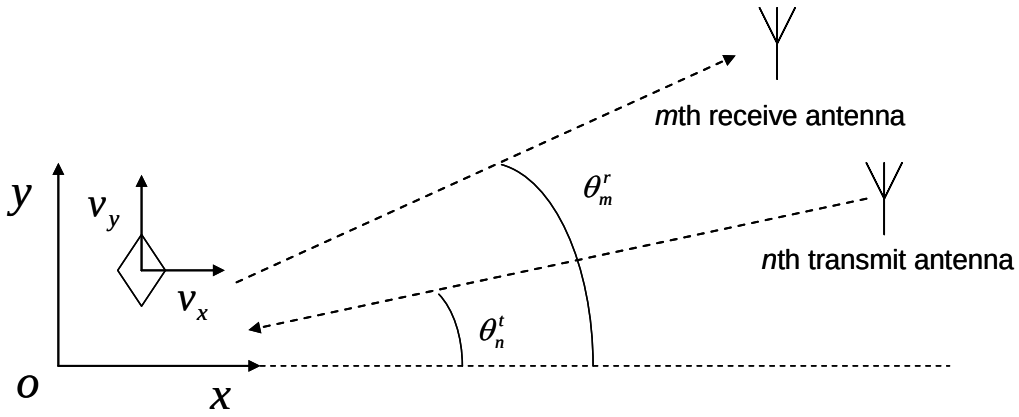


Figure 4.1: Target location and movement with respect to transmit and receive antennas.

Then, the signals received by the $m$-th receiver antenna included the reflections and noise can be expressed as

$$r_m(t) = \sum_{n=1}^{N} \alpha_{n,m} S_n\left(\beta_{n,m}(\mathbf{v})\left(t - \tau_{n,m}(\mathbf{x})\right)\right) + z_m(t) = \sum_{n=1}^{N} S_{n,m}^r(t) + z_m(t) \tag{4.1}$$

where the noise $z_m(t)$ is assumed to be ergodic, white, complex Gaussian with zero mean real and imaginary parts, equal variances $\sigma_z^2$, and independent of each other. Moreover, $\tau_{n,m}(\mathbf{x})$, $\beta_{n,m}(\mathbf{v})$, and $\alpha_{n,m}$ denote the delay time, Doppler stretch factor, and the amplitude factor for the $n$-th transmit and $m$-th receive antenna pair, respectively. The parameter $S_{n,m}^r(t)$ is introduced to simplify the notation for the reflection. Since both $v_x$ and $v_y$ are much smaller than the speed of light, $c$, the functions of $\tau_{n,m}(\mathbf{x})$, and $\beta_{n,m}(\mathbf{v})$ can be approximated, respectively, as

$$\tau_{n,m}(\mathbf{x}) \approx \frac{R_{n,m}}{c} - \frac{x}{c}\left(\cos\theta_n^t + \cos\theta_m^r\right) - \frac{y}{c}\left(\sin\theta_n^t + \sin\theta_m^r\right) \tag{4.2}$$

$$\beta_{n,m}(\mathbf{v}) \approx 1 + \frac{v_x}{c}\left(\cos\theta_n^t + \cos\theta_m^r\right) + \frac{v_y}{c}\left(\sin\theta_n^t + \sin\theta_m^r\right) \tag{4.3}$$

where $R_{n,m}$ is the distance of the propagation path starting from the $n$-th transmit antenna, though the reference point, and ending in the $m$-th receive antenna.

In the following discussion, concise notations $\tau_{n,m}$ and $\beta_{n,m}$ are applied to respectively represent $\tau_{n,m}(\mathbf{x})$ and $\beta_{n,m}(\mathbf{v})$. Also, $\alpha_{n,m} = \alpha_{R,n,m} + j\alpha_{I,n,m}$ is a complex constant in the observed duration $T_o$ and accounts for the target reflectivity and path attenuation. Moreover, the scale factor, $\beta_{n,m}^{1/2}$ is included in $\alpha_{n,m}$ in order to satisfy energy conservation, i.e. $\int_{T_o}\left|\beta_{n,m}^{1/2} S_n\left(\beta_{n,m}\left(t - \tau_{n,m}\right)\right)\right|^2 dt = \int_{T_o}\left|S_n(t)\right|^2 dt$.

If $T_o B \ll c \Big/ \left[ v_x \left( \cos\theta_n^t + \cos\theta_m^r \right) + v_y \left( \sin\theta_n^t + \sin\theta_m^r \right) \right]$, it means in the observed duration $T_o$, the change in amplitude resulting from the Doppler stretch factor is not comparable with the phase change. Therefore, the reflected signal can be closely approximated as

$$S_{n,m}^r(t) \approx \alpha_{n,m} s_n \left( t - \tau_{n,m} \right) e^{-j2\pi f_c \beta_{n,m}(\mathbf{v})\left(t - \tau_{n,m}(\mathbf{x})\right)} \tag{4.4}$$

which is a typical signal model under the narrowband assumption. However, since a UWB signal is being considered, implying that $B$ is larger than 500 MHz or the ratio $B/f_c > 0.25$, and the target could move rapidly, the narrowband condition is possibly violated, in which case equation 4.1 is the more suitable expression for further discussion.

The maximum likelihood (ML) approach can be utilized to estimate $\beta_{n,m}$, and $\tau_{n,m}$. However, in general, the value of $\alpha_{n,m}$ is unknown. Therefore, the ML estimator is too difficult to realize. A more practical approach to jointly estimate time delay and Doppler stretch is the application of wide-band ambiguity function [39]. For a single input and single output system, say the $n$-th transmit and the $m$-th receive antennas, because of the independence between $z_m(t)$ and $S_n(t)$, the Doppler stretch and delay time estimation can be formulated as a peak location problem,

$$\left[ \hat{\beta}_{n,m}, \hat{\tau}_{n,m} \right] = \arg \left\{ \max_{\tilde{\beta}_{n,m}, \tilde{\tau}_{n,m}} \left| \int_{T_o} \left( S_{n,m}^r(t) + z_m(t) \right) S_n^* \left( \tilde{\beta}_{n,m} \left( t - \tilde{\tau}_{n,m} \right) \right) \right|^2 \right\} \tag{4.5}$$

where * denotes the conjugate operation. In equation 4.5, $\tilde{\beta}_{n,m}$ and $\tilde{\tau}_{n,m}$ are the Doppler stretch and delay time parameters corresponding to the reference signal. For a MIMO radar system, two well known ambiguity functions, CAF and NCAF are respectively defined as $\left| \sum_{m=1}^{M} \sum_{n=1}^{N} \int_{T_o} S_n \left( \beta_{n,m} \left( t - \tau_{n,m} \right) \right) S_n^* \left( \tilde{\beta}_{n,m} \left( t - \tilde{\tau}_{n,m} \right) \right) dt \right|^2$ and

$\left(\sum_{m=1}^{M}\sum_{n=1}^{N}\left|\int_{T_o} S_n\left(\beta_{n,m}\left(t-\tau_{n,m}\right)\right)S_n^*\left(\widetilde{\beta}_{n,m}\left(t-\tilde{\tau}_{n,m}\right)\right)dt\right|\right)^2$ in [19]. Moreover, both ambiguity functions will achieve their maximum when $\boldsymbol{\beta}=\tilde{\boldsymbol{\beta}}$ and $\boldsymbol{\tau}=\tilde{\boldsymbol{\tau}}$, where the elements in vector $\boldsymbol{\beta}$, $\tilde{\boldsymbol{\beta}}$, $\boldsymbol{\tau}$, $\tilde{\boldsymbol{\tau}}$ are $\left[\beta_{1,1},\beta_{1,2},...,\beta_{1,M},...,\beta_{n,m},...,\beta_{N,M}\right]$, $\left[\tilde{\beta}_{1,1},...,\tilde{\beta}_{n,m},...,\tilde{\beta}_{N,M}\right]$, $\left[\tau_{1,1},...,\tau_{n,m},...,\tau_{N,M}\right]$, and $\left[\tilde{\tau}_{1,1},...,\tilde{\tau}_{n,m},...,\tilde{\tau}_{N,M}\right]$, respectively. Since the transmit signals are orthogonal to each other, applying ambiguity functions to estimate the Doppler stretch and delay time in MIMO radar system can also be formulated as a peak localization problem,

$$\left[\hat{\boldsymbol{\beta}},\hat{\boldsymbol{\tau}}\right]=\arg\left\{\max_{\tilde{\boldsymbol{\beta}},\tilde{\boldsymbol{\tau}}}\left\{\left|\sum_{m=1}^{M}\sum_{n=1}^{N}\int_{T_o} r_m(t)S_n^*\left(\widetilde{\beta}_{n,m}\left(t-\tilde{\tau}_{n,m}\right)\right)dt\right|^2\right\}\right\} \tag{4.6a}$$

$$\left[\hat{\boldsymbol{\beta}}_{nc},\hat{\boldsymbol{\tau}}_{nc}\right]=\arg\left\{\max_{\tilde{\boldsymbol{\beta}},\tilde{\boldsymbol{\tau}}}\left\{\left(\sum_{m=1}^{M}\sum_{n=1}^{N}\left|\int_{T_o} r_m(t)S_n^*\left(\widetilde{\beta}_{n,m}\left(t-\tilde{\tau}_{n,m}\right)\right)dt\right|\right)^2\right\}\right\} \tag{4.6b}$$

The integrations within the double sums in 4.6 can be discretized using $\sum_{\ell=1}^{L} r_m\left[\ell t_s\right]S_n^*\left[\widetilde{\beta}_{n,m}\left(\ell t_s-\tilde{\tau}_{n,m}\right)\right]t_s$, where $t_s$ is the sample duration and $L$ is the nearest integer less than or equal to $T_o/t_s$. Succinct notations, $A\left(\tilde{\mathbf{v}},\tilde{\mathbf{x}}\right)$ and $A_{nc}\left(\tilde{\mathbf{v}},\tilde{\mathbf{x}}\right)$, where $\tilde{\mathbf{v}}$, velocity and $\tilde{\mathbf{x}}$, location vectors are the core parameters of $\tilde{\boldsymbol{\beta}}$, and $\tilde{\boldsymbol{\tau}}$ in the reference signals which are applied to represent CAF and NCAF results respectively. Therefore, 4.6 can be simplified as

$$\left[\hat{\mathbf{v}},\hat{\mathbf{x}}\right]=\arg\left\{\max_{\tilde{\mathbf{v}},\tilde{\mathbf{x}}}\left\{A\left(\tilde{\mathbf{v}},\tilde{\mathbf{x}}\right)\right\}\right\}=\arg\left\{\max_{\tilde{\mathbf{v}},\tilde{\mathbf{x}}}\left\{A^{1/2}\left(\tilde{\mathbf{v}},\tilde{\mathbf{x}}\right)\right\}\right\} \tag{4.7a}$$

$$\left[\hat{\mathbf{v}}_{nc},\hat{\mathbf{x}}_{nc}\right]=\arg\left\{\max_{\tilde{\mathbf{v}},\tilde{\mathbf{x}}}\left\{A_{nc}\left(\tilde{\mathbf{v}},\tilde{\mathbf{x}}\right)\right\}\right\}=\arg\left\{\max_{\tilde{\mathbf{v}},\tilde{\mathbf{x}}}\left\{A_{nc}^{1/2}\left(\tilde{\mathbf{v}},\tilde{\mathbf{x}}\right)\right\}\right\} \tag{4.7b}$$

Since $A(\tilde{\mathbf{v}},\tilde{\mathbf{x}})$ is the square of a positive real number, $A(\hat{\mathbf{v}},\hat{\mathbf{x}})$ is the peak of all $A(\tilde{\mathbf{v}},\tilde{\mathbf{x}})$ if and only if $A^{1/2}(\hat{\mathbf{v}},\hat{\mathbf{x}})$ is the peak of all $A^{1/2}(\tilde{\mathbf{v}},\tilde{\mathbf{x}})$. Therefore, the second equality holds in 4.7a. Based on the similar reasoning, we collect the second equality in 4.7b.

In order to bound the number of the combinations of $[\tilde{\mathbf{v}},\tilde{\mathbf{x}}]$, setting spans for and quantizing them are necessary. Assume the spans for $\tilde{v}_x$, $\tilde{v}_y$, $\tilde{x}$, and $\tilde{y}$ are $[\tilde{v}_{x,1},\tilde{v}_{x,U}]$, $[\tilde{v}_{y,1},\tilde{v}_{y,H}]$, $[\tilde{x}_1,\tilde{x}_{\mathrm{U}}]$, and $[\tilde{y}_1,\tilde{y}_{\mathrm{H}}]$, and the corresponding step sizes are denoted as $\Delta\tilde{v}_x$, $\Delta\tilde{v}_y$, $\Delta\tilde{x}$, and $\Delta\tilde{y}$, respectively. Then, the sets for the elements can be defined as $\tilde{v}_x \in \{\tilde{v}_{x,1},\tilde{v}_{x,2},...,\tilde{v}_{x,u},...,\tilde{v}_{x,U}\}$, $\tilde{v}_y \in \{\tilde{v}_{y,1},...,\tilde{v}_{y,h},...,\tilde{v}_{y,H}\}$, $\tilde{x} \in \{\tilde{x}_1,...,\tilde{x}_{\mathrm{u}},...,\tilde{x}_{\mathrm{U}}\}$, and $\tilde{y} \in \{\tilde{y}_1,...,\tilde{y}_{\mathrm{h}},...,\tilde{y}_{\mathrm{H}}\}$, where the difference between two successive elements is equal to the step size. When $\tilde{\mathbf{v}} = (\tilde{v}_{x,u},\tilde{v}_{y,h})$ and $\tilde{\mathbf{x}} = (\tilde{x}_{\mathrm{u}},\tilde{y}_{\mathrm{h}})$, CAF and NCAF results are denoted as $A^{1/2}(\tilde{\mathbf{v}}_{u,h},\tilde{\mathbf{x}}_{\mathrm{u,h}})$ and $A_{nc}^{1/2}(\tilde{\mathbf{v}}_{u,h},\tilde{\mathbf{x}}_{\mathrm{u,h}})$ to clearly represent the concerned parameters in reference signals.

In this dissertation, we aim to analyze and compare the estimation MSE resulted from CAF and NCAF approaches. We start from collecting the information about the joint pdf of the random vectors $\mathbf{A} := \{A^{1/2}(\tilde{\mathbf{v}}_{1,1},\tilde{\mathbf{x}}_{1,1}),...,A^{1/2}(\tilde{\mathbf{v}}_{U,H},\tilde{\mathbf{x}}_{\mathrm{U,H}})\}$, and $\mathbf{ncA} := \{A_{nc}^{1/2}(\tilde{\mathbf{v}}_{1,1},\tilde{\mathbf{x}}_{1,1}),...,A_{nc}^{1/2}(\tilde{\mathbf{v}}_{U,H},\tilde{\mathbf{x}}_{\mathrm{U,H}})\}$. Then, we solve the probability of $A^{1/2}(\hat{\mathbf{v}},\hat{\mathbf{x}}) = A^{1/2}(\tilde{\mathbf{v}}_{u,h},\tilde{\mathbf{x}}_{\mathrm{u,h}})$ and of $A_{nc}^{1/2}(\hat{\mathbf{v}},\hat{\mathbf{x}}) = A_{nc}^{1/2}(\tilde{\mathbf{v}}_{u,h},\tilde{\mathbf{x}}_{\mathrm{u,h}})$ for every $u$, $h$, u, and h to complete the MSE calculation.

## 4.2. PDFs of $A^{1/2}\left(\tilde{\mathbf{v}}_{u,h},\tilde{\mathbf{x}}_{\mathrm{u,h}}\right)$ and $A_{nc}^{1/2}\left(\tilde{\mathbf{v}}_{u,h},\tilde{\mathbf{x}}_{\mathrm{u,h}}\right)$

### 4.2.1 PDFs of correlator outputs

Since $A^{1/2}\left(\tilde{\mathbf{v}}_{u,h},\tilde{\mathbf{x}}_{\mathrm{u,h}}\right)$ is the absolute value of the summation of the correlator results, and $A_{nc}^{1/2}\left(\tilde{\mathbf{v}}_{u,h},\tilde{\mathbf{x}}_{\mathrm{u,h}}\right)$ is the summation of the absolute value of the correlator results, our discussions start from the pdf of correlator results.

The $\ell$-th sample of received signal in the $m$-th receiver antenna, $r_m\left[\ell t_s\right]$ can be separated into two parts as shown in 4.8. The first term represents the reflection of the $n$-th transmit signal which is potentially correlated with the $n$-th reference signal. The second term represents the summation of other reflections and thermal noise, denoted as $w_{n,m}\left[\ell t_s\right]$, is independent of the $n$-th reference signal.

$$r_m\left[\ell t_s\right]=S_{n,m}^{r}\left[\ell t_s\right]+\sum_{\substack{\tilde{n}=1\\ \tilde{n}\neq n}}^{N}S_{\tilde{n},m}^{r}\left[\ell t_s\right]+z_m\left[\ell t_s\right]=S_{n,m}^{r}\left[\ell t_s\right]+w_{n,m}\left[\ell t_s\right] \tag{4.8}$$

The real and imaginary part of the product, $r_m\left[\ell t_s\right]S_n^{*}\left[\widetilde{\beta}_{n,m}\left(\ell t_s-\tilde{\tau}_{n,m}\right)\right]$ are represented as $\chi_{R,n,m,\ell,\tilde{\mathbf{v}},\tilde{\mathbf{x}}}^{[u,h,\mathrm{u,h}]}$, and $\chi_{I,n,m,\ell,\tilde{\mathbf{v}},\tilde{\mathbf{x}}}^{[u,h,\mathrm{u,h}]}$ respectively, where the velocity and location vectors, $\tilde{\mathbf{v}}_{u,h}$ and $\tilde{\mathbf{x}}_{\mathrm{u,h}}$ corresponding to the $\widetilde{\beta}_{n,m}$, and $\tilde{\tau}_{n,m}$, are also attached to the index. Then, the correlator outputs in the $m$-th receiver antenna with the $n$-th reference signal can be represented as the product of $t_s$ and the complex product $\overline{\chi}_{C,n,m,\tilde{\mathbf{v}},\tilde{\mathbf{x}}}^{[u,h,\mathrm{u,h}]}$, given by

$$\begin{aligned}\overline{\chi}_{C,n,m,\tilde{\mathbf{v}},\tilde{\mathbf{x}}}^{[u,h,\mathrm{u,h}]}&=\overline{\chi}_{R,n,m,\tilde{\mathbf{v}},\tilde{\mathbf{x}}}^{[u,h,\mathrm{u,h}]}+j\overline{\chi}_{I,n,m,\tilde{\mathbf{v}},\tilde{\mathbf{x}}}^{[u,h,\mathrm{u,h}]}=\sum_{\ell=1}^{K}\chi_{R,n,m,\ell,\tilde{\mathbf{v}},\tilde{\mathbf{x}}}^{[u,h,\mathrm{u,h}]}+j\chi_{I,n,m,\ell,\tilde{\mathbf{v}},\tilde{\mathbf{x}}}^{[u,h,\mathrm{u,h}]}\\&=\sum_{\ell=1}^{L}r_m\left[\ell t_s\right]S_n^{*}\left[\widetilde{\beta}_{n,m}\left(\ell t_s-\tilde{\tau}_{n,m}\right)\right]\end{aligned} \tag{4.9}$$

Moreover,

$$\begin{aligned}\chi_{R,n,m,\ell,\tilde{\mathbf{v}},\tilde{\mathbf{x}}}^{[u,h,\mathrm{u},\mathrm{h}]} &= \alpha_{R,n,m} s_n\left[\beta_{n,m}\left(\ell t_s-\tau_{n,m}\right)\right] s_n\left[\tilde{\beta}_{n,m}\left(\ell t_s-\tilde{\tau}_{n,m}\right)\right]\cos\left(2\pi f_c D_{\ell,n,m,\tilde{\mathbf{v}},\tilde{\mathbf{x}}}^{[u,h,\mathrm{u},\mathrm{h}]}\right)\\ &+\alpha_{I,n,m} s_n\left[\beta_{n,m}\left(\ell t_s-\tau_{n,m}\right)\right] s_n\left[\tilde{\beta}_{n,m}\left(\ell t_s-\tilde{\tau}_{n,m}\right)\right]\sin\left(2\pi f_c D_{\ell,n,m,\tilde{\mathbf{v}},\tilde{\mathbf{x}}}^{[u,h,\mathrm{u},\mathrm{h}]}\right)\\ &+w_{R,n,m}\left[\ell t_s\right] s_n\left[\tilde{\beta}_{n,m}\left(\ell T_s-\tilde{\tau}_{n,m}\right)\right]\cos\left(2\pi f_c\left(\tilde{\beta}_{n,m}\left(\ell t_s-\tilde{\tau}_{n,m}\right)\right)\right)\\ &-w_{I,n,m}\left[\ell T_s\right] s_n\left[\tilde{\beta}_{n,m}\left(\ell T_s-\tilde{\tau}_{n,m}\right)\right]\sin\left(2\pi f_c\left(\tilde{\beta}_{n,m}\left(\ell t_s-\tilde{\tau}_{n,m}\right)\right)\right)\end{aligned} \quad 4.10$$

where $D_{\ell,n,m,\tilde{\mathbf{v}},\tilde{\mathbf{x}}}^{[u,h,\mathrm{u},\mathrm{h}]}=\beta_{n,m}\left(\ell t_s-\tau_{n,m}\right)-\tilde{\beta}_{n,m}\left(\ell t_s-\tilde{\tau}_{n,m}\right)$, and $w_{R,n,m}\left[\ell t_s\right]$ and $w_{I,n,m}\left[\ell T_s\right]$ are the real and imaginary parts of $w_{n,m}\left[\ell t_s\right]$, respectively.

Since the transmit signals are band-limited noise, $\chi_{R,n,m,\ell,\tilde{\mathbf{v}},\tilde{\mathbf{x}}}^{[u,h,\mathrm{u},\mathrm{h}]}$ and $\chi_{R,n,m,\ell+1,\tilde{\mathbf{v}},\tilde{\mathbf{x}}}^{[u,h,\mathrm{u},\mathrm{h}]}$ are independent as long as the sample duration $t_s$ is sufficient large. However, their pdfs are not identical because the correlation between $s_n\left[\beta_{n,m}\left(\ell t_s-\tau_{n,m}\right)\right]$ and $s_n\left[\tilde{\beta}_{n,m}\left(\ell t_s-\tilde{\tau}_{n,m}\right)\right]$ depends on $\ell$. Therefore, it is not appropriate to apply the classical central limit theorem (CLT). However, a relaxed one, the Lyapunov CLT can be applied. In Lyapunov's CLT, several criteria are required to be satisfied before approximating $\chi_{R,n,m,\tilde{\mathbf{v}},\tilde{\mathbf{x}}}^{[u,h,\mathrm{u},\mathrm{h}]}$ to a normal random variable [44].

In 4.11, we define the expected value of $\chi_{R,n,m,\ell,\tilde{\mathbf{v}},\tilde{\mathbf{x}}}^{[u,h,\mathrm{u},\mathrm{h}]}$, $\mu_{R,n,m,\ell,\tilde{\mathbf{v}},\tilde{\mathbf{x}}}^{[u,h,\mathrm{u},\mathrm{h}]}$ which is finite.

$$\mu_{R,n,m,\ell,\tilde{\mathbf{v}},\tilde{\mathbf{x}}}^{[u,h,\mathrm{u},\mathrm{h}]}=\left(\alpha_{R,n,m}\cos\left(2\pi f_c D_{\ell,n,m,\tilde{\mathbf{v}},\tilde{\mathbf{x}}}^{[u,h,\mathrm{u},\mathrm{h}]}\right)+\alpha_{I,n,m}\sin\left(2\pi f_c D_{\ell,n,m,\tilde{\mathbf{v}},\tilde{\mathbf{x}}}^{[u,h,\mathrm{u},\mathrm{h}]}\right)\right)\sigma_s^2\mathrm{sinc}\left(B\times D_{\ell,n,m,\tilde{\mathbf{v}},\tilde{\mathbf{x}}}^{[u,h,\mathrm{u},\mathrm{h}]}\right) \quad 4.11$$

Secondly, finite $\left(\sigma_{R,n,m,\ell,\tilde{\mathbf{v}},\tilde{\mathbf{x}}}^{[u,h,\mathrm{u},\mathrm{h}]}\right)^2$, defined as the variance of $\chi_{R,n,m,\ell,\tilde{\mathbf{v}},\tilde{\mathbf{x}}}^{[u,h,\mathrm{u},\mathrm{h}]}$ is required, which can be expressed as

$$\left(\sigma_{R,n,m,\ell,\tilde{\mathbf{v}},\tilde{\mathbf{x}}}^{[u,h,\mathrm{u},\mathrm{h}]}\right)^2 = \sigma_s^4 \mathrm{sinc}^2\left(B \times D_{\ell,n,m,\tilde{\mathbf{v}},\tilde{\mathbf{x}}}^{[u,h,\mathrm{u},\mathrm{h}]}\right)\left(\alpha_{R,n,m}\cos\left(2\pi f_c D_{\ell,n,m,\tilde{\mathbf{v}},\tilde{\mathbf{x}}}^{[u,h,\mathrm{u},\mathrm{h}]}\right) + \alpha_{I,n,m}\sin\left(2\pi f_c D_{\ell,n,m,\tilde{\mathbf{v}},\tilde{\mathbf{x}}}^{[u,h,\mathrm{u},\mathrm{h}]}\right)\right)^2$$
$$+\sigma_s^4 \sum_{\tilde{n}=1}^{N}\left(\alpha_{R,\tilde{n},m}\cos\left(2\pi f_c D_{\ell,\tilde{n},m,\tilde{\mathbf{v}},\tilde{\mathbf{x}}}^{[u,h,\mathrm{u},\mathrm{h}]}\right) + \alpha_{I,\tilde{n},m}\sin\left(2\pi f_c D_{\ell,\tilde{n},m,\tilde{\mathbf{v}},\tilde{\mathbf{x}}}^{[u,h,\mathrm{u},\mathrm{h}]}\right)\right)^2 + \sigma_z^2\sigma_s^2$$

4.12

where $D_{\ell,\tilde{n},m,\tilde{\mathbf{v}},\tilde{\mathbf{x}}}^{[u,h,\mathrm{u},\mathrm{h}]} = \beta_{\tilde{n},m}\left(\ell t_s - \tau_{\tilde{n},m}\right) - \tilde{\beta}_{n,m}\left(\ell t_s - \tilde{\tau}_{n,m}\right)$. It is clear that $\left(\sigma_{R,n,m,\ell,\tilde{\mathbf{v}},\tilde{\mathbf{x}}}^{[u,h,\mathrm{u},\mathrm{h}]}\right)^2$ is indeed finite.

Thirdly, $\lim_{L\to\infty}\frac{1}{\eta_L^4}\sum_{\ell=1}^{L} E\left[\left|\chi_{R,n,m,\ell,\tilde{\mathbf{v}},\tilde{\mathbf{x}}}^{[u,h,\mathrm{u},\mathrm{h}]} - \mu_{R,n,m,\ell,\tilde{\mathbf{v}},\tilde{\mathbf{x}}}^{[u,h,\mathrm{u},\mathrm{h}]}\right|^4\right] = 0$, where $\eta_L^2 = \sum_{\ell=1}^{L}\left(\sigma_{R,n,m,\ell,\tilde{\mathbf{v}},\tilde{\mathbf{x}}}^{[u,h,\mathrm{u},\mathrm{h}]}\right)^2$, and the numerator is equal to the summation of the fourth central moments of $\chi_{R,n,m,\ell,\tilde{\mathbf{v}},\tilde{\mathbf{x}}}^{[u,h,\mathrm{u},\mathrm{h}]}$ for all $\ell$. According to the well defined higher moments of normal random variables in 4.10, the value of the fourth central moment is also finite for any $\ell$. Therefore, a positive constant, say $\lambda$, exists which is larger than or equal to $E\left[\left(\chi_{R,n,m,\ell,\tilde{\mathbf{v}},\tilde{\mathbf{x}}}^{[u,h,\mathrm{u},\mathrm{h}]} - \mu_{R,n,m,\ell,\tilde{\mathbf{v}},\tilde{\mathbf{x}}}^{[u,h,\mathrm{u},\mathrm{h}]}\right)^4\right]$ for any $\ell$. From 4.12, we note that the variance is always larger than $\sigma_z^2\sigma_s^2$. We can develop an inequality for the limit, i.e. $\lim_{K\to\infty}\frac{1}{\eta_L^4}\sum_{\ell=1}^{L} E\left[\left|\chi_{R,n,m,\ell,\tilde{\mathbf{v}},\tilde{\mathbf{x}}}^{[u,h,\mathrm{u},\mathrm{h}]} - \mu_{R,n,m,\ell,\tilde{\mathbf{v}},\tilde{\mathbf{x}}}^{[u,h,\mathrm{u},\mathrm{h}]}\right|^4\right] \le \lim_{L\to\infty}\frac{L\lambda}{L^2\sigma_z^4\sigma_s^4} = 0$, and conclude that this criterion is satisfied.

In summary, according to Lyapunov's CLT, $\bar{\chi}_{R,n,m,\tilde{\mathbf{v}},\tilde{\mathbf{x}}}^{[u,h,\mathrm{u},\mathrm{h}]} \sim N\left(\bar{\mu}_{R,n,m,\tilde{\mathbf{v}},\tilde{\mathbf{x}}}^{[u,h,\mathrm{u},\mathrm{h}]}, \left(\bar{\sigma}_{R,n,m,\tilde{\mathbf{v}},\tilde{\mathbf{x}}}^{[u,h,\mathrm{u},\mathrm{h}]}\right)^2\right)$ where $\bar{\mu}_{R,n,m,\tilde{\mathbf{v}},\tilde{\mathbf{x}}}^{[u,h,\mathrm{u},\mathrm{h}]} = \sum_{\ell=1}^{L}\mu_{R,n,m,\ell,\tilde{\mathbf{v}},\tilde{\mathbf{x}}}^{[u,h,\mathrm{u},\mathrm{h}]}$ and $\left(\bar{\sigma}_{R,n,m,\tilde{\mathbf{v}},\tilde{\mathbf{x}}}^{u,h,\mathrm{u},\mathrm{h}}\right)^2 = \sum_{\ell=1}^{L}\left(\sigma_{R,n,m,\ell,\tilde{\mathbf{v}},\tilde{\mathbf{x}}}^{[u,h,\mathrm{u},\mathrm{h}]}\right)^2$.

For $\bar{\chi}_{I,n,m,\tilde{\mathbf{v}},\tilde{\mathbf{x}}}^{[u,h,\mathrm{u},\mathrm{h}]}$, we can show that

$$\mu_{I,n,m,\ell,\tilde{\mathbf{v}},\tilde{\mathbf{x}}}^{[u,h,\mathrm{u},\mathrm{h}]} = \left(\alpha_{I,n,m}\cos\left(2\pi f_c D_{\ell,n,m,\tilde{\mathbf{v}},\tilde{\mathbf{x}}}^{[u,h,\mathrm{u},\mathrm{h}]}\right) - \alpha_{R,n,m}\sin\left(2\pi f_c D_{\ell,n,m,\tilde{\mathbf{v}},\tilde{\mathbf{x}}}^{[u,h,\mathrm{u},\mathrm{h}]}\right)\right)\sigma_s^2\mathrm{sinc}\left(B \times D_{\ell,n,m,\tilde{\mathbf{v}},\tilde{\mathbf{x}}}^{[u,h,\mathrm{u},\mathrm{h}]}\right)$$

4.13

$$\left(\sigma_{I,n,m,\ell,\tilde{\mathbf{v}},\tilde{\mathbf{x}}}^{[u,h,\mathrm{u},\mathrm{h}]}\right)^2 = \sigma_s^4 \mathrm{sinc}^2\left(B \times D_{\ell,n,m,\tilde{\mathbf{v}},\tilde{\mathbf{x}}}^{[u,h,\mathrm{u},\mathrm{h}]}\right)\left(\alpha_{I,n,m}\cos\left(2\pi f_c D_{\ell,n,m,\tilde{\mathbf{v}},\tilde{\mathbf{x}}}^{[u,h,\mathrm{u},\mathrm{h}]}\right) - \alpha_{R,n,m}\sin\left(2\pi f_c D_{\ell,n,m,\tilde{\mathbf{v}},\tilde{\mathbf{x}}}^{[u,h,\mathrm{u},\mathrm{h}]}\right)\right)^2$$
$$+\sigma_s^4 \sum_{\tilde{n}=1}^{N}\left(\alpha_{I,\tilde{n},m}\cos\left(2\pi f_c D_{\ell,\tilde{n},m,\tilde{\mathbf{v}},\tilde{\mathbf{x}}}^{[u,h,\mathrm{u},\mathrm{h}]}\right) - \alpha_{R,\tilde{n},m}\sin\left(2\pi f_c D_{\ell,\tilde{n},m,\tilde{\mathbf{v}},\tilde{\mathbf{x}}}^{[u,h,\mathrm{u},\mathrm{h}]}\right)\right)^2 + \sigma_z^2\sigma_s^2$$

4.14

Similarly, $\bar{\chi}_{I,n,m,\tilde{\mathbf{v}},\tilde{\mathbf{x}}}^{[u,h,\mathrm{u},\mathrm{h}]} \sim N\left(\bar{\mu}_{I,n,m,\tilde{\mathbf{v}},\tilde{\mathbf{x}}}^{[u,h,\mathrm{u},\mathrm{h}]}, \left(\bar{\sigma}_{I,n,m,\tilde{\mathbf{v}},\tilde{\mathbf{x}}}^{[u,h,\mathrm{u},\mathrm{h}]}\right)^2\right)$ where $\bar{\mu}_{I,n,m,\tilde{\mathbf{v}},\tilde{\mathbf{x}}}^{[u,h,\mathrm{u},\mathrm{h}]} = \sum_{\ell=1}^{L}\mu_{I,n,m,\ell,\tilde{\mathbf{v}},\tilde{\mathbf{x}}}^{[u,h,\mathrm{u},\mathrm{h}]}$ and $\left(\bar{\sigma}_{I,n,m,\tilde{\mathbf{v}},\tilde{\mathbf{x}}}^{[u,h,\mathrm{u},\mathrm{h}]}\right)^2 = \sum_{\ell=1}^{L}\left(\sigma_{I,n,m,\ell,\tilde{\mathbf{v}},\tilde{\mathbf{x}}}^{[u,h,\mathrm{u},\mathrm{h}]}\right)^2$ can be concluded.

Moreover, any linear combination of $\bar{\chi}_{R,n,m,\tilde{\mathbf{v}},\tilde{\mathbf{x}}}^{[u,h,\mathrm{u},\mathrm{h}]}$ and $\bar{\chi}_{I,n,m,\tilde{\mathbf{v}},\tilde{\mathbf{x}}}^{[u,h,\mathrm{u},\mathrm{h}]}$ is another normally distributed random variable according to Lyapunov's CLT. Therefore, we can conclude that $\bar{\chi}_{R,n,m,\tilde{\mathbf{v}},\tilde{\mathbf{x}}}^{[u,h,\mathrm{u},\mathrm{h}]}$ and $\bar{\chi}_{I,n,m,\tilde{\mathbf{v}},\tilde{\mathbf{x}}}^{[u,h,\mathrm{u},\mathrm{h}]}$ are bivariate normally distributed, and their correlation coefficient, $\rho_{n,m,\tilde{\mathbf{v}},\tilde{\mathbf{x}}}^{[u,h,\mathrm{u},\mathrm{h}]}$ is equal to

$$\rho_{n,m,\tilde{\mathbf{v}},\tilde{\mathbf{x}}}^{[u,h,\mathrm{u},\mathrm{h}]} = \frac{E\left[\bar{\chi}_{R.n,m,\tilde{\mathbf{v}},\tilde{\mathbf{x}}}^{[u,h,\mathrm{u},\mathrm{h}]}\bar{\chi}_{I,n,m,\tilde{\mathbf{v}},\tilde{\mathbf{x}}}^{[u,h,\mathrm{u},\mathrm{h}]}\right] - \bar{\mu}_{R.n,m,\tilde{\mathbf{v}},\tilde{\mathbf{x}}}^{u,h,\mathrm{u},\mathrm{h}}\bar{\mu}_{I,n,m,\tilde{\mathbf{v}},\tilde{\mathbf{x}}}^{[u,h,\mathrm{u},\mathrm{h}]}}{\bar{\sigma}_{R.n,m,\tilde{\mathbf{v}},\tilde{\mathbf{x}}}^{u,h,\mathrm{u},\mathrm{h}}\bar{\sigma}_{I,n,m,\tilde{\mathbf{v}},\tilde{\mathbf{x}}}^{[u,h,\mathrm{u},\mathrm{h}]}} \tag{4.15}$$

where

$$\begin{aligned}
&E\left[\bar{\chi}_{R,n,m,\tilde{\mathbf{v}},\tilde{\mathbf{x}}}^{[u,h,\mathrm{u},\mathrm{h}]}\bar{\chi}_{I,n,m,\tilde{\mathbf{v}},\tilde{\mathbf{x}}}^{[u,h,\mathrm{u},\mathrm{h}]}\right] \\
&= E\left[\sum_{\ell=1}^{L}\chi_{R,n,m,\ell,\tilde{\mathbf{v}},\tilde{\mathbf{x}}}^{[u,h,\mathrm{u},\mathrm{h}]}\sum_{\ell=1}^{L}\chi_{I,n,m,\ell,\tilde{\mathbf{v}},\tilde{\mathbf{x}}}^{[u,h,\mathrm{u},\mathrm{h}]}\right] \\
&= \sigma_s^4\sum_{\tilde{n}=1}^{N}\sum_{\ell=1}^{L}\left(\alpha_{R,\tilde{n},m}\alpha_{I,\tilde{n},m}\cos\left(4\pi f_c D_{\ell,\tilde{n},m,\tilde{\mathbf{v}},\tilde{\mathbf{x}}}^{[u,h,\mathrm{u},\mathrm{h}]}\right) + \frac{1}{2}\left(\alpha_{I,\tilde{n},m}^2 - \alpha_{R,\tilde{n},m}^2\right)\sin\left(4\pi f_c D_{\ell,\tilde{n},m,\tilde{\mathbf{v}},\tilde{\mathbf{x}}}^{[u,h,\mathrm{u},\mathrm{h}]}\right)\right) \\
&+\sum_{\ell=1}^{L}\mu_{R,n,m,\ell,\tilde{\mathbf{v}},\tilde{\mathbf{x}}}^{[u,h,\mathrm{u},\mathrm{h}]}\mu_{I,n,m,\ell,\tilde{\mathbf{v}},\tilde{\mathbf{x}}}^{[u,h,\mathrm{u},\mathrm{h}]} + \bar{\mu}_{R,n,m,\tilde{\mathbf{v}},\tilde{\mathbf{x}}}^{[u,h,\mathrm{u},\mathrm{h}]}\bar{\mu}_{I,n,m,\tilde{\mathbf{v}},\tilde{\mathbf{x}}}^{[u,h,\mathrm{u},\mathrm{h}]}
\end{aligned} \tag{4.16}$$

### 4.2.2 PDF approximations for $A^{1/2}\left(\tilde{\mathbf{v}}_{u,h},\tilde{\mathbf{x}}_{\mathrm{u,h}}\right)$ and $A_{nc}^{1/2}\left(\tilde{\mathbf{v}}_{u,h},\tilde{\mathbf{x}}_{\mathrm{u,h}}\right)$

In order to solve for the pdf of $A^{1/2}\left(\tilde{\mathbf{v}}_{u,h},\tilde{\mathbf{x}}_{\mathrm{u,h}}\right)$ and of $A_{nc}^{1/2}\left(\tilde{\mathbf{v}}_{u,h},\tilde{\mathbf{x}}_{\mathrm{u,h}}\right)$, several features of $\left(\overline{\chi}_{R,n,m,\tilde{\mathbf{v}},\tilde{\mathbf{x}}}^{[u,h,\mathrm{u,h}]},\overline{\chi}_{I,n,m,\tilde{\mathbf{v}},\tilde{\mathbf{x}}}^{[u,h,\mathrm{u,h}]}\right)$ for various $n$ and $m$ must be studied in advance. First, the pdf of the random vector, $\left\{\overline{\chi}_{R,1,1,\tilde{\mathbf{v}},\tilde{\mathbf{x}}}^{[u,h,\mathrm{u,h}]},\overline{\chi}_{I,1,1,\tilde{\mathbf{v}},\tilde{\mathbf{x}}}^{[u,h,\mathrm{u,h}]},\ldots,\overline{\chi}_{R,n,m,\tilde{\mathbf{v}},\tilde{\mathbf{x}}}^{[u,h,\mathrm{u,h}]},\overline{\chi}_{I,n,m,\tilde{\mathbf{v}},\tilde{\mathbf{x}}}^{[u,h,\mathrm{u,h}]},\ldots,\overline{\chi}_{R,N,M,\tilde{\mathbf{v}},\tilde{\mathbf{x}}}^{[u,h,\mathrm{u,h}]},\overline{\chi}_{I,N,M,\tilde{\mathbf{v}},\tilde{\mathbf{x}}}^{[u,h,\mathrm{u,h}]}\right\}$ can be shown to be a multivariate normal distribution by applying Lyapunov's CLT to prove any linear combination of its components is normally distributed. Second, the outputs of the correlators corresponding to different reference signals are uncorrelated to each other. This lack of correlation results from the independence between the transmit signals. Third, since the receiver antennas are widely separated, it is reasonable to assume that $\left|\tau_{n,m1}-\tau_{n,m2}\right|$ and $\left|\beta_{n,m1}-\beta_{n,m2}\right|$, $\forall m1\neq m2$ are sufficient large to ensure that every sample of $S_{n,m1}^{r}(t)$ is independent of the samples of $S_{n,m2}^{r}(t)$. This independence causes the correlator outputs corresponding to a certain transmit signal in different receive antenna to be uncorrelated.

According to above discussions, $\left(\overline{\chi}_{R,n1,m1,\tilde{\mathbf{v}},\tilde{\mathbf{x}}}^{[u,h,\mathrm{u,h}]},\overline{\chi}_{I,n1,m1,\tilde{\mathbf{v}},\tilde{\mathbf{x}}}^{[u,h,\mathrm{u,h}]}\right)$ are independent of $\left(\overline{\chi}_{R,n2,m2,\tilde{\mathbf{v}},\tilde{\mathbf{x}}}^{[u,h,\mathrm{u,h}]},\overline{\chi}_{I,n2,m2,\tilde{\mathbf{v}},\tilde{\mathbf{x}}}^{[u,h,\mathrm{u,h}]}\right)$, if $n1\neq n2$ or $m1\neq m2$, and this independence causes the distribution of the summation of all correlator outputs, $\left(\overline{\chi}_{R,\tilde{\mathbf{v}},\tilde{\mathbf{x}}}^{[u,h,\mathrm{u,h}]},\overline{\chi}_{I,\tilde{\mathbf{v}},\tilde{\mathbf{x}}}^{[u,h,\mathrm{u,h}]}\right)\sim N\left(\overline{\mu}_{R,\tilde{\mathbf{v}},\tilde{\mathbf{x}}}^{[u,h,\mathrm{u,h}]},\overline{\mu}_{I,\tilde{\mathbf{v}},\tilde{\mathbf{x}}}^{[u,h,\mathrm{u,h}]},\left(\overline{\sigma}_{R,\tilde{\mathbf{v}},\tilde{\mathbf{x}}}^{[u,h,\mathrm{u,h}]}\right)^{2},\left(\overline{\sigma}_{I,\tilde{\mathbf{v}},\tilde{\mathbf{x}}}^{[u,h,\mathrm{u,h}]}\right)^{2},\rho_{\tilde{\mathbf{v}},\tilde{\mathbf{x}}}^{[u,h,\mathrm{u,h}]}\right)$ where

$$\overline{\chi}_{R,\tilde{\mathbf{v}},\tilde{\mathbf{x}}}^{[u,h,\mathrm{u,h}]}=\sum_{m=1}^{M}\sum_{n=1}^{N}\overline{\chi}_{R,n,m,\tilde{\mathbf{v}},\tilde{\mathbf{x}}}^{[u,h,\mathrm{u,h}]}\quad,\quad\overline{\chi}_{I,\tilde{\mathbf{v}},\tilde{\mathbf{x}}}^{[u,h,\mathrm{u,h}]}=\sum_{m=1}^{M}\sum_{n=1}^{N}\overline{\chi}_{I,n,m,\tilde{\mathbf{v}},\tilde{\mathbf{x}}}^{[u,h,\mathrm{u,h}]}\quad,\quad\overline{\mu}_{R,\tilde{\mathbf{v}},\tilde{\mathbf{x}}}^{[u,h,\mathrm{u,h}]}=\sum_{m=1}^{M}\sum_{n=1}^{N}\overline{\mu}_{R,n,m,\tilde{\mathbf{v}},\tilde{\mathbf{x}}}^{[u,h,\mathrm{u,h}]},$$

$$\overline{\mu}_{I,\tilde{\mathbf{v}},\tilde{\mathbf{x}}}^{[u,h,\mathrm{u,h}]}=\sum_{m=1}^{M}\sum_{n=1}^{N}\overline{\mu}_{I,n,m,\tilde{\mathbf{v}},\tilde{\mathbf{x}}}^{[u,h,\mathrm{u,h}]},\ \left(\overline{\sigma}_{R,\tilde{\mathbf{v}},\tilde{\mathbf{x}}}^{[u,h,\mathrm{u,h}]}\right)^{2}=\sum_{m=1}^{M}\sum_{n=1}^{N}\left(\overline{\sigma}_{R,n,m,\tilde{\mathbf{v}},\tilde{\mathbf{x}}}^{[u,h,\mathrm{u,h}]}\right)^{2},\ \left(\overline{\sigma}_{I,\tilde{\mathbf{v}},\tilde{\mathbf{x}}}^{[u,h,\mathrm{u,h}]}\right)^{2}=\sum_{m=1}^{M}\sum_{n=1}^{N}\left(\overline{\sigma}_{I,n,m,\tilde{\mathbf{v}},\tilde{\mathbf{x}}}^{[u,h,\mathrm{u,h}]}\right)^{2},$$

and $\rho_{\tilde{\mathbf{v}},\tilde{\mathbf{x}}}^{[u,h,\mathrm{u,h}]}=\dfrac{\sum_{m=1}^{M}\sum_{n=1}^{N}\rho_{n,m,\tilde{\mathbf{v}},\tilde{\mathbf{x}}}^{[u,h,\mathrm{u,h}]}\bar{\sigma}_{R,n,m,\tilde{\mathbf{v}},\tilde{\mathbf{x}}}^{[u,h,\mathrm{u,h}]}\bar{\sigma}_{I,n,m,\tilde{\mathbf{v}},\tilde{\mathbf{x}}}^{[u,h,\mathrm{u,h}]}}{\bar{\sigma}_{R,\tilde{\mathbf{v}},\tilde{\mathbf{x}}}^{[u,h,\mathrm{u,h}]}\bar{\sigma}_{I,\tilde{\mathbf{v}},\tilde{\mathbf{x}}}^{[u,h,\mathrm{u,h}]}}$ . Since $A^{1/2}\left(\tilde{\mathbf{v}}_{u,h},\tilde{\mathbf{x}}_{\mathrm{u,h}}\right)=\sqrt{\left(\bar{\chi}_{R,\tilde{\mathbf{v}},\tilde{\mathbf{x}}}^{[u,h,\mathrm{u,h}]}\right)^2+\left(\bar{\chi}_{I,\tilde{\mathbf{v}},\tilde{\mathbf{x}}}^{[u,h,\mathrm{u,h}]}\right)^2}$, the exact pdf of $A^{1/2}\left(\tilde{\mathbf{v}}_{u,h},\tilde{\mathbf{x}}_{\mathrm{u,h}}\right)$ can be solved by applying the Jacobian transformation to the joint pdf of $\left(\bar{\chi}_{R,\tilde{\mathbf{v}},\tilde{\mathbf{x}}}^{[u,h,\mathrm{u,h}]},\bar{\chi}_{I,\tilde{\mathbf{v}},\tilde{\mathbf{x}}}^{[u,h,\mathrm{u,h}]}\right)$. However, the computation is complicated, causing considerable difficulty to exactly solve for the joint pdf of $\left\{A^{1/2}\left(\tilde{\mathbf{v}}_{1,1},\tilde{\mathbf{x}}_{1,1}\right),...,A^{1/2}\left(\tilde{\mathbf{v}}_{U,H},\tilde{\mathbf{x}}_{\mathrm{U,H}}\right)\right\}$ . Therefore, an analyzable approximation for $A^{1/2}\left(\tilde{\mathbf{v}}_{u,h},\tilde{\mathbf{x}}_{\mathrm{u,h}}\right)$ pdf needs to be developed.

We can use the first two terms of the series expansion to infer that

$$\begin{aligned}\sqrt{\left(\bar{\chi}_{R,\tilde{\mathbf{v}},\tilde{\mathbf{x}}}^{[u,h,\mathrm{u,h}]}\right)^2+\left(\bar{\chi}_{I,\tilde{\mathbf{v}},\tilde{\mathbf{x}}}^{[u,h,\mathrm{u,h}]}\right)^2}&\approx\max\left\{\left|\bar{\chi}_{R,\tilde{\mathbf{v}},\tilde{\mathbf{x}}}^{[u,h,\mathrm{u,h}]}\right|,\left|\bar{\chi}_{I,\tilde{\mathbf{v}},\tilde{\mathbf{x}}}^{[u,h,\mathrm{u,h}]}\right|\right\}+\frac{\min\left\{\left(\bar{\chi}_{R,\tilde{\mathbf{v}},\tilde{\mathbf{x}}}^{[u,h,\mathrm{u,h}]}\right)^2,\left(\bar{\chi}_{I,\tilde{\mathbf{v}},\tilde{\mathbf{x}}}^{[u,h,\mathrm{u,h}]}\right)^2\right\}}{2\max\left\{\left|\bar{\chi}_{R,\tilde{\mathbf{v}},\tilde{\mathbf{x}}}^{[u,h,\mathrm{u,h}]}\right|,\left|\bar{\chi}_{I,\tilde{\mathbf{v}},\tilde{\mathbf{x}}}^{[u,h,\mathrm{u,h}]}\right|\right\}}\\&\approx\left|\bar{\chi}_{R,\tilde{\mathbf{v}},\tilde{\mathbf{x}}}^{[u,h,\mathrm{u,h}]}\right|+\frac{\left(\bar{\chi}_{I,\tilde{\mathbf{v}},\tilde{\mathbf{x}}}^{[u,h,\mathrm{u,h}]}\right)^2}{2\left|\bar{\chi}_{R,\tilde{\mathbf{v}},\tilde{\mathbf{x}}}^{[u,h,\mathrm{u,h}]}\right|}\ \text{if}\ \left|\bar{\chi}_{R,\tilde{\mathbf{v}},\tilde{\mathbf{x}}}^{[u,h,\mathrm{u,h}]}\right|>\left|\bar{\chi}_{I,\tilde{\mathbf{v}},\tilde{\mathbf{x}}}^{[u,h,\mathrm{u,h}]}\right|,\ \text{or}\\&\approx\left|\bar{\chi}_{I,\tilde{\mathbf{v}},\tilde{\mathbf{x}}}^{[u,h,\mathrm{u,h}]}\right|+\frac{\left(\bar{\chi}_{R,\tilde{\mathbf{v}},\tilde{\mathbf{x}}}^{[u,h,\mathrm{u,h}]}\right)^2}{2\left|\bar{\chi}_{I,\tilde{\mathbf{v}},\tilde{\mathbf{x}}}^{[u,h,\mathrm{u,h}]}\right|}\ \text{if}\ \left|\bar{\chi}_{I,\tilde{\mathbf{v}},\tilde{\mathbf{x}}}^{[u,h,\mathrm{u,h}]}\right|>\left|\bar{\chi}_{R,\tilde{\mathbf{v}},\tilde{\mathbf{x}}}^{[u,h,\mathrm{u,h}]}\right|.\end{aligned}$$

4.17

If the mean of the absolute value of either the real part or the imaginary part is greater than the other, we can use the second and the third approximations in 4.17, since $\max\left\{\left|\bar{\chi}_{R,\tilde{\mathbf{v}},\tilde{\mathbf{x}}}^{[u,h,\mathrm{u,h}]}\right|,\left|\bar{\chi}_{I,\tilde{\mathbf{v}},\tilde{\mathbf{x}}}^{[u,h,\mathrm{u,h}]}\right|\right\}$ is possibly equal to $\left|\bar{\chi}_{R,\tilde{\mathbf{v}},\tilde{\mathbf{x}}}^{[u,h,\mathrm{u,h}]}\right|$ if $E\left[\left|\bar{\chi}_{R,\tilde{\mathbf{v}},\tilde{\mathbf{x}}}^{[u,h,\mathrm{u,h}]}\right|\right]>E\left[\left|\bar{\chi}_{I,\tilde{\mathbf{v}},\tilde{\mathbf{x}}}^{[u,h,\mathrm{u,h}]}\right|\right]$, and possibly equal to $\left|\bar{\chi}_{I,\tilde{\mathbf{v}},\tilde{\mathbf{x}}}^{[u,h,\mathrm{u,h}]}\right|$ if $E\left[\left|\bar{\chi}_{I,\tilde{\mathbf{v}},\tilde{\mathbf{x}}}^{[u,h,\mathrm{u,h}]}\right|\right]>E\left[\left|\bar{\chi}_{R,\tilde{\mathbf{v}},\tilde{\mathbf{x}}}^{[u,h,\mathrm{u,h}]}\right|\right]$.

We consider $E\left[\left|\bar{\chi}_{R,\tilde{\mathbf{v}},\tilde{\mathbf{x}}}^{[u,h,\mathrm{u,h}]}\right|\right] > E\left[\left|\bar{\chi}_{I,\tilde{\mathbf{v}},\tilde{\mathbf{x}}}^{[u,h,\mathrm{u,h}]}\right|\right]$ as an example for further discussion. Results are similar if $E\left[\left|\bar{\chi}_{I,\tilde{\mathbf{v}},\tilde{\mathbf{x}}}^{[u,h,\mathrm{u,h}]}\right|\right] > E\left[\left|\bar{\chi}_{R,\tilde{\mathbf{v}},\tilde{\mathbf{x}}}^{[u,h,\mathrm{u,h}]}\right|\right]$. Since $\bar{\chi}_{R,\tilde{\mathbf{v}},\tilde{\mathbf{x}}}^{[u,h,\mathrm{u,h}]}$ is normally distributed, its absolute value is a folded normally distributed random variable [45] with the pdf

$$\frac{1}{\bar{\sigma}_{R,\tilde{\mathbf{v}},\tilde{\mathbf{x}}}^{[u,h,\mathrm{u,h}]}\sqrt{2\pi}}\left[\exp\left(-\frac{\left(\left|\bar{\chi}_{R,\tilde{\mathbf{v}},\tilde{\mathbf{x}}}^{[u,h,\mathrm{u,h}]}\right|-\bar{\mu}_{R,\tilde{\mathbf{v}},\tilde{\mathbf{x}}}^{[u,h,\mathrm{u,h}]}\right)^2}{2\left(\bar{\sigma}_{R,\tilde{\mathbf{v}},\tilde{\mathbf{x}}}^{[u,h,\mathrm{u,h}]}\right)^2}\right)+\exp\left(-\frac{\left(\left|\bar{\chi}_{R,\tilde{\mathbf{v}},\tilde{\mathbf{x}}}^{[u,h,\mathrm{u,h}]}\right|+\bar{\mu}_{R,\tilde{\mathbf{v}},\tilde{\mathbf{x}}}^{[u,h,\mathrm{u,h}]}\right)^2}{2\left(\bar{\sigma}_{R,\tilde{\mathbf{v}},\tilde{\mathbf{x}}}^{[u,h,\mathrm{u,h}]}\right)^2}\right)\right] \qquad 4.18$$

When $\tilde{\mathbf{v}}_{u,h} \sim \mathbf{v}$ and $\tilde{\mathbf{x}}_{\mathrm{u,h}} \sim \mathbf{x}$, the ratio $\left|\bar{\mu}_{R,\tilde{\mathbf{v}},\tilde{\mathbf{x}}}^{[u,h,\mathrm{u,h}]}\right| \Big/ \bar{\sigma}_{R,\tilde{\mathbf{v}},\tilde{\mathbf{x}}}^{[u,h,\mathrm{u,h}]}$ can be significant because $D_{\ell,n,m,\tilde{\mathbf{v}},\tilde{\mathbf{x}}}^{[u,h,\mathrm{u,h}]}$ in 4.11 is small. If $\left|\bar{\mu}_{R,\tilde{\mathbf{v}},\tilde{\mathbf{x}}}^{[u,h,\mathrm{u,h}]}\right| \Big/ \bar{\sigma}_{R,\tilde{\mathbf{v}},\tilde{\mathbf{x}}}^{[u,h,\mathrm{u,h}]}$ is sufficiently large, the result of one of the two exponential terms in 4.18 is ignorable, and $\left|\bar{\chi}_{R,\tilde{\mathbf{v}},\tilde{\mathbf{x}}}^{[u,h,\mathrm{u,h}]}\right|$ can be approximated to $N\left(\left|\bar{\mu}_{R,\tilde{\mathbf{v}},\tilde{\mathbf{x}}}^{[u,h,\mathrm{u,h}]}\right|,\left(\bar{\sigma}_{R,\tilde{\mathbf{v}},\tilde{\mathbf{x}}}^{[u,h,\mathrm{u,h}]}\right)^2\right)$.

Then, the joint pdf of $\left(\left|\bar{\chi}_{R,\tilde{\mathbf{v}},\tilde{\mathbf{x}}}^{[u,h,\mathrm{u,h}]}\right|,\bar{\chi}_{I,\tilde{\mathbf{v}},\tilde{\mathbf{x}}}^{[u,h,\mathrm{u,h}]}\right)$ can be modeled as $\left(\left|\bar{\chi}_{R,\tilde{\mathbf{v}},\tilde{\mathbf{x}}}^{[u,h,\mathrm{u,h}]}\right|,\bar{\chi}_{I,\tilde{\mathbf{v}},\tilde{\mathbf{x}}}^{[u,h,\mathrm{u,h}]}\right) \sim N\left(\left|\bar{\mu}_{R,\tilde{\mathbf{v}},\tilde{\mathbf{x}}}^{[u,h,\mathrm{u,h}]}\right|,\bar{\mu}_{I,\tilde{\mathbf{v}},\tilde{\mathbf{x}}}^{[u,h,\mathrm{u,h}]},\left(\bar{\sigma}_{R,\tilde{\mathbf{v}},\tilde{\mathbf{x}}}^{[u,h,\mathrm{u,h}]}\right)^2,\left(\bar{\sigma}_{I,\tilde{\mathbf{v}},\tilde{\mathbf{x}}}^{[u,h,\mathrm{u,h}]}\right)^2,\bar{\rho}_{\tilde{\mathbf{v}},\tilde{\mathbf{x}}}^{[u,h,\mathrm{u,h}]}\right)$, where $\bar{\rho}_{\tilde{\mathbf{v}},\tilde{\mathbf{x}}}^{[u,h,\mathrm{u,h}]} = \rho_{\tilde{\mathbf{v}},\tilde{\mathbf{x}}}^{[u,h,\mathrm{u,h}]}$ if $\bar{\mu}_{R,\tilde{\mathbf{v}},\tilde{\mathbf{x}}}^{[u,h,\mathrm{u,h}]} > 0$, otherwise $\bar{\rho}_{\tilde{\mathbf{v}},\tilde{\mathbf{x}}}^{[u,h,\mathrm{u,h}]} = -\rho_{\tilde{\mathbf{v}},\tilde{\mathbf{x}}}^{[u,h,\mathrm{u,h}]}$. Based on the correlation between $\left|\bar{\chi}_{R,\tilde{\mathbf{v}},\tilde{\mathbf{x}}}^{[u,h,\mathrm{u,h}]}\right|$ and $\bar{\chi}_{I,\tilde{\mathbf{v}},\tilde{\mathbf{x}}}^{[u,h,\mathrm{u,h}]}$, $\bar{\chi}_{I,\tilde{\mathbf{v}},\tilde{\mathbf{x}}}^{[u,h,\mathrm{u,h}]}$ can be represented as

$$\bar{\chi}_{I,\tilde{\mathbf{v}},\tilde{\mathbf{x}}}^{[u,h,\mathrm{u,h}]} = \bar{\rho}_{\tilde{\mathbf{v}},\tilde{\mathbf{x}}}^{[u,h,\mathrm{u,h}]}\frac{\bar{\sigma}_{I,\tilde{\mathbf{v}},\tilde{\mathbf{x}}}^{[u,h,\mathrm{u,h}]}}{\bar{\sigma}_{R,\tilde{\mathbf{v}},\tilde{\mathbf{x}}}^{[u,h,\mathrm{u,h}]}}\left|\bar{\chi}_{R,\tilde{\mathbf{v}},\tilde{\mathbf{x}}}^{[u,h,\mathrm{u,h}]}\right| + \gamma_{\tilde{\mathbf{v}},\tilde{\mathbf{x}}}^{[u,h,\mathrm{u,h}]} \qquad 4.19$$

where $\gamma_{\tilde{\mathbf{v}},\tilde{\mathbf{x}}}^{[u,h,\mathrm{u,h}]} \sim N\left(\bar{\mu}_{I,\tilde{\mathbf{v}},\tilde{\mathbf{x}}}^{[u,h,\mathrm{u,h}]} - \frac{\bar{\rho}_{\tilde{\mathbf{v}},\tilde{\mathbf{x}}}^{[u,h,\mathrm{u,h}]}\bar{\sigma}_{I,\tilde{\mathbf{v}},\tilde{\mathbf{x}}}^{[u,h,\mathrm{u,h}]}\left|\bar{\mu}_{R,\tilde{\mathbf{v}},\tilde{\mathbf{x}}}^{[u,h,\mathrm{u,h}]}\right|}{\bar{\sigma}_{R,\tilde{\mathbf{v}},\tilde{\mathbf{x}}}^{[u,h,\mathrm{u,h}]}},\left(1-\left(\bar{\rho}_{\tilde{\mathbf{v}},\tilde{\mathbf{x}}}^{[u,h,\mathrm{u,h}]}\right)^2\right)\left(\bar{\sigma}_{I,\tilde{\mathbf{v}},\tilde{\mathbf{x}}}^{[u,h,\mathrm{u,h}]}\right)^2\right)$, and is independent of $\left|\bar{\chi}_{R,\tilde{\mathbf{v}},\tilde{\mathbf{x}}}^{[u,h,\mathrm{u,h}]}\right|$. Based on 4.17 and 4.19, we have

$$\sqrt{\left(\overline{\chi}_{R,\tilde{\mathbf{v}},\tilde{\mathbf{x}}}^{[u,h,\mathrm{u,h}]}\right)^2+\left(\overline{\chi}_{I,\tilde{\mathbf{v}},\tilde{\mathbf{x}}}^{[u,h,\mathrm{u,h}]}\right)^2}\approx\left(1+\frac{1}{2}\left(\overline{\rho}_{\tilde{\mathbf{v}},\tilde{\mathbf{x}}}^{[u,h,\mathrm{u,h}]}\frac{\overline{\sigma}_{I,\tilde{\mathbf{v}},\tilde{\mathbf{x}}}^{[u,h,\mathrm{u,h}]}}{\overline{\sigma}_{R,\tilde{\mathbf{v}},\tilde{\mathbf{x}}}^{[u,h,\mathrm{u,h}]}}\right)^2\right)\left|\overline{\chi}_{R,\tilde{\mathbf{v}},\tilde{\mathbf{x}}}^{[u,h,\mathrm{u,h}]}\right| \tag{4.20}$$
$$+\overline{\rho}_{\tilde{\mathbf{v}},\tilde{\mathbf{x}}}^{[u,h,\mathrm{u,h}]}\frac{\overline{\sigma}_{I,\tilde{\mathbf{v}},\tilde{\mathbf{x}}}^{[u,h,\mathrm{u,h}]}}{\overline{\sigma}_{R,\tilde{\mathbf{v}},\tilde{\mathbf{x}}}^{[u,h,\mathrm{u,h}]}}\gamma_{\tilde{\mathbf{v}},\tilde{\mathbf{x}}}^{[u,h,\mathrm{u,h}]}+\frac{\left(\gamma_{\tilde{\mathbf{v}},\tilde{\mathbf{x}}}^{[u,h,\mathrm{u,h}]}\right)^2}{\left|2\overline{\chi}_{R,\tilde{\mathbf{v}},\tilde{\mathbf{x}}}^{[u,h,\mathrm{u,h}]}\right|}$$

When $\tilde{\mathbf{v}}_{u,h}\sim\mathbf{v}$ and $\tilde{\mathbf{x}}_{\mathrm{u,h}}\sim\mathbf{x}$, the large $\left|\overline{\mu}_{R,\tilde{\mathbf{v}},\tilde{\mathbf{x}}}^{[u,h,\mathrm{u,h}]}\right|$ and $\overline{\rho}_{\tilde{\mathbf{v}},\tilde{\mathbf{x}}}^{[u,h,\mathrm{u,h}]}$ are helpful in efficiently limiting the randomness of $\left(\gamma_{\tilde{\mathbf{v}},\tilde{\mathbf{x}}}^{[u,h,\mathrm{u,h}]}\right)^2\Big/\left|2\overline{\chi}_{R,\tilde{\mathbf{v}},\tilde{\mathbf{x}}}^{[u,h,\mathrm{u,h}]}\right|$. As a result, it is appropriate to approximate the pdf of $A^{1/2}\left(\tilde{\mathbf{v}}_{u,h},\tilde{\mathbf{x}}_{\mathrm{u,h}}\right)$ as $N\left(\overline{\mu}_{\tilde{\mathbf{v}},\tilde{\mathbf{x}}}^{[u,h,\mathrm{u,h}]},\left(\overline{\sigma}_{\tilde{\mathbf{v}},\tilde{\mathbf{x}}}^{[u,h,\mathrm{u,h}]}\right)^2\right)$ where

$$\overline{\mu}_{\tilde{\mathbf{v}},\tilde{\mathbf{x}}}^{[u,h,\mathrm{u,h}]}\approx\left|\overline{\mu}_{R,\tilde{\mathbf{v}},\tilde{\mathbf{x}}}^{[u,h,\mathrm{u,h}]}\right|+\frac{\left(\overline{\mu}_{I,\tilde{\mathbf{v}},\tilde{\mathbf{x}}}^{[u,h,\mathrm{u,h}]}\right)^2+\left(1-\left(\overline{\rho}_{\tilde{\mathbf{v}},\tilde{\mathbf{x}}}^{[u,h,\mathrm{u,h}]}\right)^2\right)\left(\overline{\sigma}_{I,\tilde{\mathbf{v}},\tilde{\mathbf{x}}}^{[u,h,\mathrm{u,h}]}\right)^2}{\left|2\overline{\mu}_{R,\tilde{\mathbf{v}},\tilde{\mathbf{x}}}^{[u,h,\mathrm{u,h}]}\right|} \tag{4.21}$$

and

$$\left(\overline{\sigma}_{\tilde{\mathbf{v}},\tilde{\mathbf{x}}}^{[u,h,\mathrm{u,h}]}\right)^2\approx\left(\overline{\sigma}_{R,\tilde{\mathbf{v}},\tilde{\mathbf{x}}}^{[u,h,\mathrm{u,h}]}\right)^2+\left(\overline{\rho}_{\tilde{\mathbf{v}},\tilde{\mathbf{x}}}^{[u,h,\mathrm{u,h}]}\right)^2\left(\overline{\sigma}_{I,\tilde{\mathbf{v}},\tilde{\mathbf{x}}}^{[u,h,\mathrm{u,h}]}\right)^2-\left(\frac{\left(\overline{\mu}_{I,\tilde{\mathbf{v}},\tilde{\mathbf{x}}}^{[u,h,\mathrm{u,h}]}\right)^2+\left(1-\left(\overline{\rho}_{\tilde{\mathbf{v}},\tilde{\mathbf{x}}}^{[u,h,\mathrm{u,h}]}\right)^2\right)\left(\overline{\sigma}_{I,\tilde{\mathbf{v}},\tilde{\mathbf{x}}}^{[u,h,\mathrm{u,h}]}\right)^2}{\left|2\overline{\mu}_{R,\tilde{\mathbf{v}},\tilde{\mathbf{x}}}^{[u,h,\mathrm{u,h}]}\right|}\right)^2 \tag{4.22}$$

using $E\left[1\Big/\left|\overline{\chi}_{R,\tilde{\mathbf{v}},\tilde{\mathbf{x}}}^{[u,h,\mathrm{u,h}]}\right|\right]\approx 1\Big/\left|\overline{\mu}_{R,\tilde{\mathbf{v}},\tilde{\mathbf{x}}}^{[u,h,\mathrm{u,h}]}\right|$ since $\left(\overline{\sigma}_{R,\tilde{\mathbf{v}},\tilde{\mathbf{x}}}^{[u,h,\mathrm{u,h}]}\right)^2\Big/\left|\overline{\mu}_{R,\tilde{\mathbf{v}},\tilde{\mathbf{x}}}^{[u,h,\mathrm{u,h}]}\right|^3$ is much smaller than $1\Big/\left|\overline{\mu}_{R,\tilde{\mathbf{v}},\tilde{\mathbf{x}}}^{[u,h,\mathrm{u,h}]}\right|$ in the Taylor series expansion of $1\Big/\left|\overline{\chi}_{R,\tilde{\mathbf{v}},\tilde{\mathbf{x}}}^{[u,h,\mathrm{u,h}]}\right|$.

The above discussions about approximating the square root of the sum of two squared Gaussian random variables as another Gaussian variable can also be applied to study the distribution of $A_{nc}^{1/2}\left(\tilde{\mathbf{v}}_{u,h},\tilde{\mathbf{x}}_{\mathrm{u,h}}\right)$, which is equal to $\sum_{m=1}^{M}\sum_{n=1}^{N}\sqrt{\left(\overline{\chi}_{R,n,m,\tilde{\mathbf{v}},\tilde{\mathbf{x}}}^{[u,h,\mathrm{u,h}]}\right)^2+\left(\overline{\chi}_{I,n,m,\tilde{\mathbf{v}},\tilde{\mathbf{x}}}^{[u,h,\mathrm{u,h}]}\right)^2}$. When

$\tilde{\mathbf{v}}_{u,h} \sim \mathbf{v}$ and $\tilde{\mathbf{x}}_{\mathrm{u,h}} \sim \mathbf{x}$ , $\left|\bar{\mu}_{R,n,m,\tilde{\mathbf{v}},\tilde{\mathbf{x}}}^{[u,h,\mathrm{u,h}]}\right| \Big/ \bar{\sigma}_{R,n,m,\tilde{\mathbf{v}},\tilde{\mathbf{x}}}^{[u,h,\mathrm{u,h}]}$ is possibly sufficiently large, and if $E\left[\bar{\chi}_{R,n,m,\tilde{\mathbf{v}},\tilde{\mathbf{x}}}^{[u,h,\mathrm{u,h}]}\right] > E\left[\bar{\chi}_{I,n,m,\tilde{\mathbf{v}},\tilde{\mathbf{x}}}^{[u,h,\mathrm{u,h}]}\right]$ , the distributions of $\left(\left|\bar{\chi}_{R,n,m,\tilde{\mathbf{v}},\tilde{\mathbf{x}}}^{[u,h,\mathrm{u,h}]}\right|, \bar{\chi}_{I,n,m,\tilde{\mathbf{v}},\tilde{\mathbf{x}}}^{[u,h,\mathrm{u,h}]}\right)$ and $\sqrt{\left(\bar{\chi}_{R,n,m,\tilde{\mathbf{v}},\tilde{\mathbf{x}}}^{[u,h,\mathrm{u,h}]}\right)^2 + \left(\bar{\chi}_{I,n,m,\tilde{\mathbf{v}},\tilde{\mathbf{x}}}^{[u,h,\mathrm{u,h}]}\right)^2}$ can be approximated as $N\left(\left|\bar{\mu}_{R,n,m,\tilde{\mathbf{v}},\tilde{\mathbf{x}}}^{[u,h,\mathrm{u,h}]}\right|, \bar{\mu}_{I,n,m,\tilde{\mathbf{v}},\tilde{\mathbf{x}}}^{[u,h,\mathrm{u,h}]}, \left(\bar{\sigma}_{R,n,m,\tilde{\mathbf{v}},\tilde{\mathbf{x}}}^{[u,h,\mathrm{u,h}]}\right)^2, \left(\bar{\sigma}_{I,n,m,\tilde{\mathbf{v}},\tilde{\mathbf{x}}}^{[u,h,\mathrm{u,h}]}\right)^2, \bar{\rho}_{n,m,\tilde{\mathbf{v}},\tilde{\mathbf{x}}}^{[u,h,\mathrm{u,h}]}\right)$ and $N\left(\hat{\mu}_{n,m,\tilde{\mathbf{v}},\tilde{\mathbf{x}}}^{[u,h,\mathrm{u,h}]}, \left(\hat{\sigma}_{n,m,\tilde{\mathbf{v}},\tilde{\mathbf{x}}}^{[u,h,\mathrm{u,h}]}\right)^2\right)$ , respectively, where

$$\hat{\mu}_{n,m,\tilde{\mathbf{v}},\tilde{\mathbf{x}}}^{[u,h,\mathrm{u,h}]} \approx \left|\bar{\mu}_{R,n,m,\tilde{\mathbf{v}},\tilde{\mathbf{x}}}^{[u,h,\mathrm{u,h}]}\right| + \frac{\left(\bar{\mu}_{I,n,m,\tilde{\mathbf{v}},\tilde{\mathbf{x}}}^{[u,h,\mathrm{u,h}]}\right)^2 + \left(1 - \left(\bar{\rho}_{n,m,\tilde{\mathbf{v}},\tilde{\mathbf{x}}}^{[u,h,\mathrm{u,h}]}\right)^2\right)\left(\bar{\sigma}_{I,n,m,\tilde{\mathbf{v}},\tilde{\mathbf{x}}}^{[u,h,\mathrm{u,h}]}\right)^2}{\left|2\bar{\mu}_{R,n,m,\tilde{\mathbf{v}},\tilde{\mathbf{x}}}^{[u,h,\mathrm{u,h}]}\right|} , \tag{4.23}$$

$$\begin{aligned}\left(\hat{\sigma}_{n,m,\tilde{\mathbf{v}},\tilde{\mathbf{x}}}^{[u,h,\mathrm{u,h}]}\right)^2 \approx{}& \left(\bar{\sigma}_{R,n,m,\tilde{\mathbf{v}},\tilde{\mathbf{x}}}^{[u,h,\mathrm{u,h}]}\right)^2 + \left(\bar{\rho}_{n,m,\tilde{\mathbf{v}},\tilde{\mathbf{x}}}^{[u,h,\mathrm{u,h}]}\right)^2 \left(\bar{\sigma}_{I,n,m,\tilde{\mathbf{v}},\tilde{\mathbf{x}}}^{[u,h,\mathrm{u,h}]}\right)^2 \\ &- \left(\frac{\left(\bar{\mu}_{I,n,m,\tilde{\mathbf{v}},\tilde{\mathbf{x}}}^{[u,h,\mathrm{u,h}]}\right)^2 + \left(1 - \left(\bar{\rho}_{n,m,\tilde{\mathbf{v}},\tilde{\mathbf{x}}}^{[u,h,\mathrm{u,h}]}\right)^2\right)\left(\bar{\sigma}_{I,n,m,\tilde{\mathbf{v}},\tilde{\mathbf{x}}}^{[u,h,\mathrm{u,h}]}\right)^2}{\left|2\bar{\mu}_{R,n,m,\tilde{\mathbf{v}},\tilde{\mathbf{x}}}^{[u,h,\mathrm{u,h}]}\right|}\right)^2\end{aligned} \tag{4.24}$$

and $\bar{\rho}_{n,m,\tilde{\mathbf{v}},\tilde{\mathbf{x}}}^{[u,h,\mathrm{u,h}]}$ is the correlation coefficient between $\left|\bar{\chi}_{R,n,m,\tilde{\mathbf{v}},\tilde{\mathbf{x}}}^{[u,h,\mathrm{u,h}]}\right|$ and $\bar{\chi}_{I,n,m,\tilde{\mathbf{v}},\tilde{\mathbf{x}}}^{[u,h,\mathrm{u,h}]}$.

Otherwise, if $E\left[\bar{\chi}_{I,n,m,\tilde{\mathbf{v}},\tilde{\mathbf{x}}}^{[u,h,\mathrm{u,h}]}\right] > E\left[\bar{\chi}_{R,n,m,\tilde{\mathbf{v}},\tilde{\mathbf{x}}}^{[u,h,\mathrm{u,h}]}\right]$,

$$\hat{\mu}_{n,m,\tilde{\mathbf{v}},\tilde{\mathbf{x}}}^{[u,h,\mathrm{u,h}]} \approx \left|\bar{\mu}_{I,n,m,\tilde{\mathbf{v}},\tilde{\mathbf{x}}}^{[u,h,\mathrm{u,h}]}\right| + \frac{\left(\bar{\mu}_{R,n,m,\tilde{\mathbf{v}},\tilde{\mathbf{x}}}^{[u,h,\mathrm{u,h}]}\right)^2 + \left(1 - \left(\rho_{n,m,\tilde{\mathbf{v}},\tilde{\mathbf{x}}}^{[u,h,\mathrm{u,h}]}\right)^2\right)\left(\bar{\sigma}_{R,n,m,\tilde{\mathbf{v}},\tilde{\mathbf{x}}}^{[u,h,\mathrm{u,h}]}\right)^2}{\left|2\bar{\mu}_{I,n,m,\tilde{\mathbf{v}},\tilde{\mathbf{x}}}^{[u,h,\mathrm{u,h}]}\right|} \tag{4.25}$$

and

$$\left(\widehat{\sigma}_{n,m,\tilde{\mathbf{v}},\tilde{\mathbf{x}}}^{[u,h,\mathrm{u},\mathrm{h}]}\right)^2 \approx \left(\overline{\sigma}_{I,n,m,\tilde{\mathbf{v}},\tilde{\mathbf{x}}}^{[u,h,\mathrm{u},\mathrm{h}]}\right)^2 + \left(\rho_{n,m,\tilde{\mathbf{v}},\tilde{\mathbf{x}}}^{[u,h,\mathrm{u},\mathrm{h}]}\right)^2 \left(\overline{\sigma}_{R,n,m,\tilde{\mathbf{v}},\tilde{\mathbf{x}}}^{[u,h,\mathrm{u},\mathrm{h}]}\right)^2 - \left( \frac{\left(\overline{\mu}_{R,n,m,\tilde{\mathbf{v}},\tilde{\mathbf{x}}}^{[u,h,\mathrm{u},\mathrm{h}]}\right)^2 + \left(1-\left(\rho_{n,m,\tilde{\mathbf{v}},\tilde{\mathbf{x}}}^{[u,h,\mathrm{u},\mathrm{h}]}\right)^2\right)\left(\overline{\sigma}_{R,n,m,\tilde{\mathbf{v}},\tilde{\mathbf{x}}}^{[u,h,\mathrm{u},\mathrm{h}]}\right)^2}{\left|2\overline{\mu}_{I,n,m,\tilde{\mathbf{v}},\tilde{\mathbf{x}}}^{[u,h,\mathrm{u},\mathrm{h}]}\right|} \right)^2 \quad 4.26$$

Due to the independence between $\left(\overline{\chi}_{R,n1,m1,\tilde{\mathbf{v}},\tilde{\mathbf{x}}}^{[u,h,\mathrm{u},\mathrm{h}]}, \overline{\chi}_{I,n1,m1,\tilde{\mathbf{v}},\tilde{\mathbf{x}}}^{[u,h,\mathrm{u},\mathrm{h}]}\right)$ and $\left(\overline{\chi}_{R,n2,m2,\tilde{\mathbf{v}},\tilde{\mathbf{x}}}^{[u,h,\mathrm{u},\mathrm{h}]}, \overline{\chi}_{I,n2,m2,\tilde{\mathbf{v}},\tilde{\mathbf{x}}}^{[u,h,\mathrm{u},\mathrm{h}]}\right)$ for any $n1 \neq n2$ or $m1 \neq m2$, $\sqrt{\left(\overline{\chi}_{R,n1,m1,\tilde{\mathbf{v}},\tilde{\mathbf{x}}}^{[u,h,\mathrm{u},\mathrm{h}]}\right)^2 + \left(\overline{\chi}_{I,n1,m1,\tilde{\mathbf{v}},\tilde{\mathbf{x}}}^{[u,h,\mathrm{u},\mathrm{h}]}\right)^2}$ and $\sqrt{\left(\overline{\chi}_{R,n2,m2,\tilde{\mathbf{v}},\tilde{\mathbf{x}}}^{[u,h,\mathrm{u},\mathrm{h}]}\right)^2 + \left(\overline{\chi}_{I,n2,m2,\tilde{\mathbf{v}},\tilde{\mathbf{x}}}^{[u,h,\mathrm{u},\mathrm{h}]}\right)^2}$ are also independent of each other. Therefore, their summation, $A_{nc}^{1/2}\left(\tilde{\mathbf{v}}_{u,h}, \tilde{\mathbf{x}}_{\mathrm{u,h}}\right)$ can be approximated as $N\left(\widehat{\mu}_{\tilde{\mathbf{v}},\tilde{\mathbf{x}}}^{[u,h,\mathrm{u},\mathrm{h}]}, \left(\widehat{\sigma}_{\tilde{\mathbf{v}},\tilde{\mathbf{x}}}^{[u,h,\mathrm{u},\mathrm{h}]}\right)^2\right)$ where $\widehat{\mu}_{\tilde{\mathbf{v}},\tilde{\mathbf{x}}}^{[u,h,\mathrm{u},\mathrm{h}]} = \sum_{m=1}^{M}\sum_{n=1}^{N} \widehat{\mu}_{n,m,\tilde{\mathbf{v}},\tilde{\mathbf{x}}}^{[u,h,\mathrm{u},\mathrm{h}]}$, and $\left(\widehat{\sigma}_{\tilde{\mathbf{v}},\tilde{\mathbf{x}}}^{[u,h,\mathrm{u},\mathrm{h}]}\right)^2 = \sum_{m=1}^{M}\sum_{n=1}^{N}\left(\widehat{\sigma}_{n,m,\tilde{\mathbf{v}},\tilde{\mathbf{x}}}^{[u,h,\mathrm{u},\mathrm{h}]}\right)^2$.

### 4.3. Analytical MSE

According to the approximation presented in 4.20 and the limited randomness of its last term, the linear combination of the elements in $\left\{A^{1/2}\left(\tilde{\mathbf{v}}_{u,h}, \tilde{\mathbf{x}}_{\mathrm{u,h}}\right), \tilde{\mathbf{v}}_{u,h} \sim \mathbf{v} \cap \tilde{\mathbf{x}}_{\mathrm{u,h}} \sim \mathbf{x}\right\}$ can be approximated as the linear combination of the elements in the set $\left\{\overline{\chi}_{R,\tilde{\mathbf{v}},\tilde{\mathbf{x}}}^{[u,h,\mathrm{u},\mathrm{h}]}, \overline{\chi}_{I,\tilde{\mathbf{v}},\tilde{\mathbf{x}}}^{[u,h,\mathrm{u},\mathrm{h}]}, \tilde{\mathbf{v}}_{u,h} \sim \mathbf{v} \cap \tilde{\mathbf{x}}_{\mathrm{u,h}} \sim \mathbf{x}\right\}$ and constants $E\left[\left(\gamma_{\tilde{\mathbf{v}},\tilde{\mathbf{x}}}^{[u,h,\mathrm{u},\mathrm{h}]}\right)^2 \Big/ \left|2\overline{\chi}_{R,\tilde{\mathbf{v}},\tilde{\mathbf{x}}}^{[u,h,\mathrm{u},\mathrm{h}]}\right|\right]$. Recall that $\overline{\chi}_{R,\tilde{\mathbf{v}},\tilde{\mathbf{x}}}^{[u,h,\mathrm{u},\mathrm{h}]} = \sum_{\ell=1}^{L}\sum_{m=1}^{M}\sum_{n=1}^{N} \chi_{R,n,m,\ell,\tilde{\mathbf{v}},\tilde{\mathbf{x}}}^{[u,h,\mathrm{u},\mathrm{h}]}$ and $\overline{\chi}_{I,\tilde{\mathbf{v}},\tilde{\mathbf{x}}}^{[u,h,\mathrm{u},\mathrm{h}]} = \sum_{\ell=1}^{L}\sum_{m=1}^{M}\sum_{n=1}^{N} \chi_{I,n,m,\ell,\tilde{\mathbf{v}},\tilde{\mathbf{x}}}^{[u,h,\mathrm{u},\mathrm{h}]}$. Then, this linear combination can be considered as the linear combination of $L$ independent variables, and approximated as another normal random variable according to Lyapunov's CLT. As a result, the pdf of

$\left\{A^{1/2}\left(\tilde{\mathbf{v}}_{u,h},\tilde{\mathbf{x}}_{\mathrm{u,h}}\right),\tilde{\mathbf{v}}_{u,h}\sim\mathbf{v}\cap\tilde{\mathbf{x}}_{\mathrm{u,h}}\sim\mathbf{x}\right\}$ could be approximated as a multivariate normal distribution.

When neither $\tilde{\mathbf{v}}_{u,h}\sim\mathbf{v}$ nor $\tilde{\mathbf{x}}_{\mathrm{u,h}}\sim\mathbf{x}$, since the values of $\bar{\chi}_{R,\tilde{\mathbf{v}},\tilde{\mathbf{x}}}^{[u,h,\mathrm{u,h}]}$, and $\bar{\chi}_{I,\tilde{\mathbf{v}},\tilde{\mathbf{x}}}^{[u,h,\mathrm{u,h}]}$ are highly likely to be small, the pdf of $A^{1/2}\left(\tilde{\mathbf{v}}_{u,h},\tilde{\mathbf{x}}_{\mathrm{u,h}}\right)$ is not like a Gaussian-type bell shape at all. However, since it is highly unlikely that this $A^{1/2}\left(\tilde{\mathbf{v}}_{u,h},\tilde{\mathbf{x}}_{\mathrm{u,h}}\right)$ is selected as $A^{1/2}\left(\hat{\mathbf{v}},\hat{\mathbf{x}}\right)$, the exact pdf of $A^{1/2}\left(\tilde{\mathbf{v}}_{u,h},\tilde{\mathbf{x}}_{\mathrm{u,h}}\right)$ is not so critical for the MSE analysis. Moreover, in order to simply determine the pdf of the random vector $\mathbf{A}$, we model $A^{1/2}\left(\tilde{\mathbf{v}}_{u,h},\tilde{\mathbf{x}}_{\mathrm{u,h}}\right)$ as another normal random variable, $N\left(\bar{\mu}_{\tilde{\mathbf{v}},\tilde{\mathbf{x}}}^{[u,h,\mathrm{u,h}]},\left(\bar{\sigma}_{\tilde{\mathbf{v}},\tilde{\mathbf{x}}}^{[u,h,\mathrm{u,h}]}\right)^2\right)$ and further assume that the pdf of $\mathbf{A}$ is a multivariate normal distribution.

We note that the random variables $\bar{\chi}_{R,\tilde{\mathbf{v}},\tilde{\mathbf{x}}}^{[u,h,\mathrm{u,h}]}$ and $\bar{\chi}_{I,\tilde{\mathbf{v}},\tilde{\mathbf{x}}}^{[u,h,\mathrm{u,h}]}$, representing the real and imaginary part of the sum of all correlator outputs, can be considered to be quadrature pairs. Several computationally fast algorithms using piecewise linear formulas have been proposed to approximate the complex amplitude, such as $\left|\bar{\chi}_{R,\tilde{\mathbf{v}},\tilde{\mathbf{x}}}^{[u,h,\mathrm{u,h}]}+j\bar{\chi}_{I,\tilde{\mathbf{v}},\tilde{\mathbf{x}}}^{[u,h,\mathrm{u,h}]}\right|=\sqrt{\left(\bar{\chi}_{R,\tilde{\mathbf{v}},\tilde{\mathbf{x}}}^{[u,h,\mathrm{u,h}]}\right)^2+\left(\bar{\chi}_{I,\tilde{\mathbf{v}},\tilde{\mathbf{x}}}^{[u,h,\mathrm{u,h}]}\right)^2}$, to facilitate hardware implementations [46-49]. The simplest of these is the Robertson's formula [46], which when applied to the complex amplitude term in our development above, reduces to $\sqrt{\left(\bar{\chi}_{R,\tilde{\mathbf{v}},\tilde{\mathbf{x}}}^{[u,h,\mathrm{u,h}]}\right)^2+\left(\bar{\chi}_{I,\tilde{\mathbf{v}},\tilde{\mathbf{x}}}^{[u,h,\mathrm{u,h}]}\right)^2}\approx\max\left\{\left|\bar{\chi}_{R,\tilde{\mathbf{v}},\tilde{\mathbf{x}}}^{[u,h,\mathrm{u,h}]}\right|,\left|\bar{\chi}_{I,\tilde{\mathbf{v}},\tilde{\mathbf{x}}}^{[u,h,\mathrm{u,h}]}\right|\right\}+\min\left\{\left|\bar{\chi}_{R,\tilde{\mathbf{v}},\tilde{\mathbf{x}}}^{[u,h,\mathrm{u,h}]}\right|,\left|\bar{\chi}_{I,\tilde{\mathbf{v}},\tilde{\mathbf{x}}}^{[u,h,\mathrm{u,h}]}\right|\right\}\Big/2$ . The result is either $\left|\bar{\chi}_{R,\tilde{\mathbf{v}},\tilde{\mathbf{x}}}^{[u,h,\mathrm{u,h}]}\right|+\left|\bar{\chi}_{I,\tilde{\mathbf{v}},\tilde{\mathbf{x}}}^{[u,h,\mathrm{u,h}]}\right|\Big/2$ if $E\left[\left|\bar{\chi}_{R,\tilde{\mathbf{v}},\tilde{\mathbf{x}}}^{[u,h,\mathrm{u,h}]}\right|\right]>E\left[\left|\bar{\chi}_{I,\tilde{\mathbf{v}},\tilde{\mathbf{x}}}^{[u,h,\mathrm{u,h}]}\right|\right]$, $\left|\bar{\chi}_{I,\tilde{\mathbf{v}},\tilde{\mathbf{x}}}^{[u,h,\mathrm{u,h}]}\right|+\left|\bar{\chi}_{R,\tilde{\mathbf{v}},\tilde{\mathbf{x}}}^{[u,h,\mathrm{u,h}]}\right|\Big/2$ if $E\left[\left|\bar{\chi}_{I,\tilde{\mathbf{v}},\tilde{\mathbf{x}}}^{[u,h,\mathrm{u,h}]}\right|\right]>E\left[\left|\bar{\chi}_{R,\tilde{\mathbf{v}},\tilde{\mathbf{x}}}^{[u,h,\mathrm{u,h}]}\right|\right]$, using which we can calculate $\bar{\mu}_{\tilde{\mathbf{v}},\tilde{\mathbf{x}}}^{[u,h,\mathrm{u,h}]}$. If, without loss of

generality, we assume that $E\left[\left|\bar{\chi}_{R,\tilde{\mathbf{v}},\tilde{\mathbf{x}}}^{[u,h,\mathrm{u,h}]}\right|\right] > E\left[\left|\bar{\chi}_{I,\tilde{\mathbf{v}},\tilde{\mathbf{x}}}^{[u,h,\mathrm{u,h}]}\right|\right]$, then we have $\bar{\mu}_{\tilde{\mathbf{v}},\tilde{\mathbf{x}}}^{[u,h,\mathrm{u,h}]} \approx E\left[\left|\bar{\chi}_{R,\tilde{\mathbf{v}},\tilde{\mathbf{x}}}^{[u,h,\mathrm{u,h}]}\right|\right] + E\left[\left|\bar{\chi}_{I,\tilde{\mathbf{v}},\tilde{\mathbf{x}}}^{[u,h,\mathrm{u,h}]}\right|\right] \Big/ 2$.

The expected value of the folded normal random variable $\left|\bar{\chi}_{R,\tilde{\mathbf{v}},\tilde{\mathbf{x}}}^{[u,h,\mathrm{u,h}]}\right|$ is

$$\begin{aligned} E\left[\left|\bar{\chi}_{R,\tilde{\mathbf{v}},\tilde{\mathbf{x}}}^{[u,h,\mathrm{u,h}]}\right|\right] = &\left(\bar{\sigma}_{R,\tilde{\mathbf{v}},\tilde{\mathbf{x}}}^{[u,h,\mathrm{u,h}]}\right)\sqrt{2/\pi}\exp\left(-\left(\bar{\mu}_{R,\tilde{\mathbf{v}},\tilde{\mathbf{x}}}^{[u,h,\mathrm{u,h}]}\right)^2 \Big/ 2\left(\bar{\sigma}_{R,\tilde{\mathbf{v}},\tilde{\mathbf{x}}}^{[u,h,\mathrm{u,h}]}\right)^2\right) \\ &+\bar{\mu}_{R,\tilde{\mathbf{v}},\tilde{\mathbf{x}}}^{[u,h,\mathrm{u,h}]}\left(1-2F\left(-\bar{\mu}_{R,\tilde{\mathbf{v}},\tilde{\mathbf{x}}}^{[u,h,\mathrm{u,h}]} \Big/ \bar{\sigma}_{R,\tilde{\mathbf{v}},\tilde{\mathbf{x}}}^{[u,h,\mathrm{u,h}]}\right)\right) \end{aligned} \quad 4.27$$

where $F(\bullet)$ denotes the cumulative distribution function of a standard normal distribution [45]. Moreover, $\left(\bar{\sigma}_{\tilde{\mathbf{v}},\tilde{\mathbf{x}}}^{[u,h,\mathrm{u,h}]}\right)^2 \approx \left(\bar{\sigma}_{R,\tilde{\mathbf{v}},\tilde{\mathbf{x}}}^{[u,h,\mathrm{u,h}]}\right)^2 + \left(\bar{\mu}_{R,\tilde{\mathbf{v}},\tilde{\mathbf{x}}}^{[u,h,\mathrm{u,h}]}\right)^2 + \left(\bar{\sigma}_{I,\tilde{\mathbf{v}},\tilde{\mathbf{x}}}^{[u,h,\mathrm{u,h}]}\right)^2 + \left(\bar{\mu}_{I,\tilde{\mathbf{v}},\tilde{\mathbf{x}}}^{[u,h,\mathrm{u,h}]}\right)^2 - \left(\bar{\mu}_{\tilde{\mathbf{v}},\tilde{\mathbf{x}}}^{[u,h,\mathrm{u,h}]}\right)^2$. The correlation coefficient between elements in random vector $\mathbf{A}$ is developed in appendix.

Since the random vector $\mathbf{A}$ is modeled as a multivariate normal distribution, the analytic MSE for CAF approach is

$$\hat{\varepsilon}_{\mathbf{v}} = \sum_u \sum_h \left\|\tilde{\mathbf{v}}_{u,h} - \mathbf{v}\right\|^2 \sum_{\mathrm{u}} \sum_{\mathrm{h}} \int_{\zeta} \phi_A^{[u,h,\mathrm{u,h}]}(\zeta)\Phi_{\mathbf{A}|\zeta}^{[u,h,\mathrm{u,h}]}(\zeta)\,d\zeta \quad 4.28a$$

$$\hat{\varepsilon}_{\mathbf{x}} = \sum_{\mathrm{u}} \sum_{\mathrm{h}} \left\|\tilde{\mathbf{x}}_{\mathrm{u,h}} - \mathbf{x}\right\|^2 \sum_u \sum_h \int_{\zeta} \phi_A^{[u,h,\mathrm{u,h}]}(\zeta)\Phi_{\mathbf{A}|\zeta}^{[u,h,\mathrm{u,h}]}(\zeta)\,d\zeta \quad 4.28b$$

where $\phi_A^{[u,h,\mathrm{u,h}]}(\bullet)$ is the pdf of $A^{1/2}\left(\tilde{\mathbf{v}}_{u,h}, \tilde{\mathbf{x}}_{\mathrm{u,h}}\right)$, and $\Phi_{\mathbf{A}|\zeta}^{[u,h,\mathrm{u,h}]}(\bullet)$ is the conditional cumulative distribution function (cdf) of $\mathbf{A}$ given $A^{1/2}\left(\tilde{\mathbf{v}}_{u,h}, \tilde{\mathbf{x}}_{\mathrm{u,h}}\right) = \zeta$. Moreover, the vector $\boldsymbol{\zeta} = [\zeta, ..., \zeta]$ has all identical elements. According to the basic probability theory, it is not hard to assert that the integration is the probability of $A^{1/2}\left(\hat{\mathbf{v}}, \hat{\mathbf{x}}\right) = A^{1/2}\left(\tilde{\mathbf{v}}_{u,h}, \tilde{\mathbf{x}}_{\mathrm{u,h}}\right)$.

Similar discussions about the pdf of $\mathbf{A}$ can also applied to develop the pdf of $\mathbf{ncA}$. When $\tilde{\mathbf{v}}_{u,h} \sim \mathbf{v}$ and $\tilde{\mathbf{x}}_{\mathrm{u,h}} \sim \mathbf{x}$, each square root added in $A_{nc}^{1/2}\left(\tilde{\mathbf{v}}_{u,h}, \tilde{\mathbf{x}}_{\mathrm{u,h}}\right)$ can be approximated as

the linear combination of $\left(\overline{\chi}_{R,n,m,\tilde{\mathbf{v}},\tilde{\mathbf{x}}}^{[u,h,\mathrm{u,h}]}, \overline{\chi}_{I,n,m,\tilde{\mathbf{v}},\tilde{\mathbf{x}}}^{[u,h,\mathrm{u,h}]}\right)$. Since both $\overline{\chi}_{R,n,m,\tilde{\mathbf{v}},\tilde{\mathbf{x}}}^{[u,h,\mathrm{u,h}]}$ and $\overline{\chi}_{I,n,m,\tilde{\mathbf{v}},\tilde{\mathbf{x}}}^{[u,h,\mathrm{u,h}]}$ are the summation of $K$ independent variables, the linear combination of the elements in $\left\{A_{nc}^{1/2}\left(\tilde{\mathbf{v}}_{u,h}, \tilde{\mathbf{x}}_{\mathrm{u,h}}\right), \tilde{\mathbf{v}}_{u,h} \sim \mathbf{v} \cap \tilde{\mathbf{x}}_{\mathrm{u,h}} \sim \mathbf{x}\right\}$ can be also be approximated as the linear combination of $L$ independent variables. According to Lyapunov's CLT, this combination is a normal random variable. Therefore, we can approximate the random vector $\left\{A_{nc}^{1/2}\left(\tilde{\mathbf{v}}_{u,h}, \tilde{\mathbf{x}}_{\mathrm{u,h}}\right), \tilde{\mathbf{v}}_{u,h} \sim \mathbf{v} \cap \tilde{\mathbf{x}}_{\mathrm{u,h}} \sim \mathbf{x}\right\}$ as another multivariate normal distribution.

Also for analytical simplicity, $A_{nc}^{1/2}\left(\tilde{\mathbf{v}}_{u,h}, \tilde{\mathbf{x}}_{\mathrm{u,h}}\right)$ where neither $\tilde{\mathbf{v}}_{u,h} \sim \mathbf{v}$ nor $\tilde{\mathbf{x}}_{\mathrm{u,h}} \sim \mathbf{x}$ is modeled as a normal random variable, and the pdf of the random vector **ncA** is approximated as a multivariate normal distribution. Based on previous discussion on approximating the complex amplitude formed by quadrature pairs, $\sqrt{\left(\overline{\chi}_{R,n,m,\tilde{\mathbf{v}},\tilde{\mathbf{x}}}^{[u,h,\mathrm{u,h}]}\right)^2 + \left(\overline{\chi}_{I,n,m,\tilde{\mathbf{v}},\tilde{\mathbf{x}}}^{[u,h,\mathrm{u,h}]}\right)^2}$ can be approximated as $\left|\overline{\chi}_{R,n,m,\tilde{\mathbf{v}},\tilde{\mathbf{x}}}^{[u,h,\mathrm{u,h}]}\right| + \left|\overline{\chi}_{I,n,m,\tilde{\mathbf{v}},\tilde{\mathbf{x}}}^{[u,h,\mathrm{u,h}]}\right| \Big/ 2$ if $E\left[\left|\overline{\chi}_{R,n,m,\tilde{\mathbf{v}},\tilde{\mathbf{x}}}^{[u,h,\mathrm{u,h}]}\right|\right] > E\left[\left|\overline{\chi}_{I,n,m,\tilde{\mathbf{v}},\tilde{\mathbf{x}}}^{[u,h,\mathrm{u,h}]}\right|\right]$. Then, $\widehat{\mu}_{n,m,\tilde{\mathbf{v}},\tilde{\mathbf{x}}}^{[u,h,\mathrm{u,h}]} \approx E\left[\left|\overline{\chi}_{R,n,m,\tilde{\mathbf{v}},\tilde{\mathbf{x}}}^{[u,h,\mathrm{u,h}]}\right|\right] + E\left[\left|\overline{\chi}_{I,n,m,\tilde{\mathbf{v}},\tilde{\mathbf{x}}}^{[u,h,\mathrm{u,h}]}\right|\right] \Big/ 2$, where

$$E\left[\left|\overline{\chi}_{R,n,m,\tilde{\mathbf{v}},\tilde{\mathbf{x}}}^{[u,h,\mathrm{u,h}]}\right|\right] = \left(\overline{\sigma}_{R,n,m,\tilde{\mathbf{v}},\tilde{\mathbf{x}}}^{[u,h,\mathrm{u,h}]}\right)\sqrt{2/\pi}\exp\left(-\left(\overline{\mu}_{R,n,m,\tilde{\mathbf{v}},\tilde{\mathbf{x}}}^{[u,h,\mathrm{u,h}]}\right)^2 \Big/ 2\left(\overline{\sigma}_{R,n,m,\tilde{\mathbf{v}},\tilde{\mathbf{x}}}^{[u,h,\mathrm{u,h}]}\right)^2\right) + \overline{\mu}_{R,n,m,\tilde{\mathbf{v}},\tilde{\mathbf{x}}}^{[u,h,\mathrm{u,h}]}\left(1 - 2F\left(-\overline{\mu}_{R,n,m,\tilde{\mathbf{v}},\tilde{\mathbf{x}}}^{[u,h,\mathrm{u,h}]} \Big/ \overline{\sigma}_{R,n,m,\tilde{\mathbf{v}},\tilde{\mathbf{x}}}^{[u,h,\mathrm{u,h}]}\right)\right)}, \quad 4.29$$

and

$$\left(\widehat{\sigma}_{n,m,\tilde{\mathbf{v}},\tilde{\mathbf{x}}}^{[u,h,\mathrm{u,h}]}\right)^2 \approx \left(\overline{\mu}_{R,n,m,\tilde{\mathbf{v}},\tilde{\mathbf{x}}}^{[u,h,\mathrm{u,h}]}\right)^2 + \left(\overline{\sigma}_{R,n,m,\tilde{\mathbf{v}},\tilde{\mathbf{x}}}^{[u,h,\mathrm{u,h}]}\right)^2 + \left(\overline{\mu}_{I,n,m,\tilde{\mathbf{v}},\tilde{\mathbf{x}}}^{[u,h,\mathrm{u,h}]}\right)^2 + \left(\overline{\sigma}_{I,n,m,\tilde{\mathbf{v}},\tilde{\mathbf{x}}}^{[u,h,\mathrm{u,h}]}\right)^2 - \left(\widehat{\mu}_{n,m,\tilde{\mathbf{v}},\tilde{\mathbf{x}}}^{[u,h,\mathrm{u,h}]}\right)^2. \quad 4.30$$

As a result, the mean and variance of the $A_{nc}^{1/2}\left(\tilde{\mathbf{v}}_{u,h}, \tilde{\mathbf{x}}_{\mathrm{u,h}}\right)$ are $\widehat{\mu}_{\tilde{\mathbf{v}},\tilde{\mathbf{x}}}^{[u,h,\mathrm{u,h}]} = \sum_{m=1}^{M}\sum_{n=1}^{N}\widehat{\mu}_{n,m,\tilde{\mathbf{v}},\tilde{\mathbf{x}}}^{[u,h,\mathrm{u,h}]}$, and $\left(\widehat{\sigma}_{\tilde{\mathbf{v}},\tilde{\mathbf{x}}}^{[u,h,\mathrm{u,h}]}\right)^2 = \sum_{m=1}^{M}\sum_{n=1}^{N}\left(\widehat{\sigma}_{n,m,\tilde{\mathbf{v}},\tilde{\mathbf{x}}}^{[u,h,\mathrm{u,h}]}\right)^2$, respectively. Moreover, the correlation coefficient between

elements in **ncA** can be solved by the definition and its procedure is similar to the one in the appendix.

Since **ncA** is modeled as a multivariate normal distribution, the analytic MSE for NCAF approach is

$$\hat{\varepsilon}_{nc,\mathbf{v}} = \sum_u \sum_h \left\| \tilde{\mathbf{v}}_{u,h} - \mathbf{v} \right\|^2 \sum_{\mathrm{u}} \sum_{\mathrm{h}} \int_{\zeta} \phi_{ncA}^{[u,h,\mathrm{u},\mathrm{h}]}(\zeta) \Phi_{\mathbf{ncA}|\zeta}^{[u,h,\mathrm{u},\mathrm{h}]}(\zeta) d\zeta \qquad 4.31a$$

$$\hat{\varepsilon}_{nc,\mathbf{x}} = \sum_u \sum_h \left\| \tilde{\mathbf{x}}_{u,h} - \mathbf{x} \right\|^2 \sum_{\mathrm{u}} \sum_{\mathrm{h}} \int_{\zeta} \phi_{ncA}^{[u,h,\mathrm{u},\mathrm{h}]}(\zeta) \Phi_{\mathbf{ncA}|\zeta}^{[u,h,\mathrm{u},\mathrm{h}]}(\zeta) d\zeta \qquad 4.31b$$

where $\phi_{ncA}^{[u,h,\mathrm{u},\mathrm{h}]}(\bullet)$ is the pdf of $A_{nc}^{1/2}\left(\tilde{\mathbf{v}}_{u,h}, \tilde{\mathbf{x}}_{\mathrm{u},\mathrm{h}}\right)$, and $\Phi_{\mathbf{ncA}|\zeta}^{[u,h,\mathrm{u},\mathrm{h}]}(\bullet)$ is the conditional cdf of **ncA** given $A_{nc}^{1/2}\left(\tilde{\mathbf{v}}_{u,h}, \tilde{\mathbf{x}}_{\mathrm{u},\mathrm{h}}\right) = \zeta$ . Moreover, the integration yields the probability of $A_{nc}^{1/2}\left(\hat{\mathbf{v}}, \hat{\mathbf{x}}\right) = A_{nc}^{1/2}\left(\tilde{\mathbf{v}}_{u,h}, \tilde{\mathbf{x}}_{\mathrm{u},\mathrm{h}}\right)$.

### 4.4. Performance comparison

Since both the pdfs of random vectors **A** and **ncA** are multivariate normal distributions, the relation between $E\left[A^{1/2}\left(\tilde{\mathbf{v}}_{u,h}, \tilde{\mathbf{x}}_{\mathrm{u},\mathrm{h}}\right)\right] - E\left[A^{1/2}\left(\tilde{\mathbf{v}}_{u',h'}, \tilde{\mathbf{x}}_{\mathrm{u}',\mathrm{h}'}\right)\right]$ and $E\left[A_{nc}^{1/2}\left(\tilde{\mathbf{v}}_{u,h}, \tilde{\mathbf{x}}_{\mathrm{u},\mathrm{h}}\right)\right] - E\left[A_{nc}^{1/2}\left(\tilde{\mathbf{v}}_{u',h'}, \tilde{\mathbf{x}}_{\mathrm{u}',\mathrm{h}'}\right)\right]$ is an essential factor for comparing their estimation performance, especially when $\tilde{\mathbf{v}}_{u,h} \sim \tilde{\mathbf{v}}_{u',h'} \sim \mathbf{v}$ , $\tilde{\mathbf{x}}_{\mathrm{u},\mathrm{h}} \sim \tilde{\mathbf{x}}_{\mathrm{u}',\mathrm{h}'} \sim \mathbf{x}$ , $\left\|\tilde{\mathbf{v}}_{u,h} - \mathbf{v}\right\| \le \left\|\tilde{\mathbf{v}}_{u',h'} - \mathbf{v}\right\|$ , and $\left\|\tilde{\mathbf{x}}_{\mathrm{u},\mathrm{h}} - \mathbf{x}\right\| \le \left\|\tilde{\mathbf{x}}_{\mathrm{u}',\mathrm{h}'} - \mathbf{x}\right\|$ . For example, if the difference between $E\left[A^{1/2}\left(\tilde{\mathbf{v}}_{u,h}, \tilde{\mathbf{x}}_{\mathrm{u},\mathrm{h}}\right)\right]$ and $E\left[A^{1/2}\left(\tilde{\mathbf{v}}_{u',h'}, \tilde{\mathbf{x}}_{\mathrm{u}',\mathrm{h}'}\right)\right]$ is larger than the difference between $E\left[A_{nc}^{1/2}\left(\tilde{\mathbf{v}}_{u,h}, \tilde{\mathbf{x}}_{\mathrm{u},\mathrm{h}}\right)\right]$ and $E\left[A_{nc}^{1/2}\left(\tilde{\mathbf{v}}_{u',h'}, \tilde{\mathbf{x}}_{\mathrm{u}',\mathrm{h}'}\right)\right]$, it could imply that the probability of $A^{1/2}\left(\tilde{\mathbf{v}}_{u',h'}, \tilde{\mathbf{x}}_{\mathrm{u}',\mathrm{h}'}\right) > A^{1/2}\left(\tilde{\mathbf{v}}_{u,h}, \tilde{\mathbf{x}}_{\mathrm{u},\mathrm{h}}\right)$ is smaller than the probability of $A_{nc}^{1/2}\left(\tilde{\mathbf{v}}_{u',h'}, \tilde{\mathbf{x}}_{\mathrm{u}',\mathrm{h}'}\right) > A_{nc}^{1/2}\left(\tilde{\mathbf{v}}_{u,h}, \tilde{\mathbf{x}}_{\mathrm{u},\mathrm{h}}\right)$, causing the CAF to achieve

smaller MSE than the NCAF. According to previous discussions, under certain assumptions, the differences between the expected values could be expressed as

$$E\left[A^{1/2}\left(\tilde{\mathbf{v}}_{u,h},\tilde{\mathbf{x}}_{\mathrm{u,h}}\right)\right]-E\left[A^{1/2}\left(\tilde{\mathbf{v}}_{u',h'},\tilde{\mathbf{x}}_{\mathrm{u',h'}}\right)\right]\approx\left|\bar{\mu}_{R,\tilde{\mathbf{v}},\tilde{\mathbf{x}}}^{[u,h,\mathrm{u,h}]}\right|-\left|\bar{\mu}_{R,\tilde{\mathbf{v}},\tilde{\mathbf{x}}}^{[u',h',\mathrm{u',h'}]}\right| + \frac{\left(\bar{\mu}_{I,\tilde{\mathbf{v}},\tilde{\mathbf{x}}}^{[u,h,\mathrm{u,h}]}\right)^2+\left(1-\left(\bar{\rho}_{\tilde{\mathbf{v}},\tilde{\mathbf{x}}}^{[u,h,\mathrm{u,h}]}\right)^2\right)\left(\bar{\sigma}_{I,\tilde{\mathbf{v}},\tilde{\mathbf{x}}}^{[u,h,\mathrm{u,h}]}\right)^2}{\left|2\bar{\mu}_{R,\tilde{\mathbf{v}},\tilde{\mathbf{x}}}^{[u,h,\mathrm{u,h}]}\right|} - \frac{\left(\bar{\mu}_{I,\tilde{\mathbf{v}},\tilde{\mathbf{x}}}^{[u',h',\mathrm{u',h'}]}\right)^2+\left(1-\left(\bar{\rho}_{\tilde{\mathbf{v}},\tilde{\mathbf{x}}}^{[u',h',\mathrm{u',h'}]}\right)^2\right)\left(\bar{\sigma}_{I,\tilde{\mathbf{v}},\tilde{\mathbf{x}}}^{[u',h',\mathrm{u',h'}]}\right)^2}{\left|2\bar{\mu}_{R,\tilde{\mathbf{v}},\tilde{\mathbf{x}}}^{[u',h',\mathrm{u',h'}]}\right|}$$

4.32

and

$$E\left[A_{nc}^{1/2}\left(\tilde{\mathbf{v}}_{u,h},\tilde{\mathbf{x}}_{\mathrm{u,h}}\right)\right]-E\left[A_{nc}^{1/2}\left(\tilde{\mathbf{v}}_{u',h'},\tilde{\mathbf{x}}_{\mathrm{u',h'}}\right)\right]\approx\hat{\mu}_{\tilde{\mathbf{v}},\tilde{\mathbf{x}}}^{[u,h,\mathrm{u,h}]}-\hat{\mu}_{\tilde{\mathbf{v}},\tilde{\mathbf{x}}}^{[u',h',\mathrm{u',h'}]}$$
$$=\sum_{m=1}^{M}\sum_{n=1}^{N}\left|\bar{\mu}_{R,n,m,\tilde{\mathbf{v}},\tilde{\mathbf{x}}}^{[u,h,\mathrm{u,h}]}\right|-\left|\bar{\mu}_{R,n,m,\tilde{\mathbf{v}},\tilde{\mathbf{x}}}^{[u',h',\mathrm{u',h'}]}\right|$$
$$+\sum_{m=1}^{M}\sum_{n=1}^{N}\left[\frac{\left(\bar{\mu}_{I,n,m,\tilde{\mathbf{v}},\tilde{\mathbf{x}}}^{[u,h,\mathrm{u,h}]}\right)^2+\left(1-\left(\bar{\rho}_{n,m,\tilde{\mathbf{v}},\tilde{\mathbf{x}}}^{[u,h,\mathrm{u,h}]}\right)^2\right)\left(\bar{\sigma}_{I,n,m,\tilde{\mathbf{v}},\tilde{\mathbf{x}}}^{[u,h,\mathrm{u,h}]}\right)^2}{\left|2\bar{\mu}_{R,n,m,\tilde{\mathbf{v}},\tilde{\mathbf{x}}}^{[u,h,\mathrm{u,h}]}\right|} - \frac{\left(\bar{\mu}_{I,n,m,\tilde{\mathbf{v}},\tilde{\mathbf{x}}}^{[u',h',\mathrm{u',h'}]}\right)^2+\left(1-\left(\bar{\rho}_{n,m,\tilde{\mathbf{v}},\tilde{\mathbf{x}}}^{[u',h',\mathrm{u',h'}]}\right)^2\right)\left(\bar{\sigma}_{I,n,m,\tilde{\mathbf{v}},\tilde{\mathbf{x}}}^{[u',h',\mathrm{u',h'}]}\right)^2}{\left|2\bar{\mu}_{R,n,m,\tilde{\mathbf{v}},\tilde{\mathbf{x}}}^{[u',h',\mathrm{u',h'}]}\right|}\right]$$

4.33

where $\left|\bar{\mu}_{R,\tilde{\mathbf{v}},\tilde{\mathbf{x}}}^{[u,h,\mathrm{u,h}]}\right|-\left|\bar{\mu}_{R,\tilde{\mathbf{v}},\tilde{\mathbf{x}}}^{[u',h',\mathrm{u',h'}]}\right|$ and $\sum_{m=1}^{M}\sum_{n=1}^{N}\left|\bar{\mu}_{R,n,m,\tilde{\mathbf{v}},\tilde{\mathbf{x}}}^{[u,h,\mathrm{u,h}]}\right|-\left|\bar{\mu}_{R,n,m,\tilde{\mathbf{v}},\tilde{\mathbf{x}}}^{[u',h',\mathrm{u',h'}]}\right|$ are the more significant terms in 4.32 and 4.33 respectively. Since $\tilde{\mathbf{v}}_{u,h}\sim\tilde{\mathbf{v}}_{u',h'}$, and $\tilde{\mathbf{x}}_{\mathrm{u,h}}\sim\tilde{\mathbf{x}}_{\mathrm{u',h'}}$, the sign of $\bar{\mu}_{R,\tilde{\mathbf{v}},\tilde{\mathbf{x}}}^{[u,h,\mathrm{u,h}]}$ should be the same as the sign of $\bar{\mu}_{R,\tilde{\mathbf{v}},\tilde{\mathbf{x}}}^{[u',h',\mathrm{u',h'}]}$ in 4.32. Moreover, $\left\|\tilde{\mathbf{v}}_{u,h}-\mathbf{v}\right\|\le\left\|\tilde{\mathbf{v}}_{u',h'}-\mathbf{v}\right\|$ and $\left\|\tilde{\mathbf{x}}_{\mathrm{u,h}}-\mathbf{x}\right\|\le\left\|\tilde{\mathbf{x}}_{\mathrm{u',h'}}-\mathbf{x}\right\|$ lead to $\left|\bar{\mu}_{R,\tilde{\mathbf{v}},\tilde{\mathbf{x}}}^{[u,h,\mathrm{u,h}]}\right|>\left|\bar{\mu}_{R,\tilde{\mathbf{v}},\tilde{\mathbf{x}}}^{[u',h',\mathrm{u',h'}]}\right|$, and their difference can be represented as

$$\left|\bar{\mu}_{R,\tilde{\mathbf{v}},\tilde{\mathbf{x}}}^{[u,h,\mathrm{u,h}]}\right|-\left|\bar{\mu}_{R,\tilde{\mathbf{v}},\tilde{\mathbf{x}}}^{[u',h',\mathrm{u',h'}]}\right|=\left|\sum_{m=1}^{M}\sum_{n=1}^{N}\bar{\mu}_{R,n,m,\tilde{\mathbf{v}},\tilde{\mathbf{x}}}^{[u,h,\mathrm{u,h}]}-\bar{\mu}_{R,n,m,\tilde{\mathbf{v}},\tilde{\mathbf{x}}}^{[u',h',\mathrm{u',h'}]}\right|. \quad 4.34$$

Similarly, $\overline{\mu}_{R,n,m,\tilde{\mathbf{v}},\tilde{\mathbf{x}}}^{[u,h,\mathrm{u},\mathrm{h}]}$ and $\overline{\mu}_{R,n,m,\tilde{\mathbf{v}},\tilde{\mathbf{x}}}^{[u',h',\mathrm{u}',\mathrm{h}']}$ in 4.33 should have the same sign, and $\left|\overline{\mu}_{R,n,m,\tilde{\mathbf{v}},\tilde{\mathbf{x}}}^{[u,h,\mathrm{u},\mathrm{h}]}\right| > \left|\overline{\mu}_{R,n,m,\tilde{\mathbf{v}},\tilde{\mathbf{x}}}^{[u',h',\mathrm{u}',\mathrm{h}']}\right|$. Therefore,

$$\sum_{m=1}^{M}\sum_{n=1}^{N}\left|\overline{\mu}_{R,n,m,\tilde{\mathbf{v}},\tilde{\mathbf{x}}}^{[u,h,\mathrm{u},\mathrm{h}]}\right| - \left|\overline{\mu}_{R,n,m,\tilde{\mathbf{v}},\tilde{\mathbf{x}}}^{[u',h',\mathrm{u}',\mathrm{h}']}\right| = \sum_{m=1}^{M}\sum_{n=1}^{N}\left|\overline{\mu}_{R,n,m,\tilde{\mathbf{v}},\tilde{\mathbf{x}}}^{[u,h,\mathrm{u},\mathrm{h}]} - \overline{\mu}_{R,n,m,\tilde{\mathbf{v}},\tilde{\mathbf{x}}}^{[u',h',\mathrm{u}',\mathrm{h}']}\right| \tag{4.35}$$

Recall the expression of $\mu_{R,n,m,\ell,\tilde{\mathbf{v}},\tilde{\mathbf{x}}}^{[u,h,\mathrm{u},\mathrm{h}]}$ in 4.11. We can obtain

$$\overline{\mu}_{R,n,m,\tilde{\mathbf{v}},\tilde{\mathbf{x}}}^{[u,h,\mathrm{u},\mathrm{h}]} - \overline{\mu}_{R,n,m,\tilde{\mathbf{v}},\tilde{\mathbf{x}}}^{[u',h',\mathrm{u}',\mathrm{h}']} = \alpha_{R,n,m}\varphi_{R,n,m} + \alpha_{I,n,m}\varphi_{I,n,m} \tag{4.36}$$

where

$$\begin{aligned}
\varphi_{R,n,m} &= \sigma_s^2\sum_{\ell=1}^{L}\left(\cos\left(2\pi f_c D_{\ell,n,m,\tilde{\mathbf{v}},\tilde{\mathbf{x}}}^{[u,h,\mathrm{u},\mathrm{h}]}\right)\mathrm{sinc}\left(B\times D_{\ell,n,m,\tilde{\mathbf{v}},\tilde{\mathbf{x}}}^{[u,h,\mathrm{u},\mathrm{h}]}\right) - \cos\left(2\pi f_c D_{\ell,n,m,\tilde{\mathbf{v}},\tilde{\mathbf{x}}}^{[u',h',\mathrm{u}',\mathrm{h}']}\right)\mathrm{sinc}\left(B\times D_{\ell,n,m,\tilde{\mathbf{v}},\tilde{\mathbf{x}}}^{[u',h',\mathrm{u}',\mathrm{h}']}\right)\right)\\
\varphi_{I,n,m} &= \sigma_s^2\sum_{\ell=1}^{L}\left(\sin\left(2\pi f_c D_{\ell,n,m,\tilde{\mathbf{v}},\tilde{\mathbf{x}}}^{[u,h,\mathrm{u},\mathrm{h}]}\right)\mathrm{sinc}\left(B\times D_{\ell,n,m,\tilde{\mathbf{v}},\tilde{\mathbf{x}}}^{[u,h,\mathrm{u},\mathrm{h}]}\right) - \sin\left(2\pi f_c D_{\ell,n,m,\tilde{\mathbf{v}},\tilde{\mathbf{x}}}^{[u',h',\mathrm{u}',\mathrm{h}']}\right)\mathrm{sinc}\left(B\times D_{\ell,n,m,\tilde{\mathbf{v}},\tilde{\mathbf{x}}}^{[u',h',\mathrm{u}',\mathrm{h}']}\right)\right)
\end{aligned} \tag{4.37}$$

When the reflectivities for all transmitter and receiver antenna pairs are equal, the CAF approach outperforms the NCAF approach [19]. In our perspective, according to 4.36, the equal reflectivity causes $4.34 \approx 4.35$. On the other hand, in spatial diversity MIMO radar systems, when the reflectivity values for different transmit and receive antenna pair are totally uncorrelated with each other. This leads to 4.35 being considerably larger than 4.34, and thus the NCAF approach is able to achieve better estimation accuracy.

### 4.5. Simulation results

In this section, we will demonstrate three arguments via numerical examples. First, we will show it is proper to approximate the pdfs of $A^{1/2}\left(\tilde{\mathbf{v}}_{u,h},\tilde{\mathbf{x}}_{\mathrm{u},\mathrm{h}}\right)$ and $A_{nc}^{1/2}\left(\tilde{\mathbf{v}}_{u,h},\tilde{\mathbf{x}}_{\mathrm{u},\mathrm{h}}\right)$ as normal distributions especially when $\tilde{\mathbf{v}}_{u,h} \sim \mathbf{v}$, and $\tilde{\mathbf{x}}_{\mathrm{u},\mathrm{h}} \sim \mathbf{x}$. Then, we convince ourselves that applying

multivariate normal distributions to model the pdfs of random vectors $\mathbf{A}$ and $\mathbf{ncA}$ is sufficient. Next, we confirm NCAF outperforms CAF in spatial diversity MIMO radar systems. Several different considerations will be involved in the demonstrations. Last, we also discuss the effects of step size on the MSE.

Two different transmit and receive antennas combinations are considered in the simulation. For the first, four transmit and two receive static antennas are in the MIMO system where $\left\{\theta_1^t, \theta_2^t, \theta_3^t, \theta_4^t\right\} = \left\{35°, 45°, 55°, 65°\right\}$, and $\left\{\theta_1^r, \theta_2^r\right\} = \left\{-45°, -55°\right\}$. For the second, four transmit and four receive static antennas are in the MIMO system where all $\theta_n^t$ are the same with the angles in the first case, and $\left\{\theta_1^r, \theta_2^r, \theta_3^r, \theta_4^r\right\} = \left\{-35°, -45°, -55°, -65°\right\}$. Assume the velocity and location vectors of a moving target are $\mathbf{v} = \left(100.3, 0\right)$ m/s and $\mathbf{x} = \left(19.5, 0\right)$ cm where both $v_y$ and $y$ are assumed and known to be 0 to reduce the number of parameters to be estimated. Moreover, this target is illuminated by the noise signals with $B = 1$ GHz, and $f_c = 1.5$ GHz, and the observed and sample duration are $T_o = 0.1$ s and $t_s = 1$ ms respectively.

In order to show that approximating $A^{1/2}\left(\tilde{\mathbf{v}}_{u,h}, \tilde{\mathbf{x}}_{\mathrm{u,h}}\right)$ and $A_{nc}^{1/2}\left(\tilde{\mathbf{v}}_{u,h}, \tilde{\mathbf{x}}_{\mathrm{u,h}}\right)$ as normal random variables is indeed appropriate, we demonstrate their unbiased skewness, which is a parameter to evaluate the adequacy of the normal approximation [50], with different signal to noise power ratios (SNRs) in Figure 4.2. The skewness is obtained using Monte Carlo simulations with 2000 iterations for each $\left(\tilde{v}_{x,u}, \tilde{x}_{\mathrm{u}}\right)$ combination. The SNR is defined as $\sum_{n=1}^{N}\sum_{m=1}^{M}\left\|\alpha_{n,m}\right\|^2 \sigma_s^2 \Big/ \sigma_z^2$. Two reflectivity sets are discussed. For the first, all $\alpha_{n,m} = 1/\sqrt{NM}$. For the second, $\alpha_{n,m}$ are evenly dispersed on the circle with radius $1/\sqrt{NM}$ in a polar coordinate

system. Since in both reflectivity sets $\left|\alpha_{n,m}\right| = 1/\sqrt{NM}$ , the skewness of NCAF results do not change much in different sets, and only the skewness values with equal reflectivity are shown. Since $\sum_{n=1}^{N}\sum_{m=1}^{M}\left\|\alpha_{n,m}\right\|^2 = 1$, SNR is further equal to $\sigma_s^2/\sigma_z^2$ . The x-axis and y-axis in the figures are the values of $\tilde{x}_{\mathrm{u}} - x$ in units of $c/B$ , and the values of $\tilde{v}_{x,u} - v_x$ in units of $c/f_cT_o$ respectively.

In almost every plot in Figure 4.2, we first observe that the center is much darker than the surrounding region. This is consistent with our previous discussion that when $\tilde{\mathbf{v}}_{u,h} \sim \mathbf{v}$ and $\tilde{\mathbf{x}}_{\mathrm{u,h}} \sim \mathbf{x}$ , $A^{1/2}\left(\tilde{\mathbf{v}}_{u,h}, \tilde{\mathbf{x}}_{\mathrm{u,h}}\right)$ and $A_{nc}^{1/2}\left(\tilde{\mathbf{v}}_{u,h}, \tilde{\mathbf{x}}_{\mathrm{u,h}}\right)$ are very close to normal random variables. We also notice that the skewness of $A^{1/2}\left(\tilde{\mathbf{v}}_{u,h}, \tilde{\mathbf{x}}_{\mathrm{u,h}}\right)$ is more sensitive to SNR than the skewness of $A_{nc}^{1/2}\left(\tilde{\mathbf{v}}_{u,h}, \tilde{\mathbf{x}}_{\mathrm{u,h}}\right)$ . For example, comparing Figure 4.2 (a) and (b), the darkest area is shrunk. Moreover, in Figure 4.2 (f), even the center is not noticeably darker. However, Figure 4.2 (c) and (d) are not much different. Third, in general, the skewness of $A^{1/2}\left(\tilde{\mathbf{v}}_{u,h}, \tilde{\mathbf{x}}_{\mathrm{u,h}}\right)$ is larger than the skewness of $A_{nc}^{1/2}\left(\tilde{\mathbf{v}}_{u,h}, \tilde{\mathbf{x}}_{\mathrm{u,h}}\right)$ and this phenomenon implies the difference between analytical and simulated results in the NCAF approach will be smaller than the one in the CAF approach. Finally, the information involved in the skewness plots for $4 \times 4$ MIMO radar system were found to be very similar with the above discussions. Because of limited space, they are not shown.

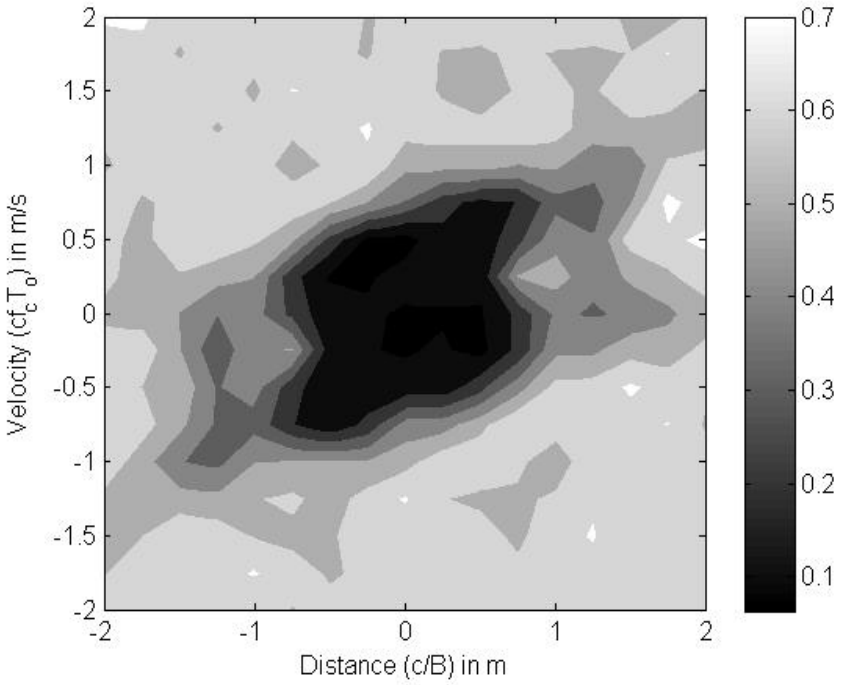
Velocity (cf$_c$T$_o$) in m/s
Distance (c/B) in m
2
1.5
1
0.5
0
-0.5
-1
-1.5
-2
0.7
0.6
0.5
0.4
0.3
0.2
0.1

(a)

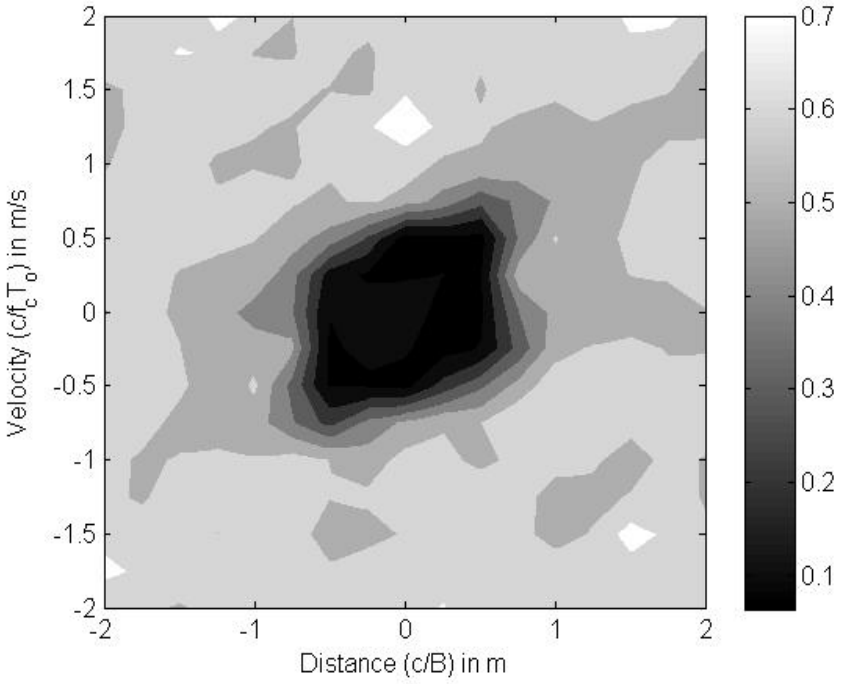
Velocity (cf$_c$T$_o$) in m/s
Distance (c/B) in m
2
1.5
1
0.5
0
-0.5
-1
-1.5
-2
0.7
0.6
0.5
0.4
0.3
0.2
0.1

(b)

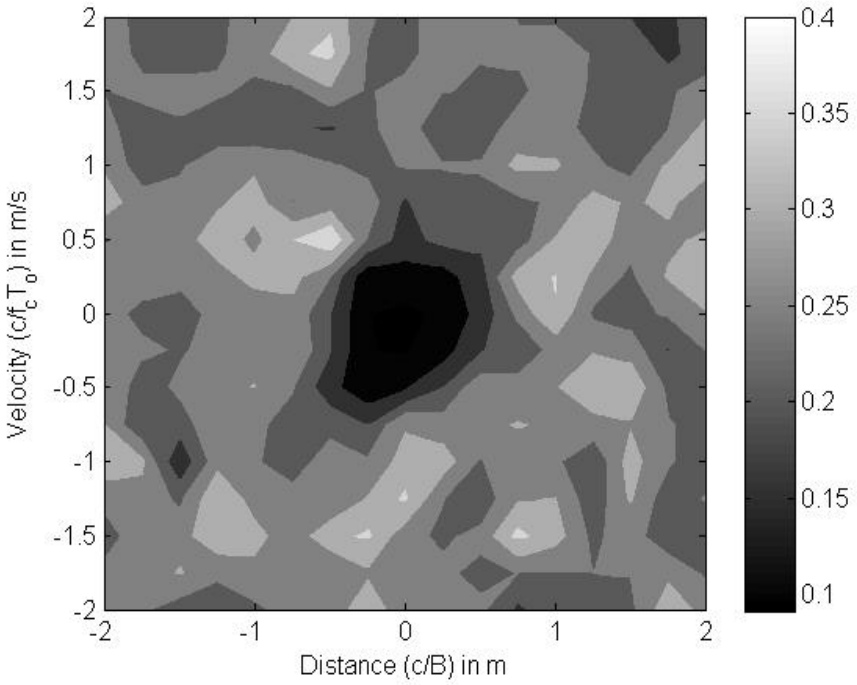
Velocity (c/f$_c$T$_o$) in m/s
Distance (c/B) in m
2
1.5
1
0.5
0
-0.5
-1
-1.5
-2
-2
-1
0
1
2
0.4
0.35
0.3
0.25
0.2
0.15
0.1

(c)

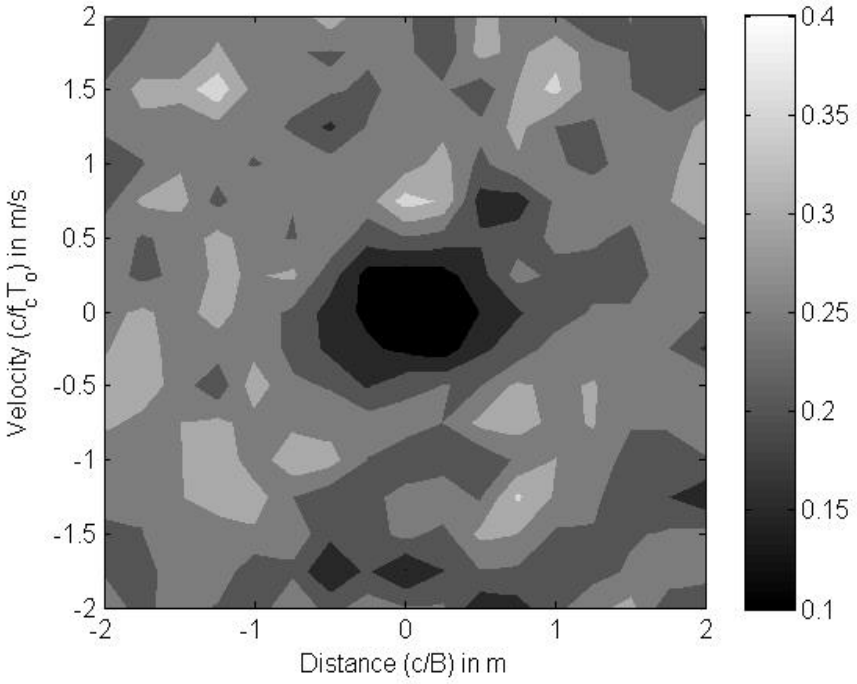
Velocity (c/f$_c$T$_o$) in m/s
Distance (c/B) in m
2
1.5
1
0.5
0
-0.5
-1
-1.5
-2
-2
-1
0
1
2
0.4
0.35
0.3
0.25
0.2
0.15
0.1

(d)

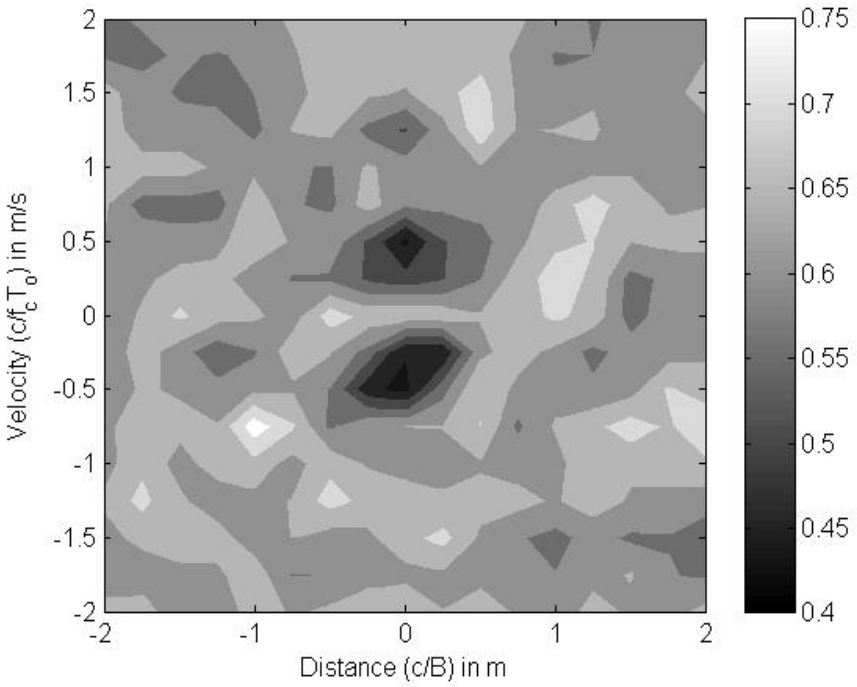
Velocity (c/f$_c$T$_o$) in m/s
Distance (c/B) in m
2
1.5
1
0.5
0
-0.5
-1
-1.5
-2
-2
-1
0
1
2
0.75
0.7
0.65
0.6
0.55
0.5
0.45
0.4

(e)

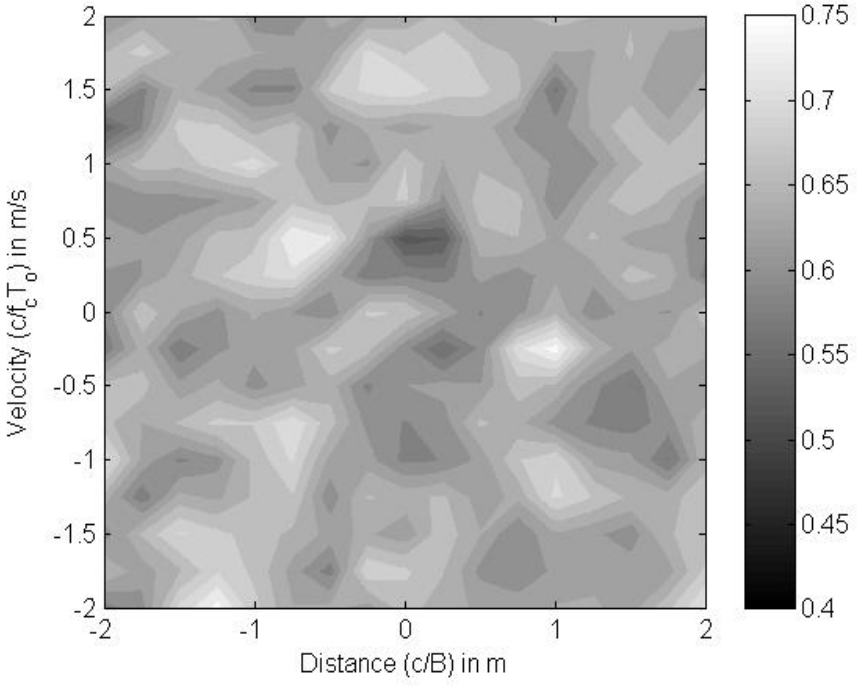
Velocity (c/f$_c$T$_o$) in m/s
Distance (c/B) in m
2
1.5
1
0.5
0
-0.5
-1
-1.5
-2
-2
-1
0
1
2
0.75
0.7
0.65
0.6
0.55
0.5
0.45
0.4

(f)

Figure 4.2: Skewness resulting from different approaches for $4\times 2$ MIMO (a) CAF, SNR= 0 dB, equal $\alpha_{n,m}$, (b) CAF, SNR= -5 dB, equal $\alpha_{n,m}$, (c) NCAF, SNR= 0 dB, equal $\alpha_{n,m}$, (d) NCAF, SNR= -5 dB, equal $\alpha_{n,m}$, (e) CAF, SNR= 0 dB, evenly dispersed $\alpha_{n,m}$, (f) CAF, SNR= -5 dB, evenly dispersed $\alpha_{n,m}$.

We also demonstrate the approximations that the distributions of the random **A** and **ncA** are multivariate normal pdfs by comparing the analytical and simulated MSE in Figure 4.3. The ranges of $(\tilde{v}_x, \tilde{x})$ for joint target velocity and location estimation are $[98,102]$ m/s and $[0,30]$ cm. Moreover, the step size, $\Delta\tilde{v}_x = c/2f_cT_o = 1$ m/s and $\Delta\tilde{x} = c/2B = 7.5$ cm. Simulation results are collected by using Monte Carlo simulations with 2000 iterations and displayed in the solid lines. The dashed lines represent analytical results which are obtained from 4.28, and 4.31. Moreover, evenly dispersed and equal reflectivity considerations are briefly denoted as "Ed. refl." and "Equ. refl." Since in both reflectivity sets $|\alpha_{n,m}| = 1/\sqrt{NM}$, the performance of NCAF approach does not depend on them at all.

According to these plots, since the analytic results are very similar with the simulations in all cases, we can conclude that multivariate normal pdfs approximate the distributions of **ncA** and **A** well. Moreover, we also substantiate that the CAF approach performance is better than the NCAF performance when all $\alpha_{n,m} = 1/\sqrt{NM}$ and is worse when $\alpha_{n,m}$ are evenly dispersed. This conclusion is consistent with the discussions in previous section that the difference between 4.34 and 4.35 determines the result of performance comparison.

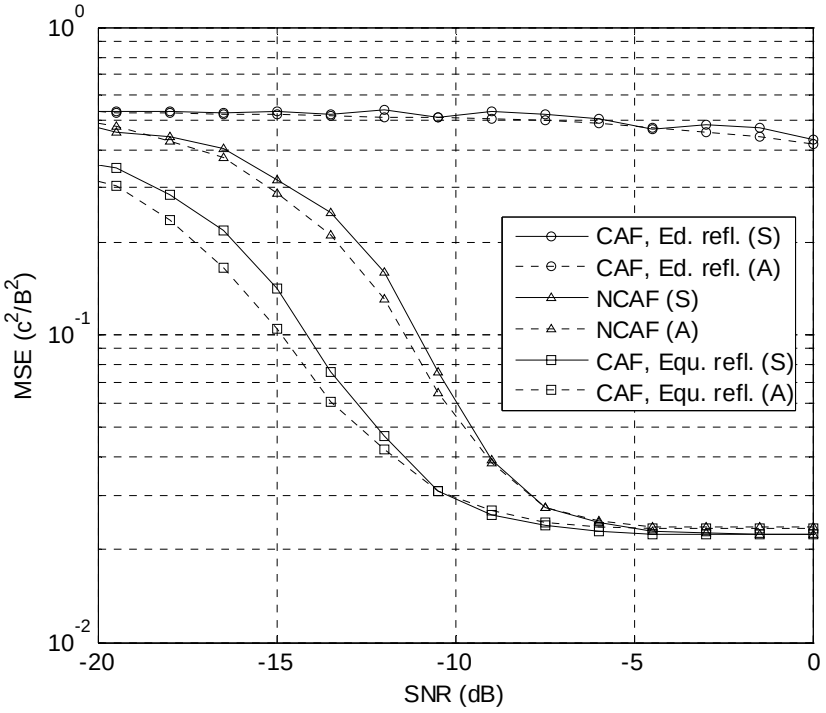
MSE (c²/B²)
SNR (dB)
CAF, Ed. refl. (S)
CAF, Ed. refl. (A)
NCAF (S)
NCAF (A)
CAF, Equ. refl. (S)
CAF, Equ. refl. (A)

(a)

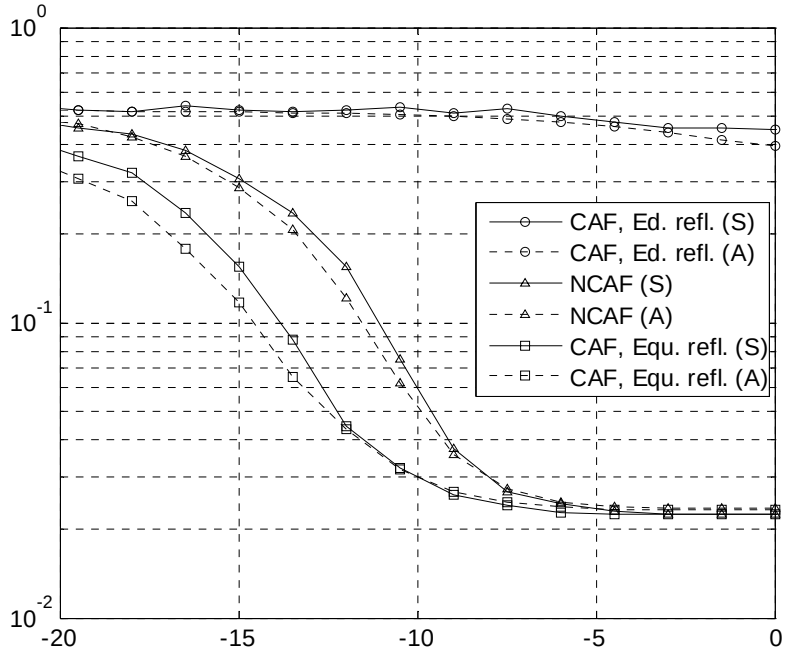
CAF, Ed. refl. (S)
CAF, Ed. refl. (A)
NCAF (S)
NCAF (A)
CAF, Equ. refl. (S)
CAF, Equ. refl. (A)

(b)

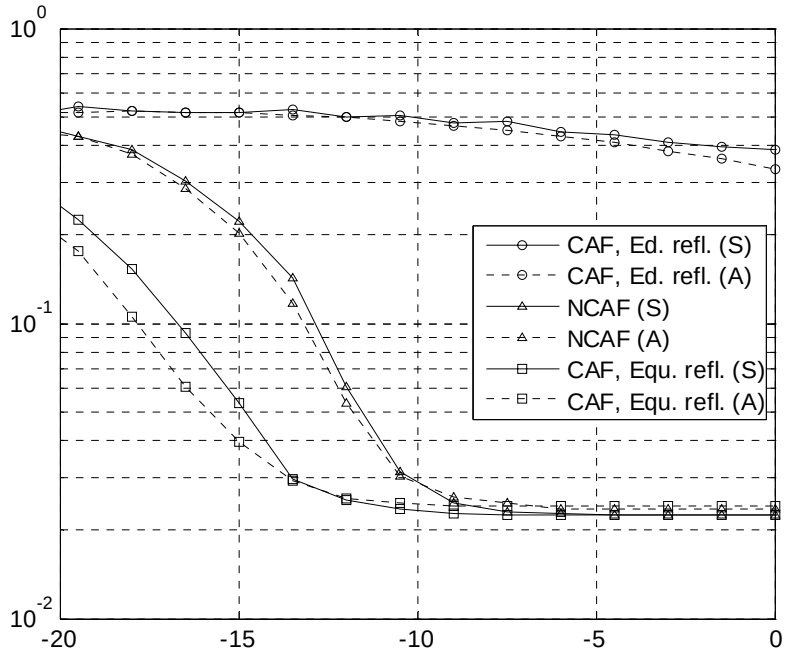
10^0
10^-1
10^-2
-20
-15
-10
-5
0
CAF, Ed. refl. (S)
CAF, Ed. refl. (A)
NCAF (S)
NCAF (A)
CAF, Equ. refl. (S)
CAF, Equ. refl. (A)

(c)

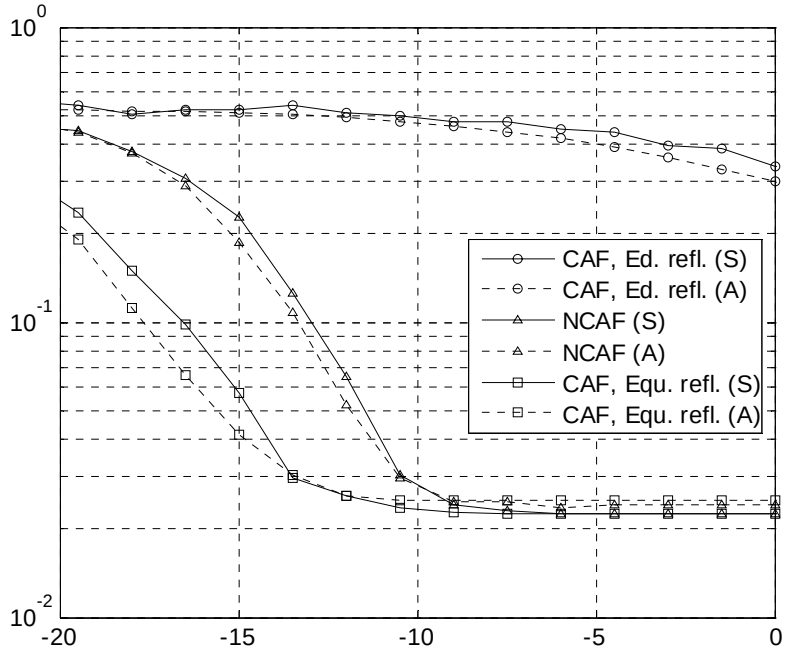
10^0
10^-1
10^-2
-20
-15
-10
-5
0
CAF, Ed. refl. (S)
CAF, Ed. refl. (A)
NCAF (S)
NCAF (A)
CAF, Equ. refl. (S)
CAF, Equ. refl. (A)

(d)

Figure 4.3: Estimation MSE of (a) location, $4\times 2$ MIMO, (b) velocity, $4\times 2$ MIMO, (c) location, $4\times 4$ MIMO, (d) velocity, $4\times 4$ MIMO with deterministic reflectivity when location and velocity are jointly estimated.

Next, we show that the NCAF approach is the better estimation option in spatial diversity MIMO radar systems. In order to simulate the variation and independence of reflectivity in spatial diversity MIMO radar system, every reflectivity changes during Monte Carlo iteration and is uncorrelated with others. Moreover, the real and imagery part of each reflectivity are model as two independent normal random variables with zero mean and variance $1/2MN$ . We do not need to adjust much in the analyses for this modification. Multivariate normal pdfs are still applied to model the distributions of $\mathbf{ncA}$ and $\mathbf{A}$ , but since the reflectivity is a random variable, the statistical parameters related with reflectivity must be recalculated. The simulation and analytical results are exhibited in Figure 4.4 which not only demonstrates that the NCAF approach surpasses the CAF approach in both $4\times 2$ and $4\times 4$ MIMO radar systems, but also reflects the discussions in Figure 4.2 that the analytical results are more accurate in the NCAF approach. Since plots for velocity and location estimation MSE are similar, only the location result is shown.

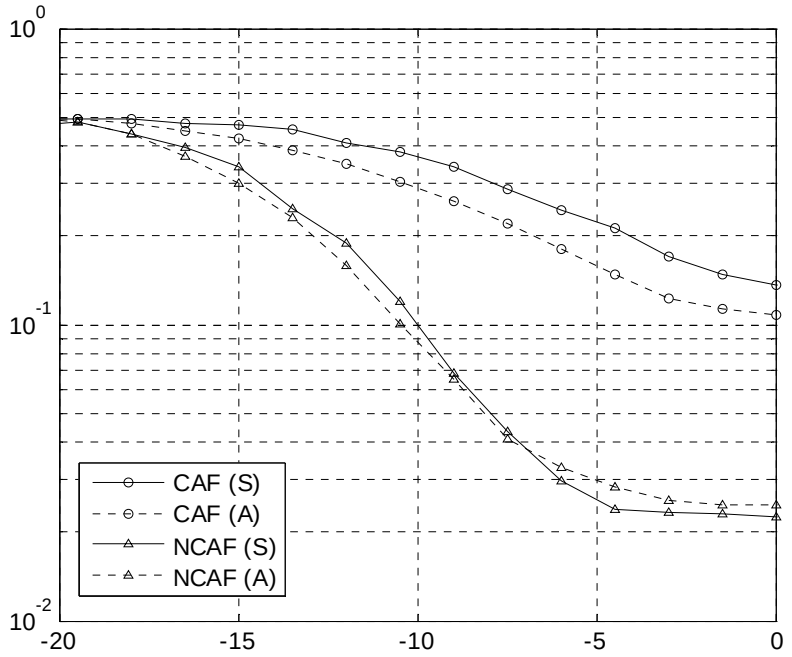
10^0
10^-1
10^-2
-20
-15
-10
-5
0
CAF (S)
CAF (A)
NCAF (S)
NCAF (A)

(a)

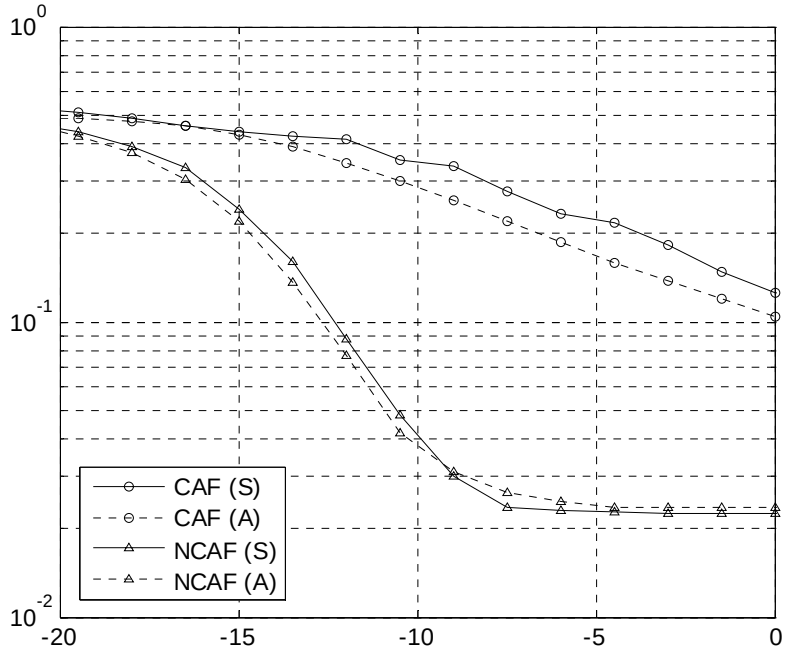
10^0
10^-1
10^-2
-20
-15
-10
-5
0
CAF (S)
CAF (A)
NCAF (S)
NCAF (A)

(b)

Figure 4.4: MSE of location estimation for (a) $4 \times 2$ MIMO, (b) $4 \times 4$ MIMO with varying reflectivity when location and velocity are jointly estimated.

Last, we concentrate on the effects of $\Delta\tilde{x}$. In Figure 4.5, we assume that the target velocity is known and the range of $\tilde{x}$ is $[-30, 60]$ cm. Two different step sizes $\Delta\tilde{x} = c/2B = 7.5$ cm and $\Delta\tilde{x} = c/4B = 3.75$ cm are considered. This figure shows the analytical conclusion can also be applied to one parameter estimation with different step sizes. Moreover, decreasing the step size is helpful in improving the estimation accuracy and reducing the error floor in the NCAF approach.

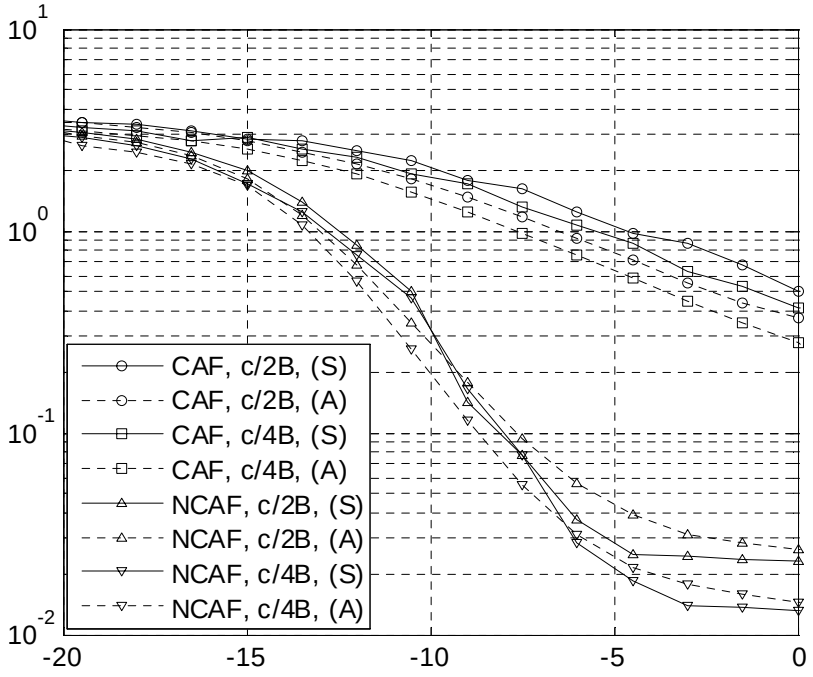


(a)

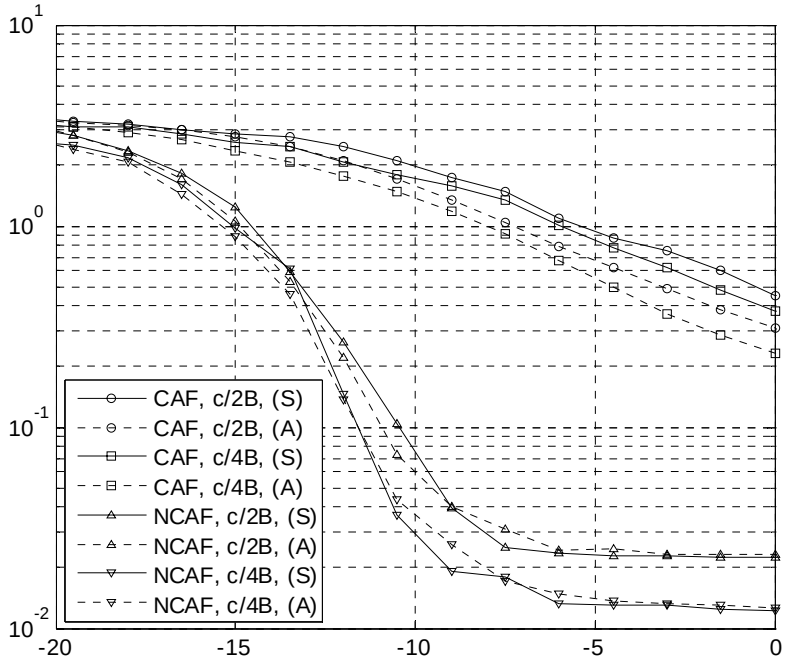


(b)

Figure 4.5: MSE of location estimation for (a) $4 \times 2$ MIMO, (b) $4 \times 4$ MIMO with varying reflectivity and different step sizes when only location is estimated.

# Chapter 5

## Conclusions and future work

We have discussed the requirements for and advantages of applying UWB noise waveform in spatial diversity MIMO radar. We notice the criteria in limiting reflected power variation for UWB noise waveform is still achieved by widely separated transmitter antennas. Moreover, its wide bandwidth is also helpful to further reduce the variation.

Then, we propose a direction finding mechanism which is able to function well in multitarget and strong jammer environments with limited observed data in UWB MIMO noise radar. This algorithm is integrated by TDL based beamforming and CGLRT. The weights in the TDL beamformer are designed to maintain the desired signal power and suppress interference. The CGLRT algorithm checks the target existence in the pre-steered direction. Since the test is the ratio of received power to the power of residual signals which results from the CLEAN algorithm, it can distinguish target reflections from jammer signals. Moreover, we further developed this mechanism and proposed an iterative CGLRT to sequentially detect targets. We have demonstrated the iteration is able to successfully extract targets which were originally embedded in other targets reflections and to sequentially improve the accuracy of target direction estimation by simulation results.

We noticed that the target direction estimation accuracy depends on the target angle and the interferences from other directions. It should be helpful to clarify their relation, if we further formulate it. The analysis should start from modeling the errors of reflectivity resulted from the CLEAN algorithm. Then, we could develop the joint pdf of likelihood ratios from different directions. According to the joint pdf, the probability that mis-decided the target direction could be determined. Finally, we can solve the mean square error of the target direction estimation.

Next, we move to estimate the velocity and location of a moving target. Doppler stretch is considered in the noise modulated amplitude. Moreover, the delay time and Doppler stretch are jointly estimated by coherent and non-coherent ambiguity function based approaches with limited data, and their results with different parameters in reference signals are denoted as random vectors, $\mathbf{A}$ and $\mathbf{ncA}$ respectively. We approximated the pdfs of $\mathbf{A}$ and of $\mathbf{ncA}$ as multivariate normal distributions to analyze the estimation MSE in MIMO UWB noise radar systems. Moreover, we demonstrated the adequacy of this approximation by illustrating the skewness of their elements and the consistence between simulation and analytical MSE results. We also noticed that the analytical results could better correspond to the simulation results in NCAF than in CAF. Based on pdf approximations and related simulation results, we explained and concluded that the NCAF approach can achieve better estimation performance in spatial diversity MIMO systems. Finally, we further studied the influence of the step size and showed smaller the step size, smaller the estimation error.

In target location and velocity estimation issues, the estimation performance should depend on the locations of observers. If the relation between estimation accuracy and the locations of observers can be determined, and if the pdf of target location could be assumed, it will be possible to solve the observers' locations for better estimation results.

Moreover, only one target is considered in our discussion. It might be advantageous to extend our results to multitarget and a strong jammer environment. In order to complete the extension, several modifications to signal model should be addressed. First of all, TDL based beamforming technique is clearly required. Then, with the proper constraint function, the TDL output of the $m$ -th subarray could be also represented as equation 4.1, where $z_m(t)$ involves not only thermal noise, but also other reflections and jamming signals. Since both the amplitudes of reflections and jamming signals are Gaussian distributed, and the operation in TDL is the linear

combination of time delay signals, $z_m(t)$ could also be modeled as a complex Gaussian random variable with correlated real and imaginary parts of $z_m(t)$. This correlation affects the following developments and the parameters for the joint Gaussian approximations need to be further investigated.

# Bibliography


[1] B. M. Horton, "Noise-modulated distance measuring systems," *Proceedings of the IRE*, vol. 47, no. 5, pp. 821-828, May 1959.

[2] S.E. Craig, W. Fishbein, and O.E. Rittenbach, "Continuous-wave radar with high range resolution and unambiguous velocity determination," *IEEE Transactions on Military Electronics*, vol. MIL-6, no. 2, pp. 153-161, April 1962.

[3] M. P. Grant, G. R. Cooper, and A. K. Kamal, "A class of noise systems," *Proceedings of the IEEE*, vol. 51, no. 7, pp. 1060-1061, July 1963.

[4] G. R. Cooper and C. D. McGillem, *Random Signal Radar*, Final Report TR-EE67-11, Purdue University School of Electrical Engineering, Lafayette, IN, June 1967.

[5] J.A. Smit and W.B.S.M. Kneefel, "RUDAR - an experimental noise radar system," *De Ingenieur,* vol. 83, no. 32, pp. 99-110, 13 August 1971.

[6] J.R. Forrest and J.P. Meeson, "Solid-state microwave noise radar," *Electronics Letters*, vol. 12, no. 15, pp. 365-366, 22 July 1976.

[7] G. Liu, X. Shi, J. Lu, G. Yang, and Y. Song, "Design of noise FM-CW radar and its implementation," *IEE Proceedings - Part F: Radar and Signal Processing*, vol. 138, no. 5, pp. 420-426, October 1991.

[8] K.A. Lukin, "Ka-band noise radar," *Proc. International Symposium on Physics and Engineering of Millimeter and Submillimeter Waves*, Kharkov, Ukraine, pp. 322-324, June 1994.

[9] R.M. Narayanan, Y. Xu, P.D. Hoffmeyer, and J.O. Curtis, "Design and performance of a polarimetric random noise radar for detection of shallow buried targets," *Proc. SPIE Conference on Detection Technologies for Mines and Minelike Targets*, Orlando, FL, vol. 2496, pp. 20-30, April 1995.

[10] E.K. Walton, V. Fillimon, and S. Gunawan, "ISAR imaging using UWB noise radar," *Proc. 18th Annual AMTA Symposium*, Seattle, WA, pp. 167-171, September-October 1996.

[11] R.M. Narayanan, Y. Xu, P.D. Hoffmeyer, and J.O. Curtis, "Design, performance, and applications of a coherent ultrawideband random noise radar," *Optical Engineering*, vol. 37, no. 6, pp. 1855-1869, June 1998.

[12] I.P. Theron, E.K. Walton, S. Gunawan, and L. Cai, "Ultrawide-band noise radar in the VHF/UHF band," *IEEE Transactions on Antennas and Propagation*, vol. 47, no. 6, pp. 1080-1084, June 1999.

[13] R. Stephan and H. Loele, "Theoretical and practical characterization of a broadband random noise radar," *IEEE MTT-S International Microwave Symposium Digest*, Boston, MA, pp. 1555-1558, June 2000.

[14] L. Turner, "The evolution of featureless waveforms for LPI communications," *Proc. IEEE 1991 National Aerospace and Electronics Conference (NAECON)*, Dayton, OH, pp. 1325-1331, May 1991.

[15] S.R.J. Axelsson, "Random noise radar/sodar with ultrawideband waveforms," *IEEE Transactions on Geoscience and Remote Sensing*, vol. 45, no. 5, pp.1099–1114, May 2007.

[16] D.A. Gray, "Multi-channel noise radar," *Proc. International Radar Symposium (IRS 2006)*, Krakow, Poland, doi : 10.1109/IRS.2006.4338086, May 2006.

[17] E. Fishler, A. Haimovich, R.S. Blum, L.J. Cimini, Jr., D. Chizhik, and R.A. Valenzuela, "Spatial diversity in radars–models and detection performance," *IEEE Transactions on Signal Processing*, vol. 54, No. 3, pp. 823–838, Mar. 2006.

[18] N.H. Lehmann, E. Fishler, A.M. Haimovich, R.S. Blum, D. Chizhik, L.J. Cimini, Jr., and R.A. Valenzuela, "Evaluation of transmit diversity in MIMO-radar direction finding," *IEEE Transactions on Signal Processing*, vol. 55, No. 5, pp. 2215–2225, May 2007.

[19] N.H. Lehmann, A.M. Haimovich, R.S. Blum, and L. Cimini, "High resolution capabilities of MIMO radar," *Proceedings of the 40th Asilomar Conference on Signals, Systems and Computers (ACSSC '06)*, Pacific Grove, CA, pp. 25–30, Oct.-Nov. 2006.

[20] X.-Z. Dai, J. Xu, Y.-N. Peng, and X.-G. Xia, "A new method of improving the weak target detection performance based on the MIMO radar," *Proc. International Conference on Radar (CIE '06),* Shanghai, China, doi: 10.1109/ICR.2006.343265, Oct. 2006.

[21] H.A. Khan and D.J. Edwards, "Doppler problems in orthogonal MIMO radars," *Proc. IEEE Conference on Radar*, Verona, NY, pp. 244-247, Apr. 2006.

[22] B. Liu, Z. He, J. Zeng, and B. Liu, "Polyphase orthogonal code design for MIMO radar systems," *Proc. International Conference on Radar (CIE '06),* Shanghai, China, doi: 10.1109/ICR.2006.343409, Oct. 2006.

[23] B. Friedlander, "On data-adaptive waveform design for MIMO radar signals," *Conference Record of the 41st Asilomar Conference on Signals, Systems and Computers, (ACSSC '07),* Pacific Grove, CA, pp.187-191, Nov. 2007.

[24] Y. Yang and R.S. Blum, "MIMO radar waveform design based on mutual information and minimum mean-square error estimation," *IEEE Transactions on Aerospace and Electronic Systems*, vol. 43, no.1, pp.330-343, Jan. 2007.

[25] D.A. Gray and R. Fry, "MIMO noise radar – element and beam space comparisons," *International Waveform Diversity and Design Conference*, pp. 344–347, June 2007.

[26] D.A. Gray and A. Capria, "MIMO noise radar – matched filters and coarrays," *IEEE Radar Conference*, pp. 1-6, May 2008.

[27] R.B. Sinitsyn, "Copula based detection algorithm for MIMO ultrawideband noise radars," *Proceedings of the 6th European Radar Conference*, pp. 121-124, Oct. 2009.

[28] L. Xu and J. Li, "Iterative generalized-likelihood ratio test for MIMO radar," *IEEE Transactions on Signal Processing*, vol. 55, no. 6, pp. 2375–2385, Jun. 2007.

[29] G. Su and M.Morf, "The signal subspace approach for multiple wide-band emitter location," *IEEE Transactions on Acoustic, Speech, and Signal processing*, vol. 31, no. 6, pp. 1502–1522, 1983

[30] V.V. Mani and R. Bose, "Smart antenna design for beamforming of UWB signals in Gaussian noise," *Proc. International ITG Workshop on Smart Antennas (WSA 2008),* Vienna, Austria, pp. 311-316, Feb. 2008.

[31] J. Mayhan, A. Simmons, W. Cummings, "Wide-band adaptive antenna nulling using tapped delay lines," *IEEE Transactions on Antenna and Propagation*, vol. 29, no.6. pp. 923-936, Nov. 1981.

[32] O.L. Frost, III, "An algorithm for linearly constrained adaptive array processing," *Proceedings of the IEEE*, vol. 60, no. 8, pp. 926-935, Aug. 1972.

[33] V.V. Mani and R. Bose, "Genetic algorithm based smart antenna design for UWB beamforming," *IEEE International Conference on Ultra-Wideband, 2007*. pp. 442-446, Sept. 2007.

[34] R.M. Narayanan, and M. Dawood, "Doppler estimation using a coherent ultrawide-band random noise radar," *IEEE Transactions on Antennas and Propagation*, vol. 48, no. 6, pp.868–878, June 2000

[35] Z. Li, and R.M. Narayanan, "Doppler visibility of coherent ultrawideband random noise radar systems," *IEEE Transactions on Aerospace and Electronic Systems*, vol. 42, no.3, pp.904-914, July. 2006.

[36] M. Meller, "Approximate Cramer-Rao bound on Doppler error in correlation-processing relatively narrowband noise radar," *IET Radar, Sonar and Navigation*, vol. 3, no. 3, pp. 245–252, June 2009.

[37] D.C. Bell, and R.M. Narayanan, "Theoretical aspects of radar imaging using stochastic waveforms," *IEEE Transactions on Signal Processing*, vol.49, No. 2, pp. 394–400, Feb. 2001.

[38] M. Dawood, and R.M. Narayanan, "Generalised wideband ambiguity function of a coherent ultrawideband random noise radar," *IEE Proceedings Radar, Sonor and Navigation*, vol. 150, no. 5, pp. 379-386, October 2003.

[39] Q. Jin, K.M. Wong and Z.Q. Luo, "The estimation of time delay and Doppler stretch of wideband signals," *IEEE Transactions on Signal Processing*, vol. 43, no. 4, pp.904–916, Apr. 1995.

[40] S.M. Kay, *Fundamentals of Statistical Signal Processing, Volume II: Detection Theory*. Upper Saddle River, NJ: Prentice Hall PTR, 1993.

[41] R. Bose, and A. Freedman, and B.D. Steinberg, "Sequence CLEAN: a modified deconvolution technique for microwave images of contiguous targets," *IEEE Transactions on Aerospace and Electronic Systems*, vol. 38, no.1, pp. 89-97, Jan. 2002.

[42] R.D. Fry and D.A. Gray, "CLEAN deconvolution for sidelobe suppression in random noise radar," *Proc. 2008 International Conference on Radar*, Adelaide, Australia, pp. 209-212, Sept. 2008.

[43] B.G. Clark, "An efficient implementation of the algorithm CLEAN," *Astronomy and Astrophysics*, vol. 89, no. 3, pp. 377-378, 1980.

[44] P. Billingsley, *Probability and Measure, third ed.*, Wiley Ser. Probab. Math. Stat., John Wiley & Sons Inc., New York, May 1995.

[45] F.C. Leone, L.S. Nelson and R.B. Nottingham, "The folded normal distribution," *Technometrics*, vol. 3, no. 4, pp. 543–550, Nov. 1961.

[46] G.H. Robertson, "A fast amplitude approximation for quadrature pairs," *Bell System Technical Journal*, vol. 50, no. 8, pp. 2849–2852, 1971

[47] M. Onoe, "Fast amplitude approximation yielding either exact mean or minimum deviation for quadrature pairs," *Proceedings of the IEEE*, vol. 60, no. 7, pp. 921–922, 1972

[48] A.E. Filip, "Linear approximations to $\sqrt{x^2 + y^2}$ having equiripple error characteristics," *IEEE Transactions on Audio and Electroacoustics*, vol. 21, no. 6, pp. 554–556, 1973

[49] B.K. Levitt, and G.A. Morris, "An improved digital algorithm for fast amplitude approximations of quadrature pairs," *NASA DSN Progress Report*, no. 42-40, pp. 97-101, 1977

[50] R. Ware and F. Lad, "Approximating the distribution for sums of products of normal variables," Research Report, Canterbury University, 2003

## Appendix

## The correlation coefficient between $A^{1/2}\left(\tilde{\mathbf{v}}_{u,h},\tilde{\mathbf{x}}_{\mathrm{u,h}}\right)$ and $A^{1/2}\left(\tilde{\mathbf{v}}_{u',h'},\tilde{\mathbf{x}}_{\mathrm{u',h'}}\right)$

The correlation coefficient $\rho_{u,h,\mathrm{u,h}}^{u',h',\mathrm{u',h'}}$ between $A^{1/2}\left(\tilde{\mathbf{v}}_{u,h},\tilde{\mathbf{x}}_{\mathrm{u,h}}\right)$ and $A^{1/2}\left(\tilde{\mathbf{v}}_{u',h'},\tilde{\mathbf{x}}_{\mathrm{u',h'}}\right)$ is defined as

$$\rho_{u,h,\mathrm{u,h}}^{u',h',\mathrm{u',h'}}=\frac{E\left[A^{1/2}\left(\tilde{\mathbf{v}}_{u,h},\tilde{\mathbf{x}}_{\mathrm{u,h}}\right)A^{1/2}\left(\tilde{\mathbf{v}}_{u',h'},\tilde{\mathbf{x}}_{\mathrm{u',h'}}\right)\right]-\bar{\mu}_{\tilde{\mathbf{v}},\tilde{\mathbf{x}}}^{\lceil u,h,\mathrm{u,h}\rceil}\bar{\mu}_{\tilde{\mathbf{v}},\tilde{\mathbf{x}}}^{\lceil u',h',\mathrm{u',h'}\rceil}}{\bar{\sigma}_{\tilde{\mathbf{v}},\tilde{\mathbf{x}}}^{\lceil u,h,\mathrm{u,h}\rceil}\bar{\sigma}_{\tilde{\mathbf{v}},\tilde{\mathbf{x}}}^{\lceil u',h',\mathrm{u',h'}\rceil}} \tag{A.1}$$

Refer to the approximation of $A^{1/2}\left(\tilde{\mathbf{v}}_{u,h},\tilde{\mathbf{x}}_{\mathrm{u,h}}\right)$ in 4.20. It can be restated as

$$\begin{aligned}A^{1/2}\left(\tilde{\mathbf{v}}_{u,h},\tilde{\mathbf{x}}_{\mathrm{u,h}}\right)\approx&\left(1-\frac{1}{2}\left(\bar{\rho}_{\tilde{\mathbf{v}},\tilde{\mathbf{x}}}^{\lceil u,h,\mathrm{u,h}\rceil}\frac{\bar{\sigma}_{I,\tilde{\mathbf{v}},\tilde{\mathbf{x}}}^{\lceil u,h,\mathrm{u,h}\rceil}}{\bar{\sigma}_{R,\tilde{\mathbf{v}},\tilde{\mathbf{x}}}^{\lceil u,h,\mathrm{u,h}\rceil}}\right)^2\right)\left|\bar{\chi}_{R,\tilde{\mathbf{v}},\tilde{\mathbf{x}}}^{\lceil u,h,\mathrm{u,h}\rceil}\right|\\&+\bar{\rho}_{\tilde{\mathbf{v}},\tilde{\mathbf{x}}}^{\lceil u,h,\mathrm{u,h}\rceil}\frac{\bar{\sigma}_{I,\tilde{\mathbf{v}},\tilde{\mathbf{x}}}^{\lceil u,h,\mathrm{u,h}\rceil}}{\bar{\sigma}_{R,\tilde{\mathbf{v}},\tilde{\mathbf{x}}}^{\lceil u,h,\mathrm{u,h}\rceil}}\bar{\chi}_{I,\tilde{\mathbf{v}},\tilde{\mathbf{x}}}^{\lceil u,h,\mathrm{u,h}\rceil}+E\left[\frac{\left(\gamma_{R,\tilde{\mathbf{v}},\tilde{\mathbf{x}}}^{\lceil u,h,\mathrm{u,h}\rceil}\right)^2}{\left|2\bar{\chi}_{R,\tilde{\mathbf{v}},\tilde{\mathbf{x}}}^{\lceil u,h,\mathrm{u,h}\rceil}\right|}\right].\end{aligned} \tag{A.2}$$

Then,

$$
\begin{aligned}
&E\left[A^{1/2}\left(\tilde{\mathbf{v}}_{u,h},\tilde{\mathbf{x}}_{\mathrm{u,h}}\right)A^{1/2}\left(\tilde{\mathbf{v}}_{u',h'},\tilde{\mathbf{x}}_{\mathrm{u',h'}}\right)\right]\\
&\approx\left(1-\frac{1}{2}f^{2}\right)\left(1-\frac{1}{2}f'^{2}\right)E\left[\left|\overline{\chi}_{R,\tilde{\mathbf{v}},\tilde{\mathbf{x}}}^{[u,h,\mathrm{u,h}]}\right|\left|\overline{\chi}_{R,\tilde{\mathbf{v}},\tilde{\mathbf{x}}}^{[u',h',\mathrm{u',h'}]}\right|\right]+\left(1-\frac{1}{2}f^{2}\right)f'^{2}E\left[\left|\overline{\chi}_{R,\tilde{\mathbf{v}},\tilde{\mathbf{x}}}^{[u,h,\mathrm{u,h}]}\right|\overline{\chi}_{I,\tilde{\mathbf{v}},\tilde{\mathbf{x}}}^{[u',g',h',I']}\right]\\
&+\left(1-\frac{1}{2}f'^{2}\right)f\times E\left[\left|\overline{\chi}_{R,\tilde{\mathbf{v}},\tilde{\mathbf{x}}}^{[u',h',\mathrm{u',h'}]}\right|\overline{\chi}_{I,\tilde{\mathbf{v}},\tilde{\mathbf{x}}}^{[u,h,\mathrm{u,h}]}\right]+f\times f'E\left[\overline{\chi}_{I,\tilde{\mathbf{v}},\tilde{\mathbf{x}}}^{[u,h,\mathrm{u,h}]}\overline{\chi}_{I,\tilde{\mathbf{v}},\tilde{\mathbf{x}}}^{[u',h',\mathrm{u',h'}]}\right]\\
&+\left\{\left(1-\frac{1}{2}f'^{2}\right)E\left[\left|\overline{\chi}_{R,\tilde{\mathbf{v}},\tilde{\mathbf{x}}}^{[u',h',\mathrm{u',h'}]}\right|\right]+f'E\left[\overline{\chi}_{I,\tilde{\mathbf{v}},\tilde{\mathbf{x}}}^{[u',h',\mathrm{u',h'}]}\right]+E\left[\frac{\left(\gamma_{\tilde{\mathbf{v}},\tilde{\mathbf{x}}}^{[u',h',\mathrm{u',h'}]}\right)^{2}}{2\overline{\chi}_{R,\tilde{\mathbf{v}},\tilde{\mathbf{x}}}^{[u',h',\mathrm{u',h'}]}}\right]\right\}E\left[\frac{\left(\gamma_{\tilde{\mathbf{v}},\tilde{\mathbf{x}}}^{[u,h,\mathrm{u,h}]}\right)^{2}}{2\overline{\chi}_{R,\tilde{\mathbf{v}},\tilde{\mathbf{x}}}^{[u,h,\mathrm{u,h}]}}\right]\\
&+\left\{\left(1-\frac{1}{2}f^{2}\right)E\left[\left|\overline{\chi}_{R,\tilde{\mathbf{v}},\tilde{\mathbf{x}}}^{[u,h,\mathrm{u,h}]}\right|\right]+f\times E\left[\overline{\chi}_{I,\tilde{\mathbf{v}},\tilde{\mathbf{x}}}^{[u,h,\mathrm{u,h}]}\right]+E\left[\frac{\left(\gamma_{\tilde{\mathbf{v}},\tilde{\mathbf{x}}}^{[u,h,\mathrm{u,h}]}\right)^{2}}{2\overline{\chi}_{R,\tilde{\mathbf{v}},\tilde{\mathbf{x}}}^{[u,h,\mathrm{u,h}]}}\right]\right\}E\left[\frac{\left(\gamma_{\tilde{\mathbf{v}},\tilde{\mathbf{x}}}^{[u',h',\mathrm{u',h'}]}\right)^{2}}{2\overline{\chi}_{R,\tilde{\mathbf{v}},\tilde{\mathbf{x}}}^{[u',h',\mathrm{u',h'}]}}\right]
\end{aligned}
\tag{A.3}
$$

where $f=\overline{\rho}_{\tilde{\mathbf{v}},\tilde{\mathbf{x}}}^{[u,h,\mathrm{u,h}]}\dfrac{\overline{\sigma}_{I,\tilde{\mathbf{v}},\tilde{\mathbf{x}}}^{[u,h,\mathrm{u,h}]}}{\overline{\sigma}_{R,\tilde{\mathbf{v}},\tilde{\mathbf{x}}}^{[u,h,\mathrm{u,h}]}}$ and $f'=\overline{\rho}_{\tilde{\mathbf{v}},\tilde{\mathbf{x}}}^{[u',h',\mathrm{u',h'}]}\dfrac{\overline{\sigma}_{I,\tilde{\mathbf{v}},\tilde{\mathbf{x}}}^{[u',h',\mathrm{u',h'}]}}{\overline{\sigma}_{R,\tilde{\mathbf{v}},\tilde{\mathbf{x}}}^{[u',h',\mathrm{u',h'}]}}$. We apply $\left|E\left[\overline{\chi}_{R,\tilde{\mathbf{v}},\tilde{\mathbf{x}}}^{[u,h,\mathrm{u,h}]}\overline{\chi}_{R,\tilde{\mathbf{v}},\tilde{\mathbf{x}}}^{[u',h',\mathrm{u',h'}]}\right]\right|$, $\pm E\left[\overline{\chi}_{R,\tilde{\mathbf{v}},\tilde{\mathbf{x}}}^{[u,h,\mathrm{u,h}]}\overline{\chi}_{I,\tilde{\mathbf{v}},\tilde{\mathbf{x}}}^{[u',h',\mathrm{u',h'}]}\right]$, and $\pm E\left[\overline{\chi}_{R,\tilde{\mathbf{v}},\tilde{\mathbf{x}}}^{[u',h',\mathrm{u',h'}]}\overline{\chi}_{I,\tilde{\mathbf{v}},\tilde{\mathbf{x}}}^{[u,h,\mathrm{u,h}]}\right]$ to approximate $E\left[\left|\overline{\chi}_{R,\tilde{\mathbf{v}},\tilde{\mathbf{x}}}^{[u,h,\mathrm{u,h}]}\right|\left|\overline{\chi}_{R,\tilde{\mathbf{v}},\tilde{\mathbf{x}}}^{[u',h',\mathrm{u',h'}]}\right|\right]$, $E\left[\left|\overline{\chi}_{R,\tilde{\mathbf{v}},\tilde{\mathbf{x}}}^{[u,h,\mathrm{u,h}]}\right|\overline{\chi}_{I,\tilde{\mathbf{v}},\tilde{\mathbf{x}}}^{[u',h',\mathrm{u',h'}]}\right]$ and $E\left[\left|\overline{\chi}_{R,\tilde{\mathbf{v}},\tilde{\mathbf{x}}}^{[u',h',\mathrm{u',h'}]}\right|\overline{\chi}_{I,\tilde{\mathbf{v}},\tilde{\mathbf{x}}}^{[u,h,\mathrm{u,h}]}\right]$, respectively. For example, if $\overline{\mu}_{R,n,m,\tilde{\mathbf{v}},\tilde{\mathbf{x}}}^{[u,h,\mathrm{u,h}]}>0$, $+E\left[\overline{\chi}_{R,\tilde{\mathbf{v}},\tilde{\mathbf{x}}}^{[u,h,\mathrm{u,h}]}\overline{\chi}_{I,\tilde{\mathbf{v}},\tilde{\mathbf{x}}}^{[u',h',\mathrm{u',h'}]}\right]\approx E\left[\left|\overline{\chi}_{R,\tilde{\mathbf{v}},\tilde{\mathbf{x}}}^{[u,h,\mathrm{u,h}]}\right|\overline{\chi}_{I,\tilde{\mathbf{v}},\tilde{\mathbf{x}}}^{[u',h',\mathrm{u',h'}]}\right]$. Since each variable is the summation of the samples of correlator outputs in different receiver antennas corresponding to different reference signals, those expected values are obtained by calculating the correlation between the samples. Taking $E\left[\overline{\chi}_{R,\tilde{\mathbf{v}},\tilde{\mathbf{x}}}^{[u,h,\mathrm{u,h}]}\overline{\chi}_{R,\tilde{\mathbf{v}},\tilde{\mathbf{x}}}^{[u',h',\mathrm{u',h'}]}\right]$ as an example,

$$
\begin{aligned}
&E\left[\overline{\chi}_{R,\tilde{\mathbf{v}},\tilde{\mathbf{x}}}^{[u,h,\mathrm{u,h}]}\overline{\chi}_{R,\tilde{\mathbf{v}},\tilde{\mathbf{x}}}^{[u',h',\mathrm{u',h'}]}\right]\\
&\quad=E\left[\sum_{\ell=1}^{L}\sum_{m=1}^{M}\sum_{n=1}^{N}\chi_{R,n,m,\ell}^{[u,h,\mathrm{u,h}]}\sum_{\ell=1}^{L}\sum_{m=1}^{M}\sum_{n=1}^{N}\chi_{R,n,m,\ell}^{[u',h',\mathrm{u',h'}]}\right]=\sum_{\ell=1}^{L}\sum_{m=1}^{M}\sum_{n=1}^{N}\Psi_{n,m,\ell}+\overline{\mu}_{R,\tilde{\mathbf{v}},\tilde{\mathbf{x}}}^{[u,h,\mathrm{u,h}]}\overline{\mu}_{R,\tilde{\mathbf{v}},\tilde{\mathbf{x}}}^{[u',h',\mathrm{u',h'}]}
\end{aligned}
\tag{A.4}
$$

$$
\Psi_{n,m,\ell}=\Psi_{1,n,m,\ell}+\Psi_{2,n,m,\ell}+\Psi_{3,n,m,\ell} \tag{A.5}
$$

$$\Psi_{1,n,m,\ell} = \left(\alpha_{R,n,m}\cos\left(2\pi f_c D_{\ell,n,m}^{[u,h,\mathrm{u},\mathrm{h}]}\right) + \alpha_{I,n,m}\sin\left(2\pi f_c D_{\ell,n,m}^{[u,h,\mathrm{u},\mathrm{h}]}\right)\right)$$
$$\times\left(\alpha_{R,n,m}\cos\left(2\pi f_c D_{\ell,n,m}^{[u',h',\mathrm{u}',\mathrm{h}']}\right) + \alpha_{I,n,m}\sin\left(2\pi f_c D_{\ell,n,m}^{[u',h',\mathrm{u}',\mathrm{h}']}\right)\right)$$
$$\times\left(\sigma_s^4\mathrm{sinc}\left(B\times\left(D_{\ell,n,m}^{[u,h,\mathrm{u},\mathrm{h}]} - D_{\ell,n,m}^{[u',h',\mathrm{u}',\mathrm{h}']}\right)\right) + \sigma_s^4\mathrm{sinc}\left(B\times D_{\ell,n,m}^{[u,h,\mathrm{u},\mathrm{h}]}\right)\mathrm{sinc}\left(B\times D_{\ell,n,m}^{[u',h',\mathrm{u}',\mathrm{h}']}\right)\right) \tag{A.6}$$

$$\Psi_{2,n,m,\ell} = \sum_{\substack{\tilde{n}=1\\ n\neq\tilde{n}}}^{N}\Bigg[\left(\alpha_{R,\tilde{n},m}\cos\left(2\pi f_c D_{\ell,\tilde{n},m}^{[u,h,\mathrm{u},\mathrm{h}]}\right) + \alpha_{I,\tilde{n},m}\sin\left(2\pi f_c D_{\ell,\tilde{n},m}^{[u,h,\mathrm{u},\mathrm{h}]}\right)\right)$$
$$\times\left(\alpha_{R,\tilde{n},m}\cos\left(2\pi f_c D_{\ell,\tilde{n},m}^{[u',h',\mathrm{u}',\mathrm{h}']}\right) + \alpha_{I,\tilde{n},m}\sin\left(2\pi f_c D_{\ell,\tilde{n},m}^{[u',h',\mathrm{u}',\mathrm{h}']}\right)\right) \tag{A.7}$$
$$\times\sigma_s^4\mathrm{sinc}\left(B\times\left(D_{\ell,\tilde{n},m}^{[u,h,\mathrm{u},\mathrm{h}]} - D_{\ell,\tilde{n},m}^{[u',h',\mathrm{u}',\mathrm{h}']}\right)\right)\Bigg]$$

$$\Psi_{3,n,m,\ell} = \sigma_z^2\sigma_s^2\mathrm{sinc}\left(B\times\left(D_{\ell,\tilde{n},m}^{[u,h,\mathrm{u},\mathrm{h}]} - D_{\ell,\tilde{n},m}^{[u',h',\mathrm{u}',\mathrm{h}']}\right)\right)\cos\left(2\pi f_c\left(D_{\ell,\tilde{n},m}^{[u,h,\mathrm{u},\mathrm{h}]} - D_{\ell,\tilde{n},m}^{[u',h',\mathrm{u}',\mathrm{h}']}\right)\right)$$

(A.8)

Similar calculations can be applied to find $\pm E\left[\bar{\chi}_{R,\tilde{\mathbf{v}},\tilde{\mathbf{x}}}^{[u,h,\mathrm{u},\mathrm{h}]}\bar{\chi}_{I,\tilde{\mathbf{v}},\tilde{\mathbf{x}}}^{[u',h',\mathrm{u}',\mathrm{h}']}\right]$, and $\pm E\left[\bar{\chi}_{R,\tilde{\mathbf{v}},\tilde{\mathbf{x}}}^{[u',h',\mathrm{u}',\mathrm{h}']}\bar{\chi}_{I,\tilde{\mathbf{v}},\tilde{\mathbf{x}}}^{[u,h,\mathrm{u},\mathrm{h}]}\right]$. Then, the $\rho_{u,h,\mathrm{u},\mathrm{h}}^{u',h',\mathrm{u}',\mathrm{h}'}$ is solved.

# VITA

**Wei-Jen Chen**

## RESEARCH INTERESTS

Signal processing, Communication theory, UWB MIMO radar system

## EDUCATION

The Pennsylvania State University, Ph.D. in Electrical Engineering, Aug. 2010.

The National Chiao-Tung University, M.S. in Communication Engineering, Jun. 2002.

The National Chiao-Tung University, B.S. in Communication Engineering, Jun. 2000.

## PUBLICATIONS

1. Li-Chun Wang and Wei-Jen Chen, "Fully Distributed Joint Closed-loop Power Control and Open-loop Rate Adaptation for the Multi-Rate WCDMA System," *Proc. Sixth International Symposium on Wireless Personal Multimedia Communications*, Yokosuka, Japan, pp. 312-316, Oct. 2003.

2. Wei-Jen Chen and Ram M. Narayanan, "Adaptive MIMO Radar Detection Algorithm in a Spatially Correlated Clutter Environment," *Proc. SPIE Conference on Wireless Sensing and Processing III*, Orlando, FL, Vol. 6980, pp. 69800M-1–69800M-12, doi:10.1117/12.777395, March 2008.

3. Wei-Jen Chen and Ram M. Narayanan, "Tapped-Delay Line Beamforming in Spatial Diversity MIMO Noise Radar using Conditional Generalized Likelihood Ratio Test," *Proc. International Conference on Electromagnetics in Advanced Applications (ICEAA'09)*, Torino, Italy, pp. 343–346, September 2009.

4. Wei-Jen Chen and Ram M. Narayanan, "Integration of Conditional Generalized Likelihood Ratio Test and Tapped Delay Line Beamforming for Ultrawideband MIMO Noise Radar," *IEEE Transactions on Aerospace and Electronic Systems*, submitted December 2008, revised and resubmitted July 2009.

5. Wei-Jen Chen and Ram M. Narayanan, "Target location and velocity estimation in Ultrawideband MIMO Noise Radar" *IET Radar, Sonar and Navigation*, submitted February 2010.